Technical Report

A Systems Study of Fiber Optics for Broadband Communications

Activity No. 5
System Design Rules
and Guidelines

BNR Project TR 6259
August 1977

Bell-Northern Research

A Systems Study of Fiber Optics for Broadband Communications

BNR Project TR6259
August 1977

for
Communications Research Centre
Department of Communications
Government of Canada

under DSS Contract
File number: 12ST. 36001-6-2350
Contract number: OST 76-00054

Activity No. 5
System Design Rules
and guidelines

M. Larose

Bell-Northern Research Ltd.

TABLE OF CONTENTS

ACKNOWLEDGEMENTS

The author acknowledges the contribution to this report of N. Toms who is responsible for the Appendixes A and B of this report.

INTRODUCTION

In the broadband communication systems considered in Activities 2, 3 and 4 of the Systems Study of Fiber Optics for Broadband Communications, the provision of video signals is the most transmission demanding service. Telephony and data could be added to the video signals without significantly affecting the system performance. The system performance is evaluated in terms of the maximum achievable transmission length (which is given as a function of the number of video channels transmitted, the hardware characteristics, and the video performance requirements).

This report is concerned primarily with the transmission of video using the intensity modulation of the light source output by an amplitude-modulated electrical signal - the signal format compatible with present TV sets. Frequency modulation and digital video transmission are also considered for transportation trunk applications.

Even though this report is mainly concerned with frequency division multiplexing (FDM), the results can readily be applied to space division multiplexing (SDM) or to a combination of the two (SDM-FDM). The results can also be applied to wavelength division multiplexing (WDM) if each optical wavelength is considered individually. The requirements imposed on the disperser isolation between the wavelengths is studied in Appendix B.

SUMMARY

Formulas for intermodulation, crossmodulation, signal-to-noise ratio, differential gain, and system frequency response are derived. For a signal-to-noise ratio objective of 40 dB, a low number of repeaters, and single-channel transmission (especially baseband transmission), the use of a low gain avalanche photodiode is advantageous. The magnitude of this gain depends on the relative level of the non-signal-dependent noise and on the excess noise factor associated with the avalanche process. However, as the number of channels, the number of repeaters, or the signal-to-noise ratio requirement increases, the PIN photodiode becomes the optimum detector for video transmission.

Graded index fiber should be used for video transmission. For long transmission lines, in the order of 50 km, equalization for the fiber frequency response may be required depending on the number of channels transmitted and the light source used.

For systems meeting BP-23 specifications, present LED's with linearization circuits could accommodate up to five low frequency video channels. A higher number of channels could be transmitted over a repeatered line with laser sources if they can be sufficiently stabilized and linearized. In FDM systems, the law for the power compounding of intermodulation beats with the number of repeaters is found to have a very limiting effect on the system performance. This law depends on the relationship between the phase and the frequency in the fiber frequency

response. This needs clarification if the practical implementation of a multichannel video system is considered.

The use of harmonically related carriers (HRC) presents advantages in signal-to-noise ratio and linearity requirements. However, the crossmodulation in HRC systems requires further study on the influence of second-order distortion.

For long high quality transportation trunks, the transmission of a single channel per light source is preferable. For trunk lengths exceeding the capability of AM-VSB transmission, FM and digital video transmissions represent viable alternatives.

LIST OF FIGURES

LIST OF FIGURES (Cont)

LIST OF TABLES

GLOSSARY

REPS	- repeater spacing
P_{max}	- mean optical power coupled into the fiber
P_{min}	- mean optical power received at the detector
α	- fiber attenuation (dB/km)
F	- fiber type factor
NA	- numerical aperture of the fiber
IR_x	- radiant intensity on axis at a reference driving current x
I_{max}	- maximum driving current
K_e	- laser-fiber coupling efficiency
$\frac{dP}{dI}$	- laser external quantum efficiency
η	- photodiode quantum efficiency
e	- electron charge
G	- photodiode avalanche gain
$h\nu$	- photon energy
$\langle i_T^2 \rangle$	- thermal noise rms power
N_T	- thermal noise rms power
k	- Boltzmann's constant
T	- absolute temperature
b	- video channel bandwidth
F_t	- amplifier noise figure
R_{eq}	- equivalent load resistance
$\langle i_Q^2 \rangle$	- quantum noise rms power
N_Q	- quantum noise rms power
P_{avg}	- average power received on the detector

F_D - excess avalanche noise factor

$\langle i_D^2 \rangle$ - dark current rms power

N_D - dark current rms power

I_D - dark current of the photodiode

I_L - leakage current of the photodiode

N_L - leakage current rms power

$\langle i_L^2 \rangle$ - leakage current rms power

$\langle i_B^2 \rangle$ - beat noise rms power

$\langle N_B \rangle$ - beat noise rms power

J - number of spatial modes of the source

W - spectral width of the source

F_s - source excess noise factor

m_c - RF modulation index

ω_c - carrier angular frequency

m_{Ic} - optical modualtion index (carrier)

i_{DC} - bias current at the source

P_{DC} - mean optical power received at the detector (bias)

SNR - signal-to-noise ratio

SNR_{NCTA} - signal-to-noise ratio, NCTA definition

N - number of repeaters

m_{Ib} - optical modulation index (baseband)

SNR_{BTL} - signal-to-noise ratio, BTL definition

m_I - (global) optical modulation index

K - number of video channels (carriers)

N_Q' - quantum noise factor

N_B' - beat noise factor

Z - video signal factor

G_{opt} - optimum avalanche gain

k - ionization factor

A' - intrinsic photodiode responsitivity

Q' - quantum noise constant

IM_x - relative power of an intermodulation beat of type x

$H_{2\alpha_x}$ - relative second harmonic of a fundamental of x mA peak-to-peak

$H_{3\alpha_x}$ - relative third harmonic of a fundamental of x mA peak-to-peak

S_i - peak-to-peak signal of a modulated carrier

C - coefficient of the beats addition

n_b, n_c, n_d - number of beats used in the crossmodulation evaluation

m - modulation index (crossmodulation)

D_{2nd}, D_{3rd} - relative second and third harmonic in current

σ_T - total dispersion

σ_s - rms spectral half-width of the source

n - refractive index

λ - wavelength

L - fiber length

c - speed of light

σ_m - modal dispersion per unit of length

n_1 - core refractive index

Δ - fractional index difference between core and cladding

L_{eff} - effective length

B_{-3dB} - -3 dB electrical bandwidth

B - highest signal frequency

C_i - input capacitance

1. DESCRIPTION OF BASEBAND AND AM-VSB TRANSMISSION SYSTEMS

1.1 BASEBAND TRANSMISSION

The baseband video signal format considered in this report is the NTSC 525/60 which is standard in North America. The dc component of the baseband video signal gives the average value of the brightness of the picture which is information required by the TV receiver. However, it is not necessary to transmit the dc component; it can be reintroduced at the receiver end using a clamper. Thus the baseband video signal can be transmitted either with or without the dc component. These are designated as dc and ac transmission, respectively.

In the case of dc transmission, the source-driving current is the baseband video signal added to a bias current. At the receiver end, a clamper is required because ac coupling is used between the detector and the amplifier. For a repeatered line, clampers are required at all repeaters in order to restore the dc component. However, since clampers introduced nonlinear distortions and cascading many of them should therefore be avoided, dc transmission should be limited to short systems.

In the case of ac transmission, the dc component is not restored at every repeater. A clamper is required only at the last

receiver of the line. In ac transmission, the dc level wandering increase the peak-to-peak signal amplitude. For example, after many white lines at full intensity the dc level corresponds to a level of +80 units of the IRE video scale and the peak negative signal excursion during the synch pulse is 120 units. Similarly, during the vertical field interval, if preceded by many black lines, the dc level corresponds to about -10 IRE units and the peak possible positive excursion is 130 units. Thus the peak-to-peak signal excursion equals 1.6 of the peak-to-peak video signal.

In a repeatered ac transmission line, each detector-amplifier combination acts as a first-order high-pass filter. A video signal varying from the blanking level to the peak luminance level appears as a step function being applied to a cascade of first-order high-pass filters. Consequently low frequency damped oscillations result. These low frequency damped oscillations are not objectionable in themselves, and they are removed by the clamper. However, they do increase the signal dynamic range which can, in turn, cause saturation of the amplifiers if care is not taken. It is shown that for a cascade of first-order high-pass filters, where the number of repeaters tends to infinite, the maximum overshoot is 40.3 percent.[1] The preceding is based on the assumption that all high-pass filters are of the first order and have the same time constant. If for some reason (e.g., higher order filters) the damped oscillations grow exponentially, clampers are required at intermediate repeaters in order to limit the signal dynamic range.

Baseband ac transmission requires a wider dyanmic range than dc transmission, but the number of repeater sections is not limited by the maximum number of clampers that can be placed in tandem. In present copper-based systems, the maximum number of clampers permitted is in the order of ten. A maximum of seven are cascaded in the Canadian network, and no more than twelve is recommended by the Bell System.[2] Thus for long systems, ac transmission should be preferred.

For both dc and ac transmission, the RC coupling circuit must have a long time constant. The cutoff frequency must be less than 30 Hz in order to be transparent to the lower frequencies of the video signal. The absence of good response at low frequencies can cause tilt, which is the deviation from straightness when a constant level signal is applied. These deviations are also called field-time waveform distortion and can be measured using the field bar test signal. In fiber optics systems, the clamper should correct for any field time tilt, assuming that the system frequency response is flat and without phase distortions around 60 Hz.

1.2 AM-VSB TRANSMISSION

Presently in broadcast television and CATV, the video signals are distributed using the analog modulation of a RF carrier. The modulated carrier is passed through a vestigial sideband filter before transmission, thus limiting the video channel bandwidth to 6 MHz, which includes the FM sound carrier. This type of transmission is also known as transmission on a modulated carrier.

Many video channels can be multiplexed using frequency division multiplexing (FDM). The carrier frequencies usually used are the ones corresponding to channels from T7 to W of the VHF spectrum. In these systems, the intermodulation and crossmodulation due to the system nonlinearity can cause picture impairments and limit the system capability.

Harmonically Related Carrier Systems

HRC systems are a special class of AM-VSB FDM systems in which the picture carriers are all harmonics of a primary frequency, e.g., 6 MHz. This has the advantage that all intermodulation beats fall precisely on carrier frequencies and the resulting zero beat is not visible in the picture. Thus the BP-23 requirement for intermodulation in HRC systems can be relaxed from -56 dB to about -40 dB below the picture carrier level. This, in turn, reduces the linearity requirements imposed on the transmission system. However, HRC operation does not affect the system crossmodulation performance requirement.

2. SYSTEM PERFORMANCE ANALYSIS OF BASEBAND AND AM-VSB TRANSMISSION SYSTEMS

In this section mathematical expressions are derived to permit the evaluation of the maximum system length given the transmission objectives and the hardware characteristics.

2.1 REPEATER SPACING

A N-repeater fiber optic transmission line is schematically represented in Figure 2.1. The maximum system length can be determined by evaluating the repeater spacing first and then multiplying the repeater spacing by the number of repeaters. The repeater spacing equals

$$REPS = \frac{10\log\left(\frac{P_{max}}{P_{min}}\right)}{\alpha} \qquad (2.1)$$

where

P_{max} = optical power coupled into the fiber

P_{min} = optical power received at each repeater detector

α = fiber attenuation including the connector and splice losses in dB/km.

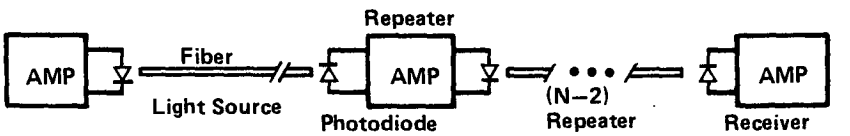

Figure 2.1: N–Repeater Fiber Optic Transmission Line

P_{max} and P_{min} are evaluated with consideration to the end-to-end transmission objectives. The power coupled in the fiber, P_{max}, is limited by the source quantum efficiency and the source-to-fiber coupling efficiency. For a given optical modulation index, the minimum power that must be received at each repeater detector, P_{min}, depends on the signal-to-noise ratio that must be achieved at the end of the transmission line. P_{min} is thus limited by the total noise in the system. However, for the chosen optical modulation index, linearity requirements should be met. If not, the modulation index should be reduced accordingly.

2.2 MAXIMUM OPTICAL POWER COUPLED INTO THE FIBER

Surface emitting LED's and double-heterostructure injection laser sources are the two types of sources considered in this study. Edge-emitting LED's are not considered because their CW output characteristic is not sufficiently linear.[3]

The coupling efficiency is a function of many characteristics of the source and the fiber. To consider them all would be time consuming without guaranteeing better results. The lambertian source approximation for the surface-emitting LED is found to give values that correspond with the experimental results.[4] For a LED with the emitting area smaller than the fiber core, the power coupled into the fiber can

be evaluated from

$$P_{max} = \pi F (NA)^2 IR_x \cdot \frac{I_{max}}{x} \qquad (2.2)$$

where

F = fiber type factor

- step index fiber F = 1.0

- graded index fiber F = 0.5

NA = numerical aperture of the fiber

IR_x = radiant intensity on axis at a reference driving current x

I_{max} = maximum current compatible with a long life CW operation

Injection Laser Sources

The coupling efficiency of injection lasers can be improved using melted lenses, tapered fiber, and fiber lenses. High coupling efficiencies have been reported for these techniques.[5,6,7] Coupling efficiencies of 60 percent for step index fibers and 40 percent for graded index fibers are assumed to be typical of what can be achieved now without putting stringent tolerances on the alignment of the fiber and the laser source.

The power coupled into the fiber equals

$$P_{max} = K_e \frac{dP}{dI} I_{max} \qquad (2.3)$$

where

K_e = coupling efficiency

- step index K = 60 percent

- graded index K = 40 percent

$\frac{dP}{dI}$ = external quantum efficiency

I_{max} = maximum driving current above threshold compatible with long CW operation

2.3 SIGNAL-TO-NOISE RATIO (SNR) CONSIDERATIONS

In this section, the mean optical power required for each detector (P_{min}) is determined. For every transmitted video channel, the signal must meet a given SNR requirement. This imposes a limitation on the minimum optical power received. SNR expressions for different types of transmission are derived first; then the minimum power is deduced from these expressions.

2.3.1 Signal

The only detectors considered in this study are photodiodes. These devices convert the received optical power into electrical current. The signal can be related to the received optical power

$$I_{signal} = \frac{P\eta eG}{h\nu} \qquad (2.4)$$

where

P = optical signal power upon the detector

η = photodiode quantum efficiency

e = electron charge

$h\nu$ = photon energy

G = internal gain of the photodiode

The electrical signal power is proportional to the square of the signal current (I^2signal).

2.3.2 Noise

There are different noise sources associated with detection: thermal, quantum, dark current, leakage current, background radiation, and beat noise due to an incoherent source.[8] The noise due to background radiation can be neglected since guided optical transmission is used and the noise source can be eliminated by minimal care in the receiver design. The expressions for the other types of noise are

$$\langle i_T^2 \rangle = 4kTb\frac{F_t}{R_{eq}} = N_T \text{ (thermal)} \quad (2.5)$$

$$\langle i_Q^2 \rangle = 2e\frac{e}{h\nu}\eta G^2 F_D b P_{avg} = N_Q \text{ (quantum)} \quad (2.6)$$

$$\langle i_D^2 \rangle = 2eI_D G^2 F_D b = N_D \text{ (dark current)} \quad (2.7)$$

$$\langle i_L^2 \rangle = 2eI_L b = N_L \text{ (leakage current)} \quad (2.8)$$

$$\langle i_B^2 \rangle = 2\left(\frac{e}{h\nu} G\eta P_{avg}\right)^2 \frac{b}{JW}\left(1 - \frac{1}{2}\frac{b}{W}\right) = N_B \text{ (beat noise)} \quad (2.9)$$

where

k = Boltzmann's constant

T = absolute temperature

b = electrical bandwidth

F_t = amplifier noise figure

R_{eq} = equivalent load resistance

e = electron charge

$h\nu$ = photon energy

G = photodiode avalanche gain

F_D = excess noise factor associated with the avalanche process

P_{avg} = average power incident on the detector

I_D = dark current of the photodiode

I_L = leakage current of the photodiode

J = number of spatial modes of the source viewed by the receiver

W = spectral width of the source in cycles per second

For applications of interest the beat noise is negligible. The spectral width (W) of a typical LED is about equal to 2×10^{13} Hz. The number of modes (J) transmitted in a graded index fiber with a 45 micron core radius and a NA of 0.2 is about 1000. Consequently, the beat noise equals 2.5×10^{-17} G^2 $P_{avg}{}^2$ Watts/Hz, which is about 20 dB below the quantum noise for a P_{avg} equal to 100 microwatts.

The leakage current of a state-of-the-art PIN photodiode can be less than 1 nA. Thus, the leakage current noise is 17 dB below the quantum noise level at an incident average power as low as 0.1 microwatt. One tenth of a microwatt is a low signal level when video transmission at a SNR of more than 40 dB is considered.

Furthermore, the dark current of an avalanche photodiode can be as low as 0.05 nA[9] which results in a dark current noise that is 30 dB below the quantum noise for 0.1 microwatt average incident power. This demonstrates that beat noise, dark and leakage current noise are negligible compared to the quantum noise in video transmission for incident powers ranging from 0.1 to 100 microwatts.

The total rms noise associated with the detection is equal to

$$\langle i^2_{TOTAL} \rangle = \langle i^2_T \rangle + \langle i^2_Q \rangle + \langle i^2_D \rangle + \langle i^2_L \rangle + \langle i^2_B \rangle \qquad (2.10)$$

which can be approximated by

$$\langle i^2_{TOTAL} \rangle \cong \langle i^2_T \rangle + \langle i^2_Q \rangle \qquad (2.11)$$

The generation of light inside the source is also a noisy process. It was found that under some conditions the light received by a detector introduced more noise than the expected pure shot (quantum) noise. This supplementary noise has been characterized by an excess noise factor (F_s), which is defined as the ratio of the actual noise over the pure shot noise corresponding to the incident optical power. The expression for the quantum noise (2.6) can be modified to reflect the influence of the source noise

$$\langle i^2_Q \rangle = 2e \frac{e}{h\nu} \eta G^2 F_s F_D b P_{avg} \qquad (2.12)$$

It has been found that at frequencies above 5 kHz the LED is almost an ideal light source $F_s \simeq 1$.[10] At lower frequencies the noise shows a 1/f dependency with the frequency. This low frequency noise can be removed using optoelectronic feedback techniques.[11]

Thus, for most practical purposes, the LED can be considered an ideal light source, $F_s \approx 1$.

The excess noise produced by injection laser sources depends on the driving current. For driving currents 10 percent above threshold, amplitude-stabilized lasers show no significant excess noise.[12] At low frequencies, lasers also show a 1/f noise, which can be eliminated by the use of optoelectronic feedback techniques.[13]

2.3.3 Transmission on a Modulated Carrier

The current coming from the modulator is

$$i(t) = A\left(1 + m_c f(t)\right) \cos \omega_c t \qquad (2.13)$$

where

$|f(t)| \leq 1$ = baseband video signal

m_c = RF modulation index (North American standard)

$m_c = 0.778$

ω_c = carrier angular frequency

Bipolar signals cannot be transmitted directly on fiber optic transmission lines. A bias current must be added to the RF signal of equation 2.13. The source driving current becomes

$$i_s(t) = i_{DC}\left(1 + m_{Ic}\, y(t)\right) \qquad (2.14)$$

where

i_{dc} = bias current

m_{I_c} = optical modulation index

$$m_{Ic} = \frac{i_{Smax} - i_{DC}}{i_{DC}} \qquad (2.15)$$

y(t) = normalized RF video current ($|y(t)| \leq 1$)

$$y(t) = \frac{i(t)}{A(1+m_c)} \qquad (2.16)$$

This driving current is schematically represented in Figure 2.2.

At the receiver end, the optical signal must be converted back into a bipolar RF electrical signal. The ac coupling between the photodiode and the amplifier subtracts the bias current. Thus the signal current at the amplifier end equals

$$i_{signal} = P_{DC}\, m_{Ic}\, \frac{(1+m_c f(t))}{1+m_c} \cos\omega_c t \left(\frac{\eta e G}{h\nu}\right) \qquad (2.17)$$

The NCTA signal-to-noise ratio which is equivalent to the BP-23 SNR definition applies to this video signal. It is defined as the ratio of the rms power of the RF signal during the synch pulse over the rms noise power in a 4-MHz wide RF channel.

Since negative video transmission is used, f(t) = +1 during the synchronization pulse. Also, the expression for the transmission of one video channel over a N-repeater line becomes

$$SNR_{NCTA} = \frac{\left(\frac{\eta e G}{h\nu}\right)^2 \frac{m_{Ic}^2 P_{DC}^2}{2}}{N(N_T + N_Q + N_D + N_L + N_B)} \qquad (2.18)$$

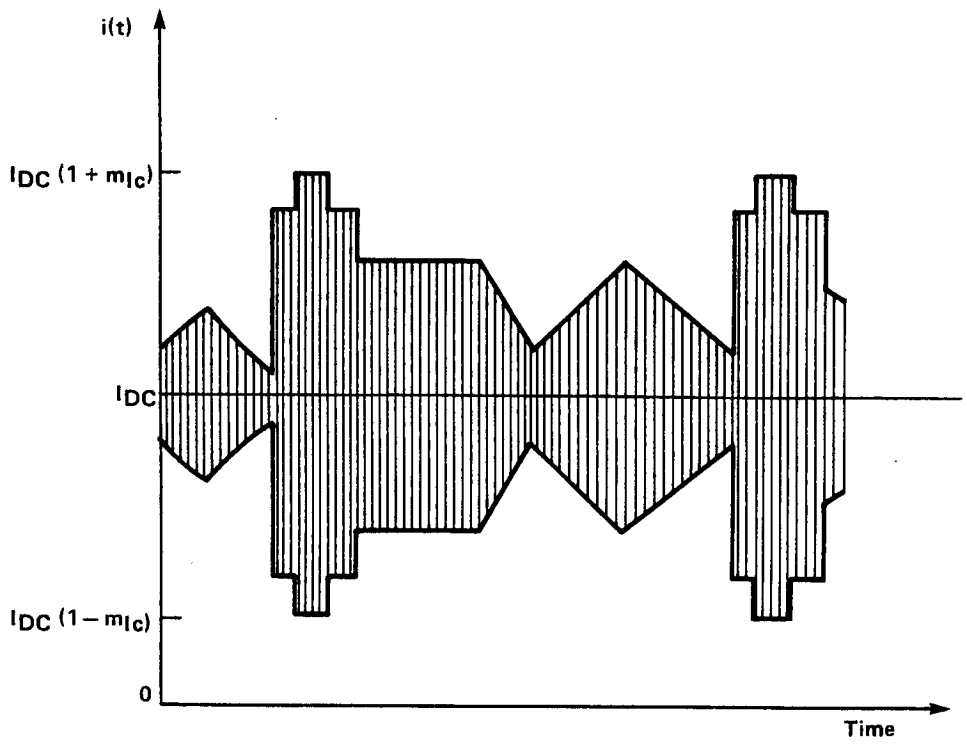

Figure 2.2: Source Driving Current Modulated Carrier

2.3.4 Baseband Video Transmission

DC Transmission

The baseband video signal is also bipolar. Hence, a bias current must be added to it before it drives the light source. For a baseband video signal transmitted with its dc component, the driving current is

$$i(t) = i_{DC}\left(1 + m_{Ib} f(t)\right) \qquad (2.19)$$

where

i_{dc} = bias current

m_{Ib} = optical modulation index

$f(t)$ = baseband video signal

$$|f(t)| \leq 1$$

The optical power received at the detector is illustrated in Figure 2.3

The BTL unweighted SNR definition is used for baseband transmission because the NCTA definition does not apply. The BTL SNR is defined as the ratio of the difference in voltage (current)

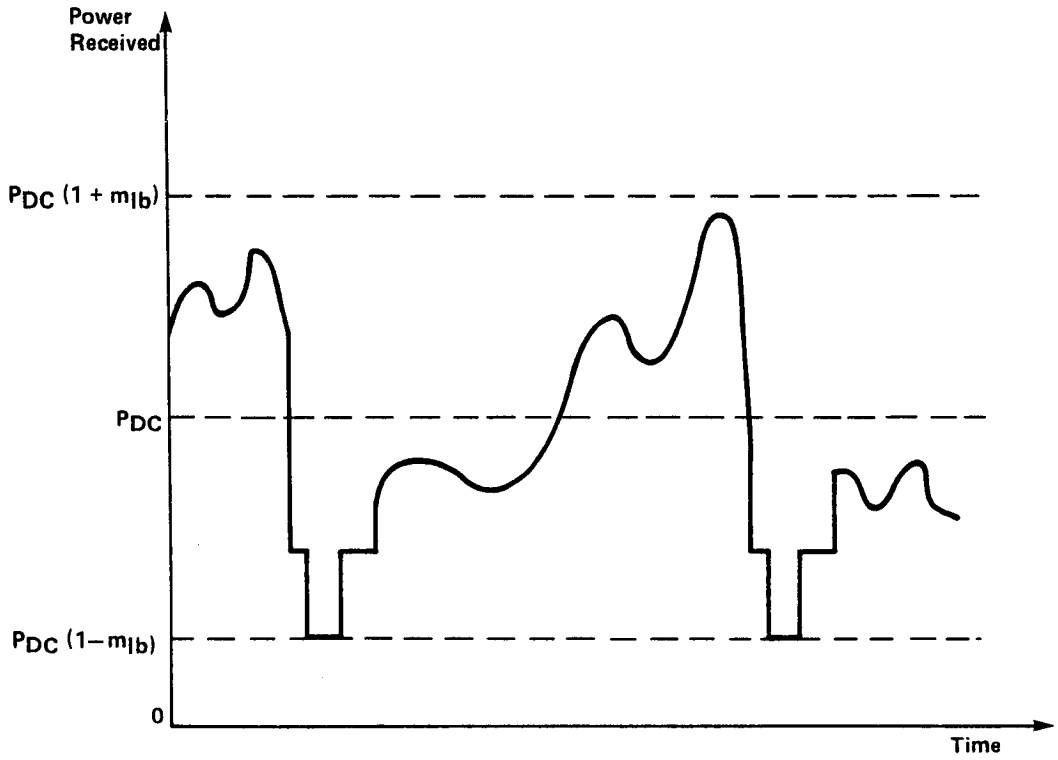

Figure 2.3: Received Optical Power DC BAseband Transmission

between the reference white level and the synch tip level over the rms noise voltage (current).

In positive transmission, the reference white level corresponds to f(t) = 1 and the synch tip to f(t) = -1. Thus the current difference equals

$$\Delta i = 2 m_{Ib} P_{DC} \left(\frac{\eta e G}{h\nu}\right) \qquad (2.20)$$

The rms current noise depends on the average optical power received on the detector. If the average is taken over the duration of one line scan and the picture line is completely white, the average optical power equals

$$P_{avg} = P_{DC}\left(1 + m_{Ib}\right) \qquad (2.21)$$

This corresponds to the worst case situation for the noise in a baseband system. Taking this value for the average power, the SNR expression for the transmission of one baseband video channel over an N-repeater line becomes

$$SNR_{BTL} = \frac{\left(\frac{\eta e G}{h\nu}\right)^2 \left(2 m_{Ib} P_{DC}\right)^2}{N\left(N_T + N_Q + N_D + N_L + N_{IB}\right)} \qquad (2.22)$$

SNR requirements are usually given in terms of the NCTA signal-to-noise ratio definition (e.g., BP-23). However, an equivalence between both signal-to-noise ratio definitions exists.[14] For signals giving the same pricture quality

$$SNR_{NCTA} = SNR_{BTL} + 4.0\,dB \qquad (2.23)$$

Thus the baseband transmission of a video channel achieving a BTL SNR of 36 dB is equivalent in quality to the transmission of one video channel on modulated carrier that achieves a NCTA SNR of 40 dB.

AC Transmission

A baseband video signal transmitted without its dc component requires a wider dynamic range because of the dc wandering and the damped oscillations. The required dynamic range equals 2.24 (i.e. 1.4 x 1.6) of the peak-to-peak video signal. The preceding SNR expression can be modified accordingly.

$$SNR_{BTL} = \frac{\left(\frac{\eta e G}{h\nu}\right)^2 \left(\frac{m_I}{1.12} P_{DC}\right)^2}{N(N_T + N_Q + N_D + N_L + N_B)} \qquad (2.24)$$

where m_I is the modulation index.

2.3.5 Multichannel Transmission

Standard FDM System

The expression "standard FDM system" means a non-HRC system with no transmission at baseband. For systems carrying many channels (more than ten), the channels can be assumed to add on a power basis. Since the carriers are at different frequencies, their phases are random and the video signals different. The probability that the synch pulses of all the video channels occur at the same time and all the carriers are in phase is negligible. However, this may not be true for a low number of channels because the averaging effect is lost. Thus it will be safer to assume that the video channels add on a voltage basis.

For a K-video channel system, the global optical modulation index (m_I) becomes

$$m_I = K\, m_{I_c} \qquad (2.25)$$

where m_{I_c} is the optical modulation index of an individual video channel. This equation relates the individual optical modulation index to the global modulation index. Thus, the NCTA signal-to-noise ratio expression (2.18) can be used by substituting m_{I_c} with m_I/K in the equation.

Mixed Mode Transmission

The expression "mixed mode transmission" means the transmission of one baseband video channel in addition to others on modulated carriers. Equation 2.23 equates BTL and NCTA SNR definitions. For dc baseband transmission and for the same picture quality, it follows that

$$\frac{4 m_{I_b}^2 P_{DC}^2}{noise} \times 10^{0.4} = \frac{\frac{m_{I_C}^2}{2} P_{DC}^2}{noise} \qquad (2.26)$$

and

$$m_{I_b} = 0.223\ m_{I_c} \qquad (2.27)$$

Thus, for K-modulated carriers and a baseband channel with the dc component transmitted, the global modulation index becomes

$$m_I = (K + 0.223)\ m_{I_c} \qquad (2.28)$$

The average power, assuming a worst case situation for the noise, is

$$P_{avg} = \left(1 + \frac{0.223}{K+0.223}\right) \cdot P_{DC} \qquad (2.29)$$

and replacing M_{I_c} and P_{avg} with their corresponding values, the NCTA SNR expression (2.18) can be used for the mixed-mode transmission case.

Similarly, for the ac transmission of one baseband video channel with others on modulated carriers, the global modulation index equals

$$m_I = (0.5 + K)\, m_{Ic} \qquad (2.30)$$

and the average optical power

$$P_{avg} = \left(1 + \frac{0.5}{K+0.5}\right) P_{Dc} \qquad (2.31)$$

HRC Systems

In a HRC system, since the carrier frequencies are harmonics derived from the same primary frequency, the carriers should add regularly in phase and the resulting peak signal should be K m_{Ic}. However, it is possible to reduce this peak signal by varying the relative phase of the carriers. It has been found that channels add following a 14 log law.[15] Thus, for a K channel system, the global modulation index equals

$$m_I = K^{0.7} m_{Ic} \qquad (2.32)$$

2.3.6 Minimum Optical power Upon the Detector

From the SNR expressions, the minimum dc optical power required at the detector to meet a given SNR objective (NCTA definition) is

$$P_{min} = \frac{1}{2}\left[B + \sqrt{B^2 + 4C}\right] \qquad (2.33)$$

where

$$B = \frac{SNR \cdot N'_Q \, N}{AZ - SNR \cdot N'_B N} \qquad (2.34)$$

$$C = \frac{SNR \cdot N\left(N_T + N_D + N_L\right)}{AZ - SNR \cdot N'_B \, N} \qquad (2.35)$$

$$N'_Q = 2e\frac{e}{h\nu}\,\eta\, G^2 F_s F_D\, b\, F_{avg} \qquad (2.36)$$

$$A = \left(\frac{\eta e G}{h\nu}\right)^2 \qquad)$$

$$N'_B = 2\left(\frac{eG}{h\nu}\,\eta\right)^2 \frac{b}{JW}\left(1 - \frac{1}{2}\frac{b}{W}\right) \qquad (2.38)$$

and

F_{avg} = average power factor

- for baseband transmission

$$F_{avg} = 1 + m_I \qquad (2.39)$$

- for modulated carriers transmission

$$F_{avg} = 1 \qquad (2.40)$$

- for mixed mode dc baseband transmission

$$F_{avg} = 1 + \frac{0.223\, m_I}{K + 0.223} \qquad (2.41)$$

- for mixed mode ac baseband transmission

$$F_{avg} = 1 + \frac{0.5\, m_I}{K + 0.5} \qquad (2.42)$$

z = video signal factor

- for baseband dc transmission

$$z = 4m_I^2 \times 10^{0.4} \qquad (2.43)$$

- for baseband ac transmission

$$z = \frac{m_I^2 \times 10^{0.4}}{1.254} \qquad (2.44)$$

- for modulated carrier transmission

$$z = \frac{m_I^2}{2K^2} \qquad (2.45)$$

- for mixed mode dc baseband transmission

$$z = \frac{1}{2}\left(\frac{m_I}{K+0.223}\right)^2 \qquad (2.46)$$

- for mixed mode ac baseband transmission

$$z = \frac{1}{2}\left(\frac{m_I}{K+0.5}\right)^2 \qquad (2.47)$$

2.3.7 Optimum Avalanche Gain

An excess noise factor (F_D) is associated with the avalanche multiplication process in an avalanche photodiode. This excess noise factor varies as a function of the gain. The following expression is found to closely approximate experimental results when the photocurrent before multiplication consists solely of electrons

$$F_D = kG + \left(2 - \frac{1}{G}\right)(1-k) \qquad (2.48)$$

where k is an ionization factor characteristic of the APD.[16]

An expression for the avalanche gain that maximizes the signal-to-noise ratio for a given incident power has been found,[17] as follows

$$G_{opt} = \left[q/2 + \left\{(q/2)^2 + (p/3)^3\right\}^{1/2}\right]^{1/3} + \left[q/2 - \left\{(q/2)^2 + (p/3)^3\right\}^{1/2}\right]^{1/3}$$

where

$$p = (1 - k)/k$$

$$q = 2\ v/yk$$

$$v = N\ (N_Q + N_D)/G^2\ F_D$$

$$y = N\ (N_T + N_L)$$

However, in video transmission, the signal-to-noise ratio is usually a fixed requirement, and the maximization of the repeater spacing is, rather, the design objective. The repeater spacing can be maximized by minimizing the power required at the detector. Considering only the quantum and thermal noises in equation 2.33 and deriving P_{min} with respect to G, the condition which G must satisfy to minimize the required incident power is

$$\frac{2 N_T A' Z}{SNR \cdot NQ'^2} = \left[\frac{3}{2}k^2\right]G^4 + \left[2k(1-k)\right]G^3 + \left[k(1-k)\right]G^2 + \left[2(1-k)^2\right]G - \left[\frac{1}{2}(1-k)^2\right] \qquad (2.49)$$

where

$$A' = \frac{e\eta}{h\nu}$$

$$Q' = 2e \cdot \frac{e\eta}{h\nu} \, b \, F_s \, F_{avg}$$

The above equation can be solved iteratively by gradually increasing G until the right value is found. The equation has only one real solution that is greater than or equal to one, since all the coefficients of the G terms are positive. Thus, the optimum avalanche gain can first be found and then be used for the evaluation of the minimum power required at the detector.

2.4 NONLINEAR DISTORTIONS

Intermodulation, crossmodulation differential gain and phase are the main nonlinear distortions encountered in video transmission. In a fiber optic transmission line, the light source is the dominant cause of nonlinearity. Since present CATV amplifiers have sufficient linearity to transmit more than 30 channels, it is assumed that the nonlinearity of the system electronic circuitry is negligible compared to the source nonlinearity. The nonlinearity of photodiodes has been measured, and their contribution is also negligible.[18]

The source ac output is approximated by the following transfer function of a memoryless system

$$p(t) = a_1 i(t) + a_2 i(t)^2 + a_3 i(t)^3 \qquad (2.50)$$

where p(t) is the ac optical power output as a function of time, i(t) is the signal portion of the driving current, and a_1, a_2, a_3 are expansion coefficients which depend on the source and on its bias current.

This model is valid for surface-emitting LED's when the frequencies involved are within the device bandwidth.[19] Furthermore, preliminary measurements on lasers indicate that they would behave similarly to LED's.[20]

The source output could also be represented by a Volterra series. However, the use of Volterra series would require a thorough evaluation of the source characteristics. This refinement would be

appropriate if experimental results deviate objectionably from the values predicted by the present model.

2.4.1 Intermodulation

Intermodulation is a form of interference involving the generation of interfering beats between two or more carriers. Harmonic distortion is a special form of intermodulation involving a single carrier frequency.[21] In this report, intermodulation is used in its wider sense to include harmonic distortion.

In a CATV system, the picture carriers largely dominate the other carriers present in the video signal. The sound carrier and the color subcarrier are typically more than 15 dB down. Thus the intermodulation caused by the sound and color carriers can be neglected. The picture carrier level depends on the dc content of the modulating signal which varies with time. The intermodulation gets worse as the picture carrier levels increase. The video signal, in a worst case situation, would consist of the synch pulses superimposed on a continuous signal at the blanking level, as illustrated in Figure 2.4. Evaluating the Fourier transform of the resulting RF signal, it is found that the picture carrier level is 2.1 dB less than the total RF power during the synch pulse.

By replacing i(t) in equation 2.50 by three sinewaves of dif - ferent frequencies, the relative power of thedifferent intermodulation beats can be found.[22] For each dB increase in the sinewave power, the

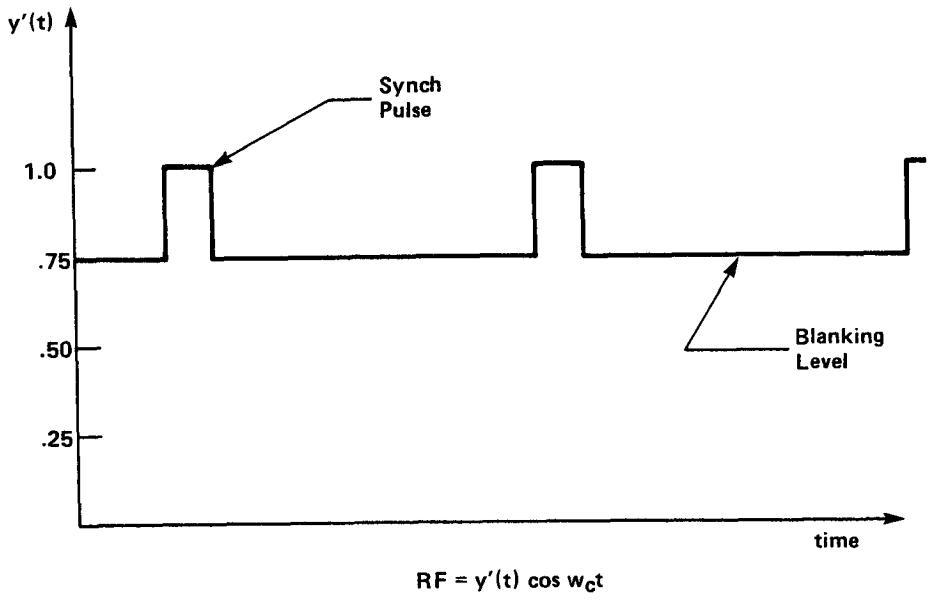

Figure 2.4: RF Signal Worst Case Situation

relative second-order distortions increase by 1 dB and the third order distortions by 2 dB. Thus the linearity of a device is uniquely defined by the second and third harmonics of a reference fundamental. Consequently, the power of the different intermodulation beats, relative to the picture carrier level, can be expressed by

$$IM_{2\alpha} = H_{2\alpha_x} + \left[10\log\left(\frac{si}{x}\right)^2 - 2.1\,dB\right] + C\log N \qquad (2.51)$$

$$IM_{\alpha\pm\beta} = H_{2\,2\alpha_x} + \left[10\log\left(\frac{si}{x}\right)^2 - 2.1\,dB\right] + C\log N + 6\,dB \qquad (2.52)$$

$$IM_{3\alpha} = H_{3\alpha_x} + \left[20\log\left(\frac{si}{x}\right)^2 - 4.2\,dB\right] + C\log N \qquad (2.53)$$

$$IM_{2\alpha\pm\beta} = H_{3\alpha_x} + \left[20\log\left(\frac{si}{x}\right)^2 - 4.2\,dB\right] + C\log N + 9.6\,dB \qquad (2.54)$$

$$IM_{\alpha\pm\beta\pm\gamma} = H_{3\alpha_x} + \left[20\log\left(\frac{si}{x}\right)^2 - 4.2\,dB\right] + C\log N + 15.5\,dB \qquad (2.55)$$

where

$H_{2\alpha_x}$ = relative level of the second harmonic referred to a fundamental of x mA peak-to-peak

$H_{3\alpha_x}$ = relative level of the third harmonic referred to a fundamental of x mA peak-to-peak

si = peak-to-peak signal current during the synch pulse of one video channel

$$si = 2M_{IC}\,I_{DC} \qquad (2.56)$$

x = peak-to-peak current of the reference fundamental

C = factor depending on the compounding law of the beats with the number of repeaters. It can vary with the

type of beats involved

$10 \leq C \leq 20$

N = number of repeaters in tandem

The compounding law of beats with the number of repeaters depends on the relationship between the phase and the frequency in the fiber transfer function. The results of Cohen, et al., indicate that the phase-frequency relation is not linear.[23] However, the phase shift between dc and the -3 dB frequency is less than 0.1 radian for the lengths of fiber they used. This indicates that beats from one repeater to another would add on a quasi-voltage basis (C=20) for a low number of repeaters, but as the number of repeaters increases, it will deviate and approach addition on a power basis (C=10). These results apply to a single-step index fiber when illuminated with a laser source. The phase-frequency relation could be different for a graded index fiber and with significant chromatic dispersion.

In conclusion, the few experimental results available indicate a quasi-voltage addition when the number of repeaters is low. However, the subject of beats compounding definitively requires further experimental study before a reliable addition law for the intermodulation beats is derived.

2.4.2 Crossmodulation

Crossmodulation is the transfer of modulation from one or many RF carriers to another as a result of the system nonlinearity. The crossmodualtion ratio is defined as the ratio of the peak-to-peak variation, due to crossmodulation, of the test signal to its amplitude with all other carriers removed. The measurement is usually made by modulating all the RF carriers except the one under test with a 15.75-kHz frequency signal.

An analytical expression for the crossmodulation has been derived for the case where the modulating signal is a sinewave and the RF carriers are modulated synchronously.[24] However, BP-24 does not require synchronous modulation and the above expression has been modified accordingly. This gives

$$XM = H_3 \alpha_x + 20 \log \left(\frac{s_i}{x}\right)^2 + 11.3\ dB + C \log N \qquad (2.57)$$

$$+ 10 \log \left[\left\{ (k-1) + n_b \right\} \frac{16m^2}{(1+m)^4} + \left(\frac{3n_c}{4} + \frac{nd}{16} \right) \frac{16m^2 + m^6}{(1+m)^6} \right]$$

where

k = number of RF carriers

n_b = number of beats such as $f_a + f_b - f_t = f_t$

f_a and f_b are carrier frequencies and f_t is the carrier frequency under test

n_c = number of beats such as $f_a + f_b - f_c = f_t$

n_d = number of beats such as $2 f_a - f_b = f_t$

m = modulation index of the sinewave

Good engineering practice requires that the peak-to-peak modulating signal should equal at least 87.5 percent of the peak RF amplitude. Thus m should be greater or equal to 0.78.

2.4.3 Differential Gain

The differential gain in color TV is defined as the dB difference in gain for the 3.58-MHz color subcarrier when the level of the luminance signal is varied from blanking to reference white levels. The test signal consists of synchronizing pulses and a stairstep signal with a superimposed 3.58 MHz sinewave signal, the peak-to-peak amplitude of which is 20 percent of the stairstep signal amplitude between blanking and reference white. The system nonlinearity cannot introduce significant differential gain when the video signal is transmitted on a modulated carrier.[25]

For baseband transmission, when the above test signal is used, the differential gain is expressed by[26]

$$\text{diff gain} = 20\log\left[\frac{1 + 3D_{2nd} + 8.0625\,D_{3rd}}{1 - 2D_{2nd} + 2.4375\,D_{3rd}}\right] \qquad (2.58)$$

where

D_{2nd}, D_{3nd} = second and third harmonics in current relative to a fundamental sinewave having the same peak-to-peak amplitude as the baseband video signal

The relative second and third harmonics in power of the fundamental sinewave are

$$IM_{2K} = H_{2\alpha_x} + 10\log\left(\frac{2m_{Ib}\, I_{DC}}{x}\right)^2 + C\log N \qquad (2.59)$$

$$IM_{3K} = H_{3\alpha_x} + 20\log\left(\frac{2m_{Ib}\, I_{DC}}{x}\right)^2 + C\log N \qquad (2.60)$$

and the harmonics in current become

$$D_{2nd} = 10^{IM_{2\alpha}/20} \qquad (2.61)$$

$$D_{3rd} = 10^{IM_{3\alpha}/20} \qquad (2.62)$$

2.4.4 Differential Phase

The differential phase is defined as the variation in phase of the color subcarrier of a TV signal as the level of the luminance signal is varied from blanking to white. A system with the transfer function

$$e_{out} = a_1 e_i + a_2 e_i^2 + a_3 e_i^3 \qquad (2.63)$$

where the coefficinets a_1, a_2, and a_3 are not signal frequency dependent and no phase delay is introduced does not cause differential phase.

It is presumed that the differential phase is mainly caused by the feedback loop of the repeater amplifier. Thus, with careful design the repeater could be built to satisfy the transmission requirements. In fact, baseband repeaters show very little differential phase, less than 0.2 degrees.[27,28]

2.5 FIBER FREQUENCY RESPONSE

The influence of light sources and detectors on the system bandwidth is negligible because these devices can have electrical bandwidths well in excess of 100 MHz. For transmission over short distances, the fiber frequency response is usually also negligible. However, due to the length dependence of the fiber response, the fiber frequency response for transmission over long distances limits the number of video channels that can be transmitted by the fiber.

In this study, only multimode fibers are considered. The derivations in this section are mainly based on references 29 and 30, which use the WKB approximation. The modal and material dispersions are the two main contributors to the fiber total dispersion.

The amplitude term of the fiber transfer function can be approximated by a Gaussian for amplitudes greater than 0.75.[31] Thus

$$|H(f)| = e^{-(2\pi f \sigma_T)^2/2} \qquad (2.64)$$

where σ_T is the total dispersion occuring in the fiber which results from the sum of the material and modal contributions

$$\sigma_T^2 = \sigma_{material}^2 + \sigma_{modal}^2 \qquad (2.65)$$

2.5.1 Material Dispersion

Different light frequencies of the source spectrum do not travel at the same speed in the glass. This results in material dispersion

$$\sigma_{material} = \frac{\lambda \sigma_s}{c} \cdot \frac{d^2 n}{d\lambda^2} L \qquad (2.66)$$

where

n = refractive index

λ = center emission wavelength

σ_s = rms spectral half-width of the source

$\frac{d^2n}{d\lambda 2}$ = second derivative of the refractive index with respect to wavelength

L = fiber length

c = light velocity (vacuum)

The second derivative of the refractive index with respect to wavelength can be deduced from a three-term Sellmeier law, which applies to the bulk material considered.

For a pure fused silica fiber, the material dispersion is 0.106 ns/nm-km at a center wavelength of 0.8 micron[32] and 0.064 ns/nm-km at a center wavelength of 0.9 micron.[33] Many fibers are doped silica fibers. The dopant (e.g., Germania, boron) also affects the material dispersion figure and should be considered in precise evaluation of the chromatic dispersion.

For a GaAs LED laving a half-intensity spectral width of 40 nm, the corresponding rms spectral half-width is approximately 16.5 nm. A typical semiconductor laser source has a rms spectral half-width of 1 nm.

2.5.2 Modal Dispersion

Modal dispersion is due to the presence of distinct optical transmission paths in a multimode fiber. It depends on the refractive index profile over the fiber section.

Step Index Fiber

For a step index fiber, the dispersion per unit of fiber length is approximately

$$\sigma_M = 0.289 \frac{n_1 \Delta}{c} \quad (s/m) \tag{2.67}$$

where

n_1 = core refractive index

Δ = fractional index difference between core and cladding

$$\Delta = \frac{n_{core} - n_{CLADDING}}{n_{core}} \tag{2.68}$$

Graded Index Fiber

For an ideal graded index fiber (near parabolic index profile)

$$\sigma_M = .037 \frac{n_1 \Delta^2}{c} \quad (s/m)$$

and for a practical graded index fiber with a five percent error in the refractive index profile

$$\sigma_M = .00591 \frac{n_1 \Delta}{c} \quad (p/m) \qquad (2.69)$$

For graded index fibers Δ is defined as

$$\Delta = \frac{n(0) - n(a)}{n(0)} \qquad (2.70)$$

where

n(o) = refractive index at the core center

n(a) = refractive index at the core limit

Δ is also related to the numerical aperture (NA) of the fiber. For step or graded index fibers

$$\Delta = \frac{NA^2}{2n_1^2} \qquad (2.71)$$

where n_1 is the refractive index at the core center.

Mode coupling generally occurs for fiber lengths in the order of a kilometer. The mode coupling is characterized by the fiber effective length (L_{eff}), which is the fiber length required to achieve the dynamic equilibrium between the propagating modes. For distances longer than the effective length, the modal dispersion varies as the square root of the distance. The modal dispersion becomes

$$\sigma_{modal} = \sigma_m \sqrt{L_{eff} L} \qquad (2.72)$$

2.5.3 System Bandwidth

The total dispersion, σ_T, is equal to the rms sum of the material and modal dispersions (2.65).

For a one-section line, the -3 dB electrical bandwidth is related to the total dispersion

$$B_{-3dB} \simeq \frac{0.133}{\sigma_T} \qquad (2.73)$$

For an N-repeater line, the system frequency response is

$$H_T(f) = H_1(f) * H_2(f) * \ldots * H_N(f) \qquad (2.74)$$

where $H_1(f)$ is the frequency response to the repeater section, i, assuming that the repeater sections are identical and considering the amplitude term only

$$|H(f)| = e^{-\frac{N}{2}(2\pi f \sigma_T)^2} \qquad (2.75)$$

Then the system electrical bandwidth becomes

$$B_{-3dB} \simeq \frac{0.133}{\sqrt{N}\,\sigma_T} \qquad (2.76)$$

3. CALCULATIONS ON INDIVIDUAL ASPECTS OF THE SYSTEM

In this section, sensitivity analyses are made on individual aspects of the system performance. Knowledge of the influence of certain hardware characteristics or transmission methods on aspects of the performance is useful in the determination of the optimum transmission system.

3.1 OPTIMUM AVALANCHE GAIN

Internal gain in the detector is useful when the subsequent amplification of the electrical signal introduces a significant amount of noise. There is a tradeoff between the excess noise associated with the avalanche process and the reduction in relative level of the thermal noise. This tradeoff depends on the SNR requirement and on the transmission method employed. To have to meet a given SNR requirement at the end of an N-repeater line is equivalent to requiring for each individual repeater section a signal-to-noise ratio of SNR + 10 log N, assuming that the repeater sections are identical.

In Figure 3.1, the optimum avalanche gain is shown as a function of the thermal noise at room temperature of the equivalent SNR required at each repeater section for the dc transmission of one video channel. The thermal noise is indicated by the ratio of the amplifier noise figure over the detector load resistance. SNR's are given in terms of the equivalent NCTA

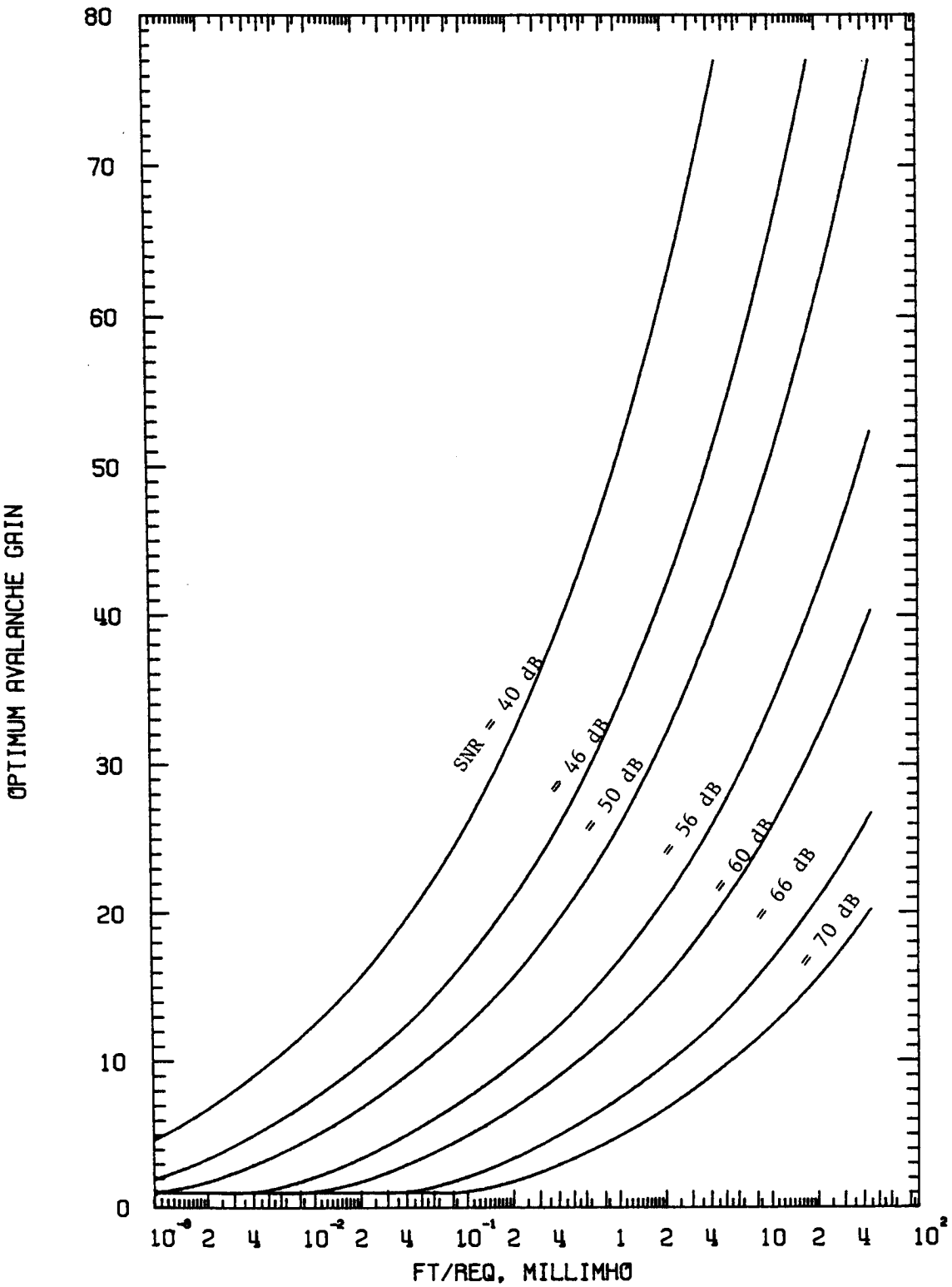

Figure 3.1 Optimum Avalanche Gain DC Baseband Transmission

signal-to-noise ratio. In Figure 3.2 the same is shown for the transmission of one video channel on a modulated carrier assuming the same optical modulation index, $m_I = 0.75$. The quantum efficiency of the photodiode is 0.85 and the excess noise factor k equals 0.03.

These figures indicate that the optimum avalanche gain decreases as the thermal noise decreases and as the required signal-to-noise ratio increases.

In Figure 3.3 the optimum avalanche gain is given for a multichannel FDM AM-VSB system as a function of the SNR and the number of video channels. The thermal noise is minimized by choosing the highest load resistance compatible with an amplifier input capacitance of 0.12 picofarad. The amplifier noise figure is set to 3 dB. The input capacitance can be reduced to that level using feedback techniques.[34,35] It is assumed that the stray capacitances are eliminated by proper packaging or by integrating the detector with the buffer amplifier.

A high impedance front end amplifier followed by an equalizer like the ones proposed for digital transmission is not considered in this report for analog video transmission because it is believed that the front end and the equalizer cannot be matched well enough to avoid signal distortions. Moreover, this approach decreases the SNR at the high frequencies which could be objectionable in color TV transmission due to the presence of the colour subcarrier at 3.58 MHz above the picture carrier frequency.

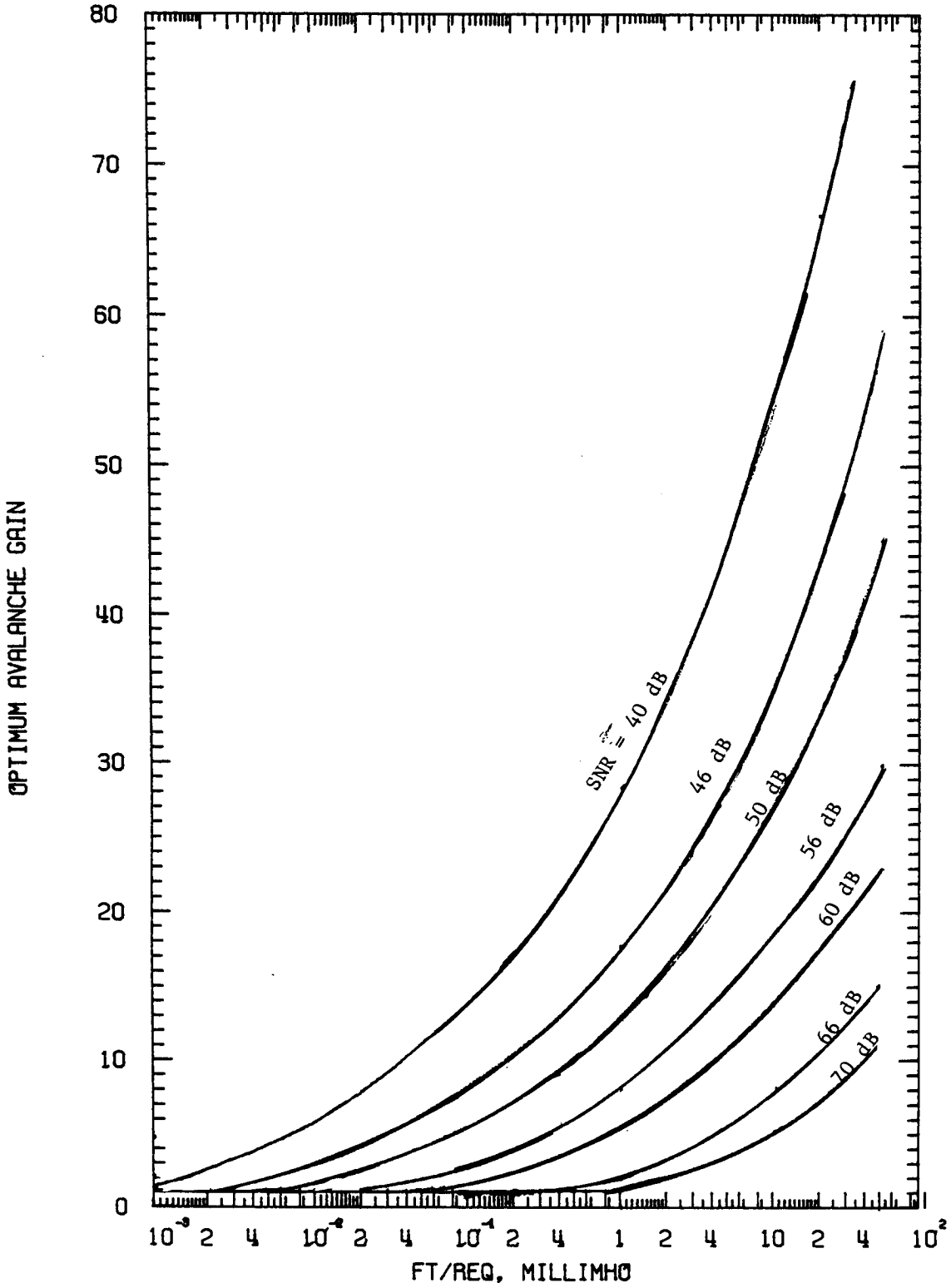

Figure 3.2 Optimum Avalanche Gain Modulated Carrier

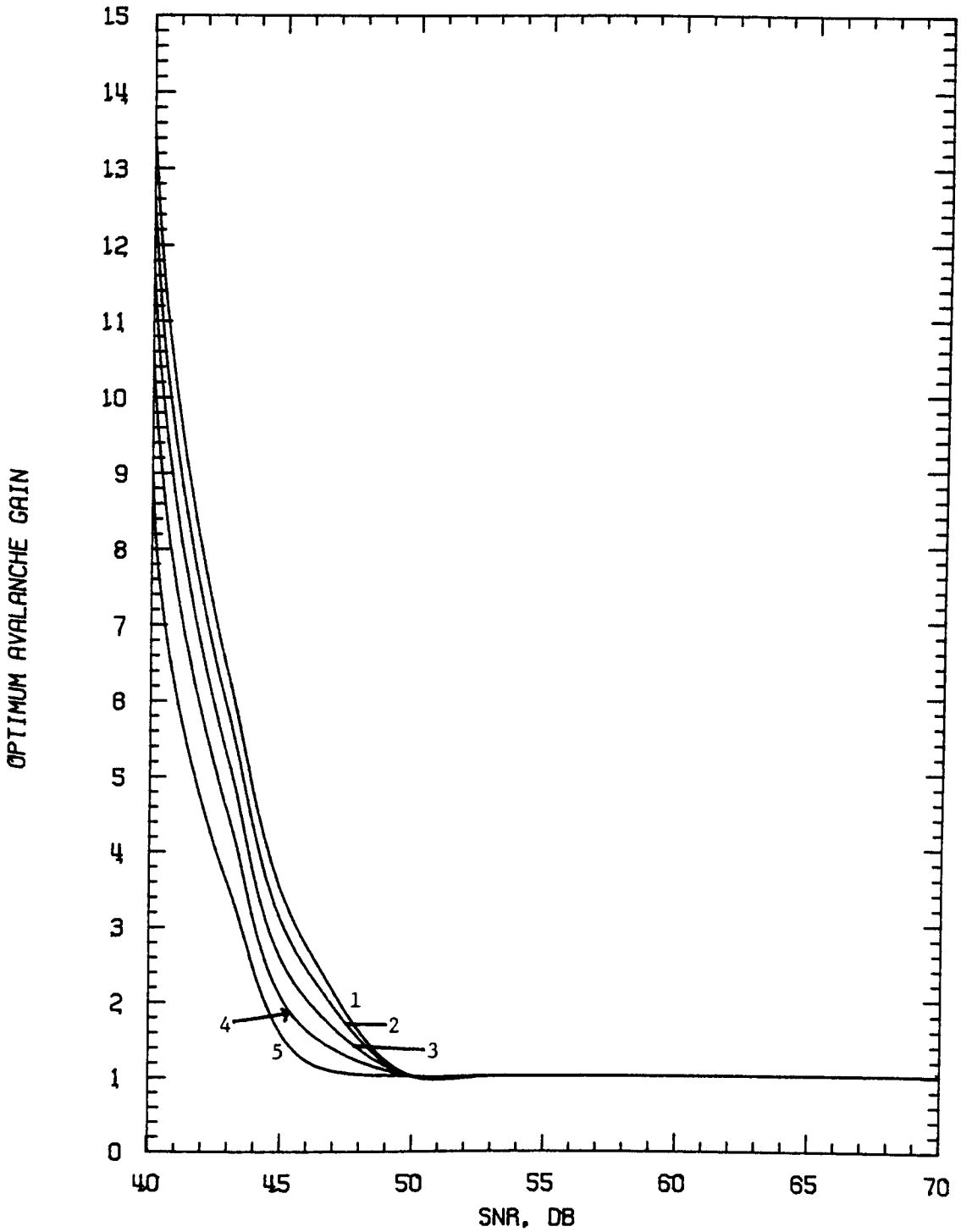

Figure 3.3 Optimum Avalanche Gain - Number of Modulated Carriers

Thus the buffer amplifier should have a flat frequency response over the total band and the maximum equivalent load resistance becomes

$$R_{eq} = \frac{1}{2\pi C_i B} \qquad (3.1)$$

where C_i is the input capacitance, and B the highest signal frequency.

For most practical purposes, a PIN photodiode is the optimum detector for a multichannel FDM system. Figure 3.4 shows the influence of the excess noise factor, k, on the value of the optimum avalanche gain for dc baseband transmission and different SNR's. The preceding calculations are based on the analysis of Section 2.3.7.

3.2 MINIMUM OPTICAL POWER

The minimum optical power required upon the detector in order to meet a given SNR requirement is evaluated as a function of the number of repeaters and the number of video channels. In Figure 3.5 the mean power required to meet a SNR of 40 dB is given both for the cases where an APD with the optimum avalanche gain is used (solid line) and where a PIN photodiode is used (dotted line). The APD and the PIN photodiode considered both have a quantum efficiency of 0.85. The excess noise factor of the APD is 0.03. The thermal noise is minimized assuming again a 0.12 pf input capacitance and the use of lower adjacent channels (e.g., T7 and T8 for the two modulated carrier cases). In Figure 3.6, the same is done for a SNR requirement of 56 dB.

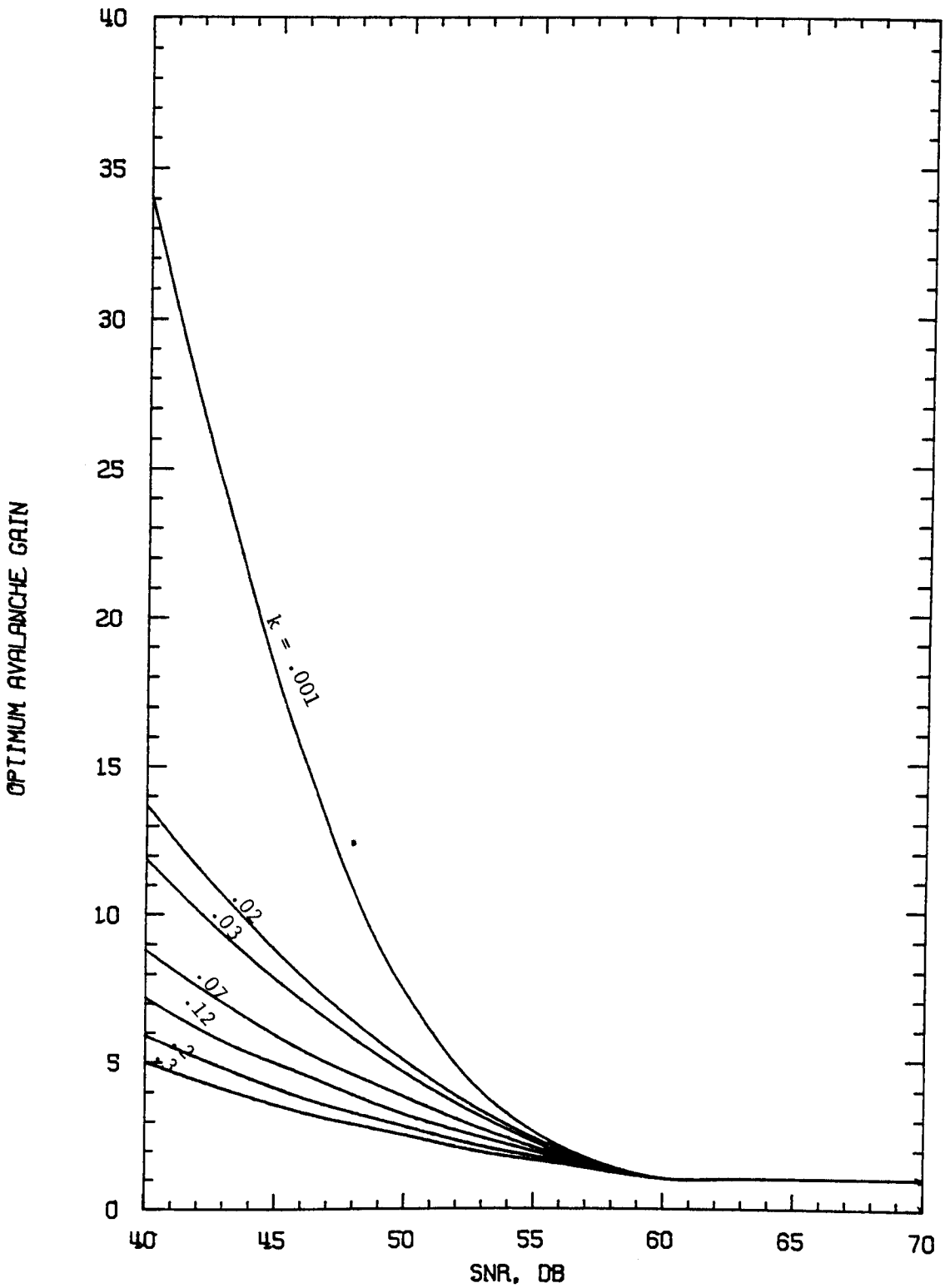

Figure 3.4 Optimum Avalanche Gain - DC Baseband Transmission

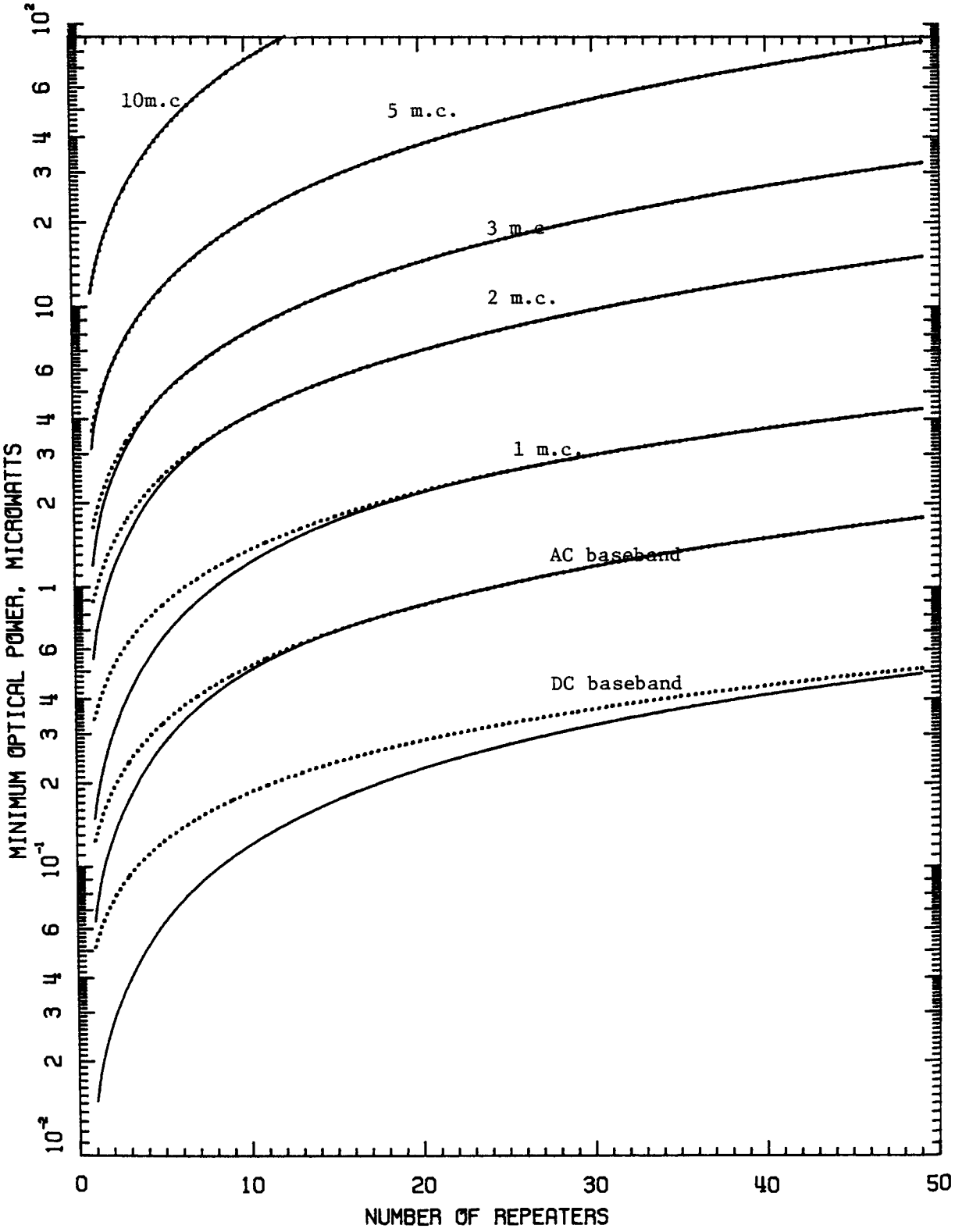

Figure 3.5 Minimum Optical Power: SNR Objective of 40 dB

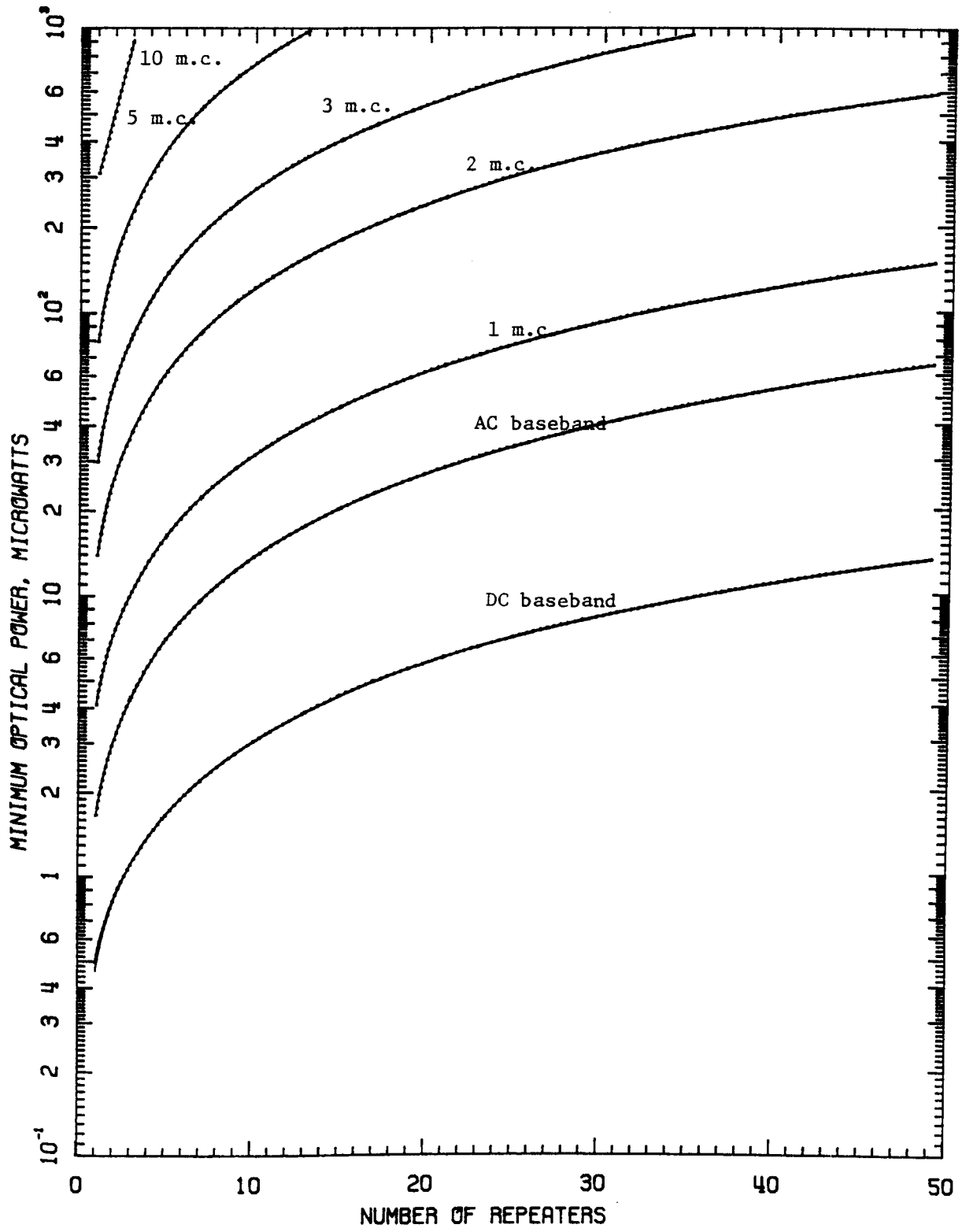

Figure 3.6 Minimum Optical Power: SNR Objective of 56 dB

It is again verified that the PIN photodiode is the optimum detector for a repeatered FDM system. For single channel transmission at 40-dB SNR and for a low number of repeaters, the use of a low gain avalanche photodiode, especially for dc baseband transmission is advantageous. A PIN photodiode is the optimum detector for transmission at a SNR of 56 dB.

In Figure 3.7, the sensitivity of the required minimum power to variations of the thermal noise level is illustrated for the transmission of a single modulated carrier meeting a 40 dB SNR objective. It is seen in Figure 3.8 that P_{min} is less sensitive to variations of the thermal noise level when a APD is used.

3.3 LINEARITY REQUIREMENTS

The linearity requirements resulting from the maximum tolerable intermodulation and crossmodulation according to BP-23 standards are evaluated for different numbers of video channels and for different carrier frequency allocation schemes. The cross-modulation required in BP-23 is -48 dB, and the curve for the intermodulation is given in Figure 3.8. The procedures for evaluating the corresponding linearity requirements are illustrated in Figures 3.9 and 3.10.

The minimum linearity required by intermodulation is expressed in terms of the second and third harmonics of a picture

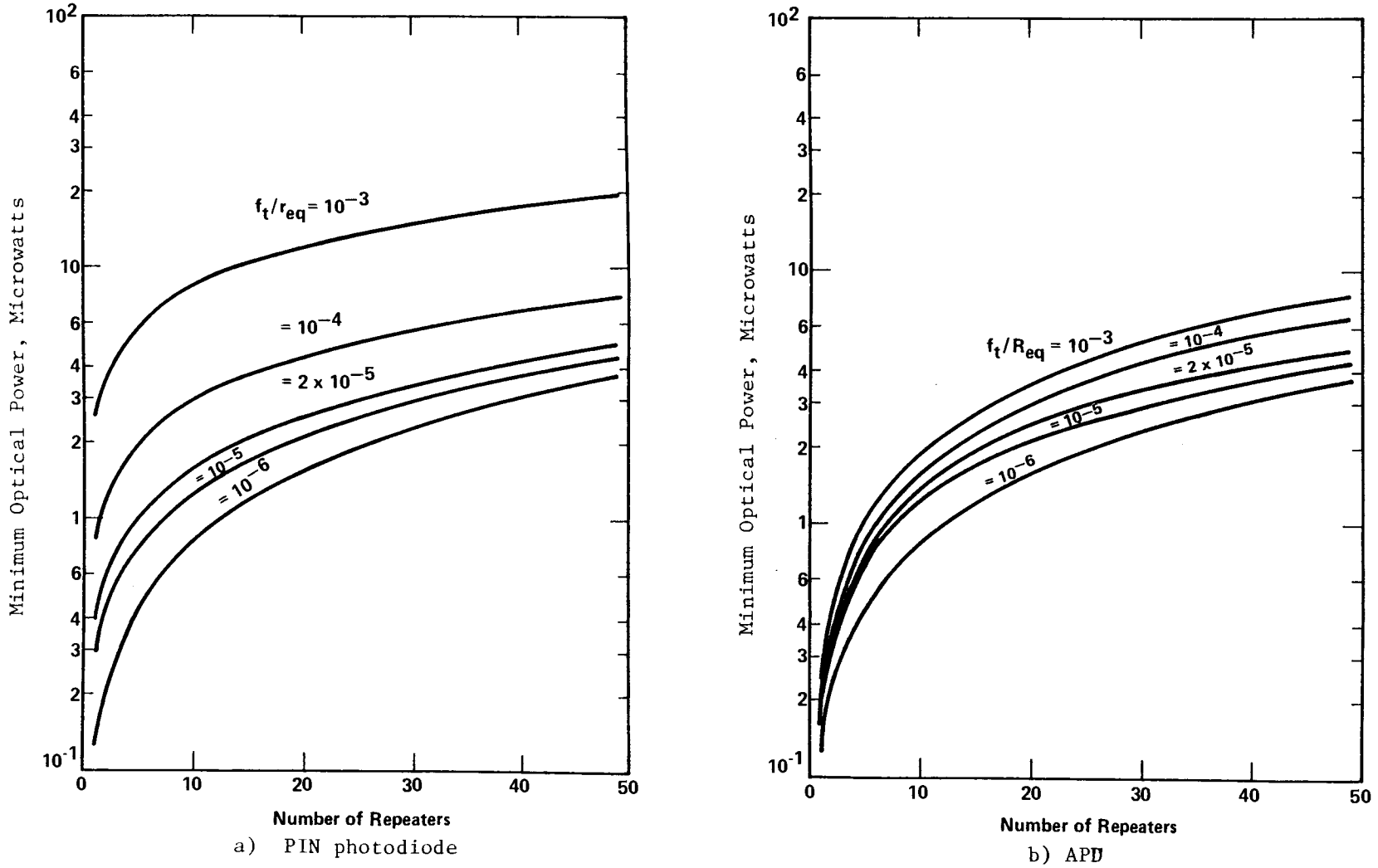

Figure 3.7 Minimum Optical Power: SNR Objective of 40 dB
One Modulated Carrier

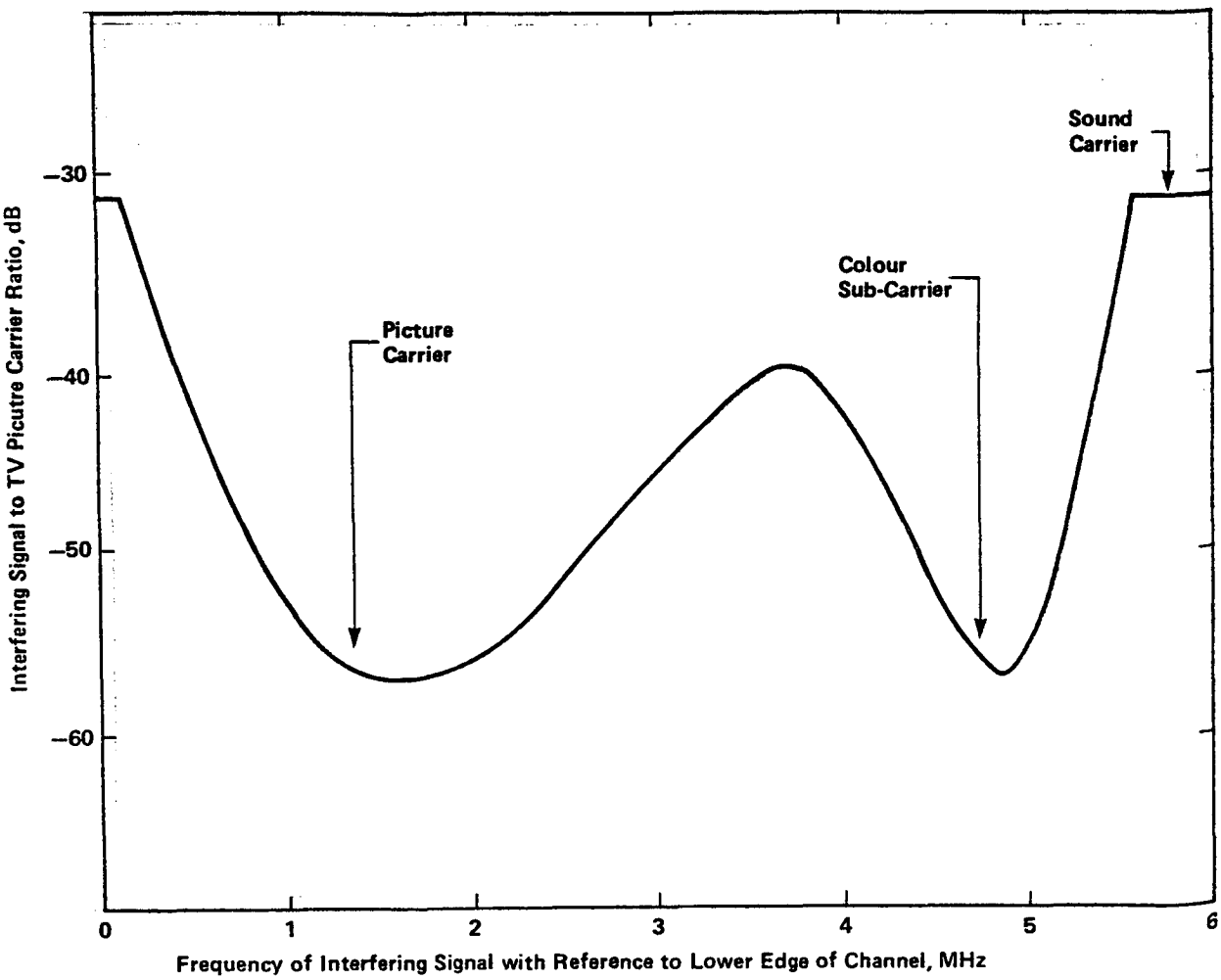

Figure 3.8 BP-23 Intermodulation Requirements

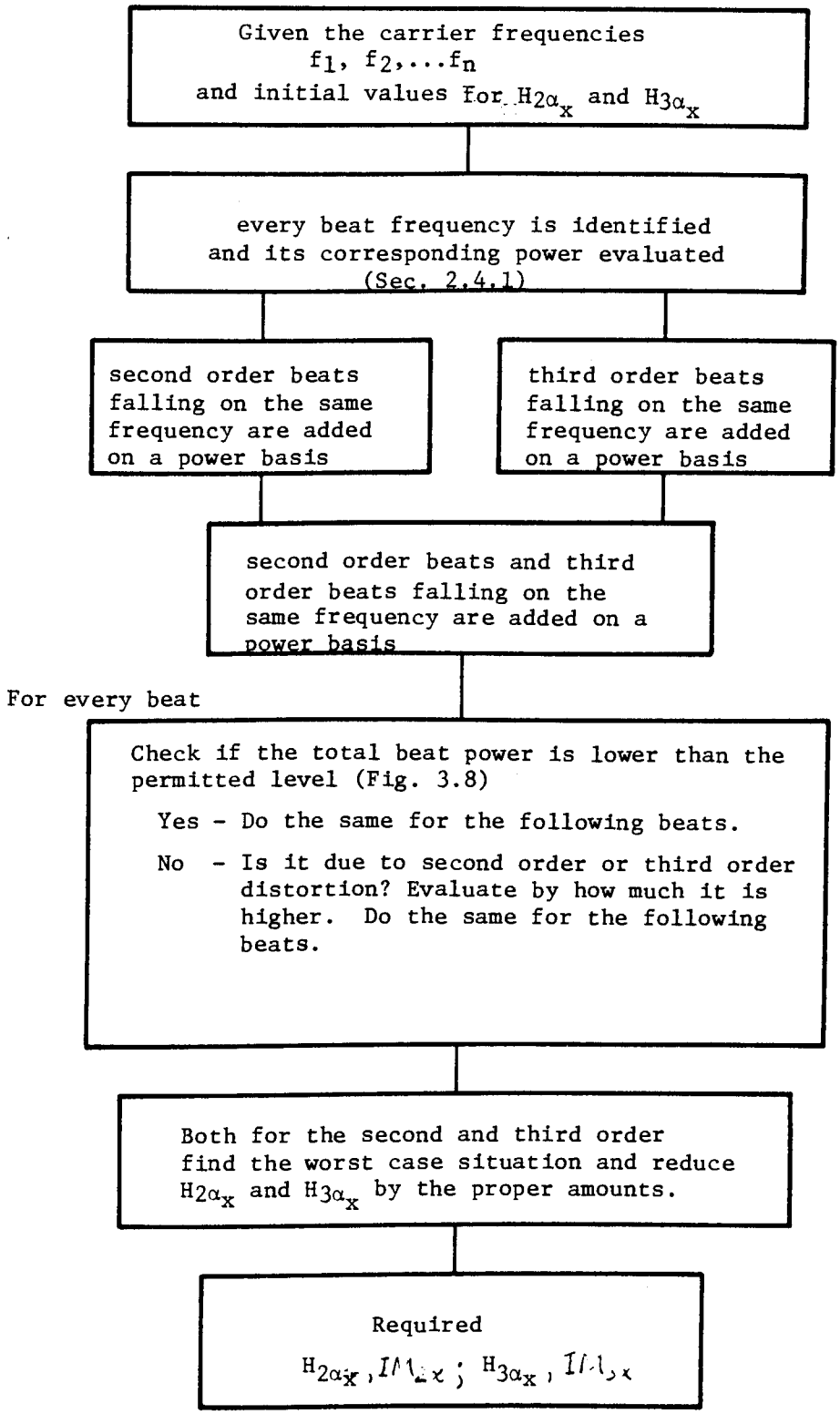

Figure 3.9 Linearity Requirements - Procedure for Intermodulation

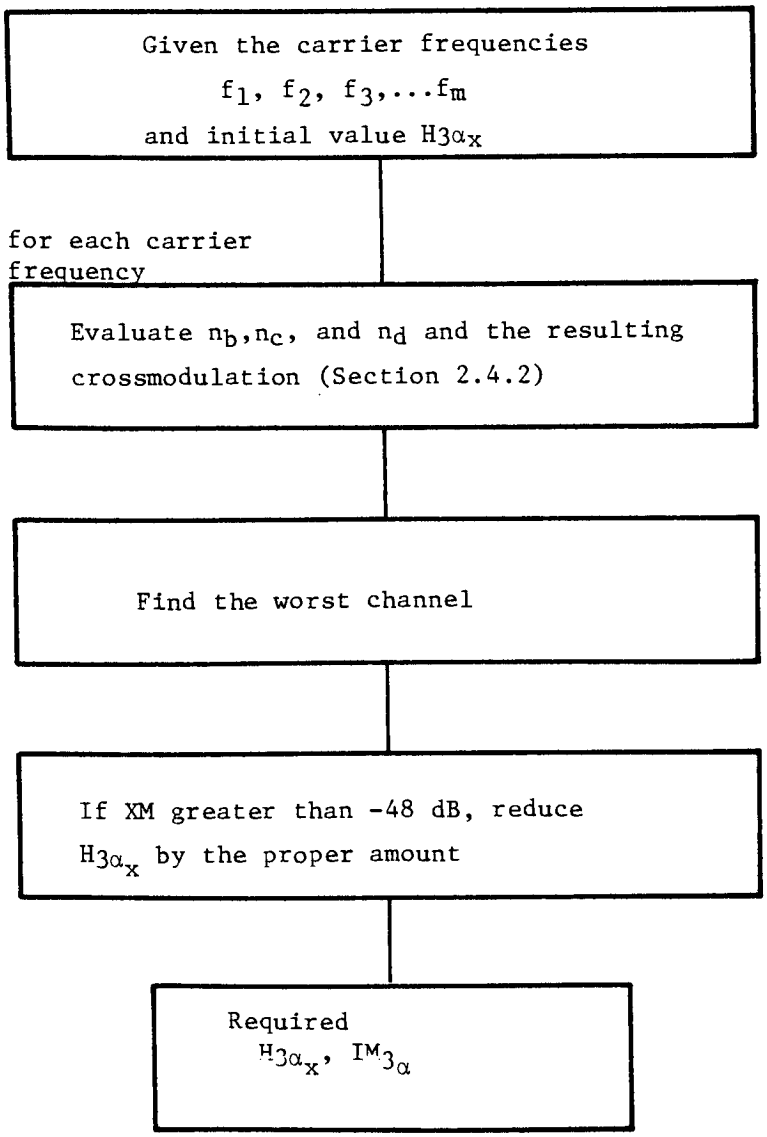

Figure 3.10 Linearity Requirements - Procedure for Crossmodulation

carrier. The crossmodulation requirement is expressed in terms of the third harmonic of a picture carrier.

The linearity of a light source is usually specified in terms of the relative power of the second and third harmonics ($H_{2\alpha_x}$, $H_{3\alpha_x}$) observed when a sinewave of x mA peak-to-peak amplitude is applied to the bias driving current of the source. If x equals the peak-to-peak amplitude of a K-channel composite current, for a FDM system

$$H2\alpha_x = IM_{2\alpha} + 20 \log K + 2.1 \text{ dB} \quad (3.2)$$

$$H3\alpha_x = IM_{3\alpha} + 40 \log K + 4.2 \text{ dB} \quad (3.3)$$

and for an HRC system whose peak-to-peak amplitude is minimized by adjusting the relative phases of the carriers

$$H2\alpha_x = IM_{2\alpha} + 14 \log K + 2.1 \text{ dB} \quad (3.4)$$

$$H3\alpha_x = IM_{3\alpha} + 28 \log K + 4.2 \text{ dB} \quad (3.5)$$

The linearity requirements for a nonrepeatered FDM system are given in Table 3.1 for systems using the K lower adjacent channels starting at T7 and for 12-channel systems which use the standard broadcast frequencies (channels 2 to 13). The carrier frequencies for these channels are listed in Table 3.2.

Table 3.1

LINEARITY REQUIREMENTS - NONREPEATERED LINE
FDM SYSTEM

K LOWER ADJACENT CHANNELS + 12 BROADCAST

NUMBER OF CHANNELS	INTERMODULATION REQUIREMENTS dB				CROSSMODULATION REQUIREMENTS dB	
	$H_{2\alpha_x}$	$H_{3\alpha_x}$	$IM_{2\alpha}$	$IM_{3\alpha}$	$H_{3\alpha_x}$	$IM_{3\alpha}$
2	-46.2	-	-54.3	-	-47.1	-59.2
3	-48.7	-49.2	-60.3	-72.5	-44.9	-63.9
4	-47.2	-47.7	-61.3	-76.0	-41.4	-65.4
5	-47.3	-46.9	-63.4	-79.0	-39.3	-67.3
6	-46.2	-45.9	-63.9	-81.3	-37.2	-68.3
7	-46.1	-45.1	-65.1	-83.1	-35.8	-69.6
8	-45.3	-44.2	-65.5	-84.5	-34.2	-70.3
9	-47.8	-42.1	-69.0	-85.0	-32.4	-70.6
10	-46.9	-40.8	-69.0	-85.0	-31.0	-71.0
12	-45.3	-38.5	-69.0	-85.9	-28.6	-71.8
15	-43.4	-36.0	-69.0	-87.2	-25.6	-72.7
12*	-	-38.0	-	-85.4	-28.5	-71.7

*Broadcast frequencies: channels 2-13.

Table 3.2

CARRIER FREQUENCIES

	CHANNEL NAME	CARRIER FREQUENCY (MHz)		CHANNEL NAME	CARRIER FREQUENCY (MHz)
1	T7	7.0	16	C	133.25
2	T8	13.0	17	D	139.25
3	T9	19.0	18	E	145.25
4	T10	25.0	19	F	151.25
5	T11	31.0	20	G	157.25
6	T12	37.0	21	H	163.25
7	T13	43.0	22	I	169.25
8	T14	49.0	23	7	175.25
9	2	55.25	24	8	181.25
10	3	61.25	25	9	187.25
11	4	67.25	26	10	193.25
12	5	77.25	27	11	199.25
13	6	83.25	28	12	205.25
14	A*	121.25	29	13	211.25
15	B	127.25	30	J	217.25

*The BP-23 supplement restriction on the use of this channel does not apply in fiber optic systems.

The third-order linearity requirement is given in Table 3.3 for nonrepeatered HRC systems. The chosen carrier frequencies are harmonics of 6 MHz starting at 12 MHz. The maximum tolerated intermodulation is 40 dB below the picture carrier level.

For an N-repeater line, the linearity requirements must be increased by a factor of C log N where C is between 10 and 20. The use of HRC systems represents a reduction in the linearity required of about 10 to 15 dB in third-order distortion.

3.4 FIBER FREQUENCY RESPONSE

The maximum system length permitted by the fiber frequency response is evaluated for different types of fiber, different signal bandwidths, and different source spectral widths. The calculations are based on the analysis of Section 2.5.

Step index fibers should not be considered for broadband communications because even if the numerical aperture and the effective length are decreased (decreasing the coupling efficiency and increasing the fiber attenuation), the fiber bandwidth is not sufficient for multichannel transmission, as shown in Figures 3.11 and 3.12. In these figures the highest signal frequency is indicated above the corresponding curve.

For systems using LED sources and graded index fiber, line equalization is required unless the system is short or a single channel is transmitted at baseband, as shown in Figures 3.13 and 3.14.

Table 3.3

LINEARITY REQUIREMENTS
NONREPEATERED LINE HRC SYSTEMS

NUMBER OF CHANNELS	INTERMODULATION REQUIREMENTS (dB)				CROSSMODULATION REQUIREMENTS (dB)	
	$H_{2\alpha_x}$	$H_{3\alpha_x}$	$IM_{2\alpha}$	$IM_{3\alpha}$	$H_{3\alpha_x}$	$IM_{3\alpha}$
2	-	-	-	-	-47.1	-59.2
3	-37.2	-37,9	-46.0	-55.5	-46.3	-63.9
4	-38.5	-37,9	-49.0	-59.0	-44.3	-65.4
5	-38,9	-38.2	-50.8	-62.0	-43.5	-67.3
6	-39.0	-38.3	-52.0	-64.3	-42.3	-68.3
7	-39.1	-38.2	-53.0	-66.1	-41.7	-69.6
8	-39.1	-38.0	-53.8	-67.5	-40.8	-70.3
9	-39.0	-38.0	-54.5	-68.9	-40.3	-71.2
10	-38.9	-37.8	-55.0	-70.0	-39.6	-71.8
12	-38.8	-37.6	-56.0	-72.0	-38.6	-73.0
15	-38.5	-37.2	-57.1	-74.3	-37.6	-74.7

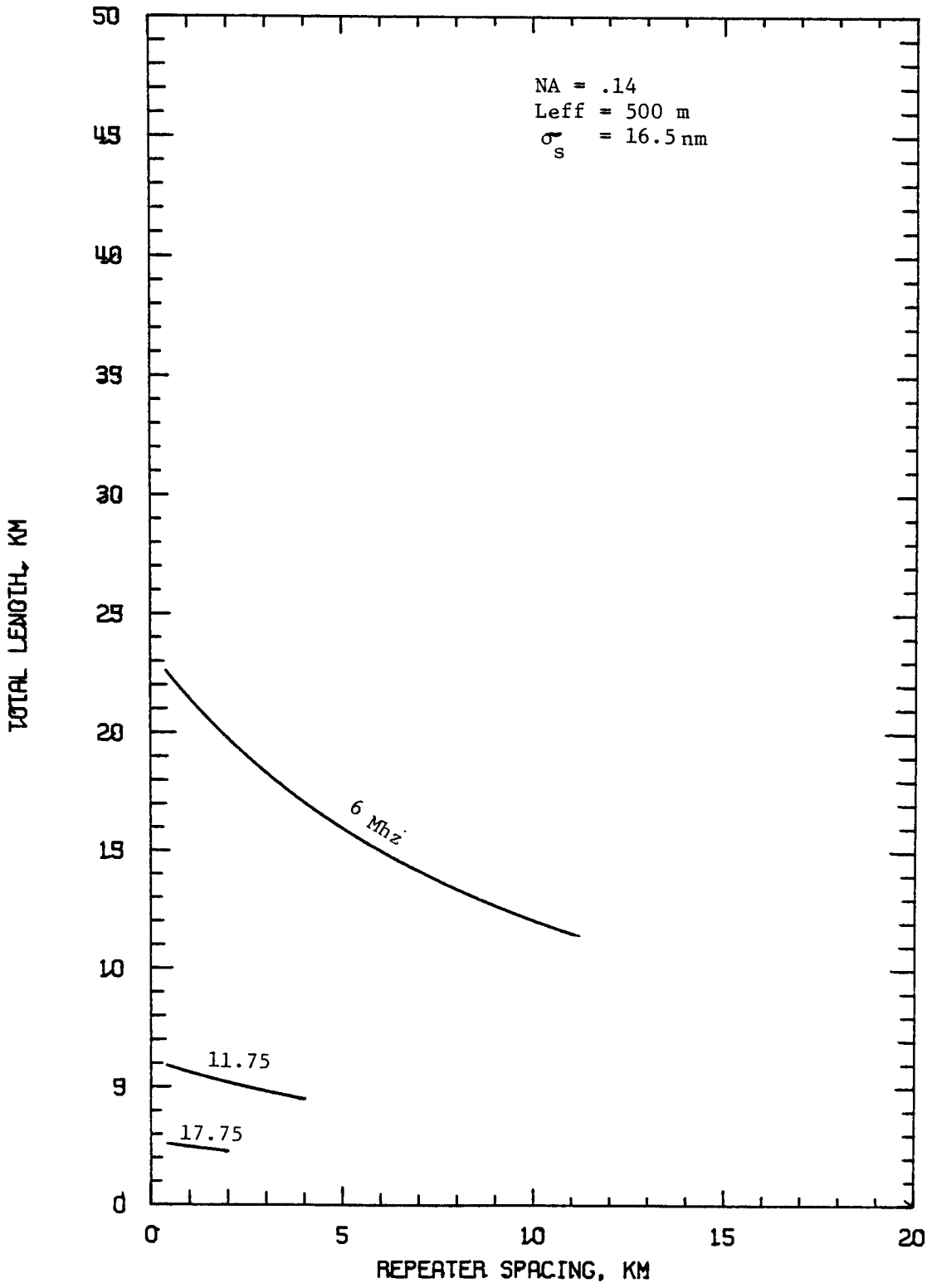

Figure 3.11 Step Index Fiber Frequency Response: LED Source

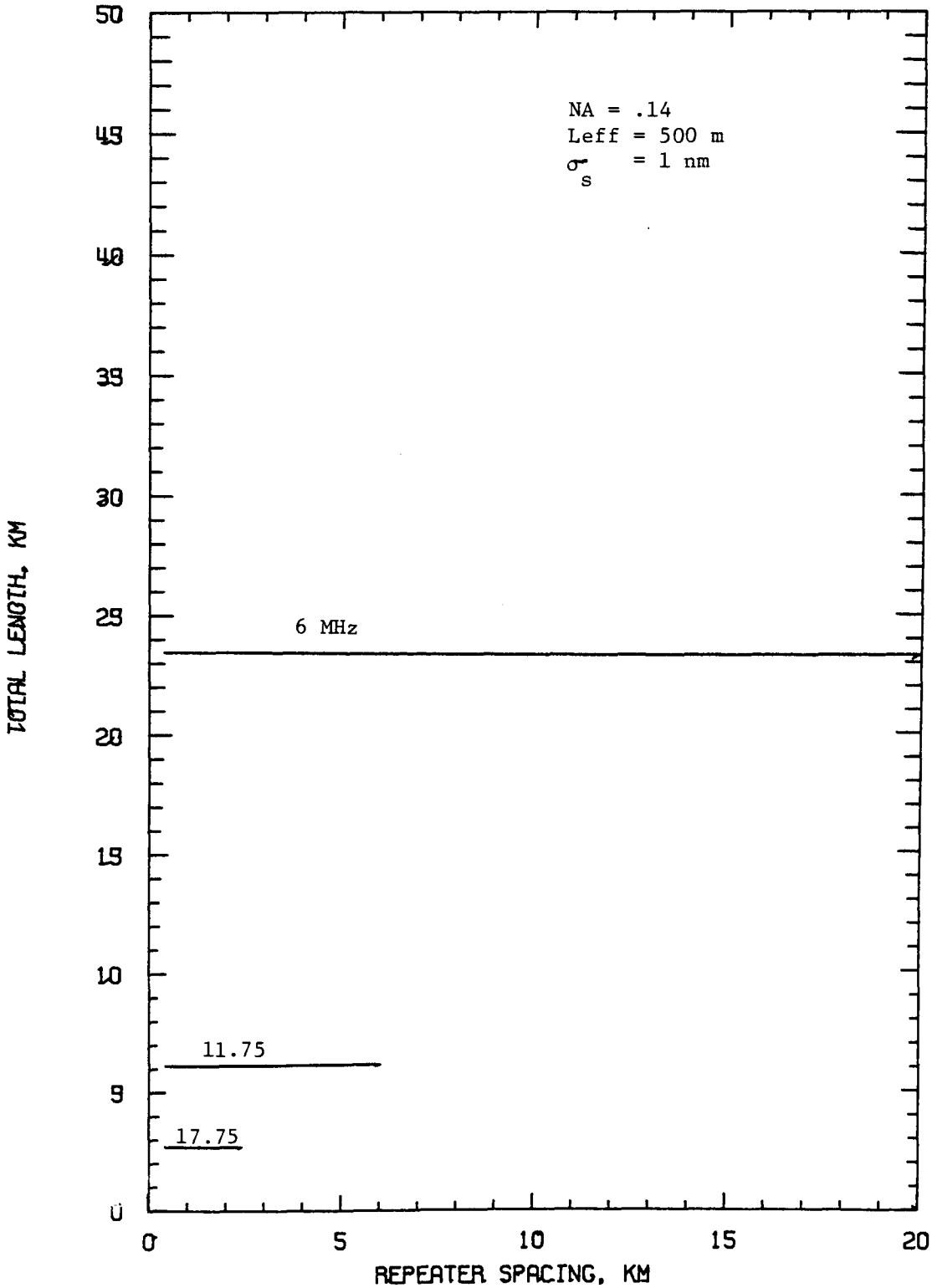

Figure 3.12 Step Index Fiber Frequency Response : Laser Source

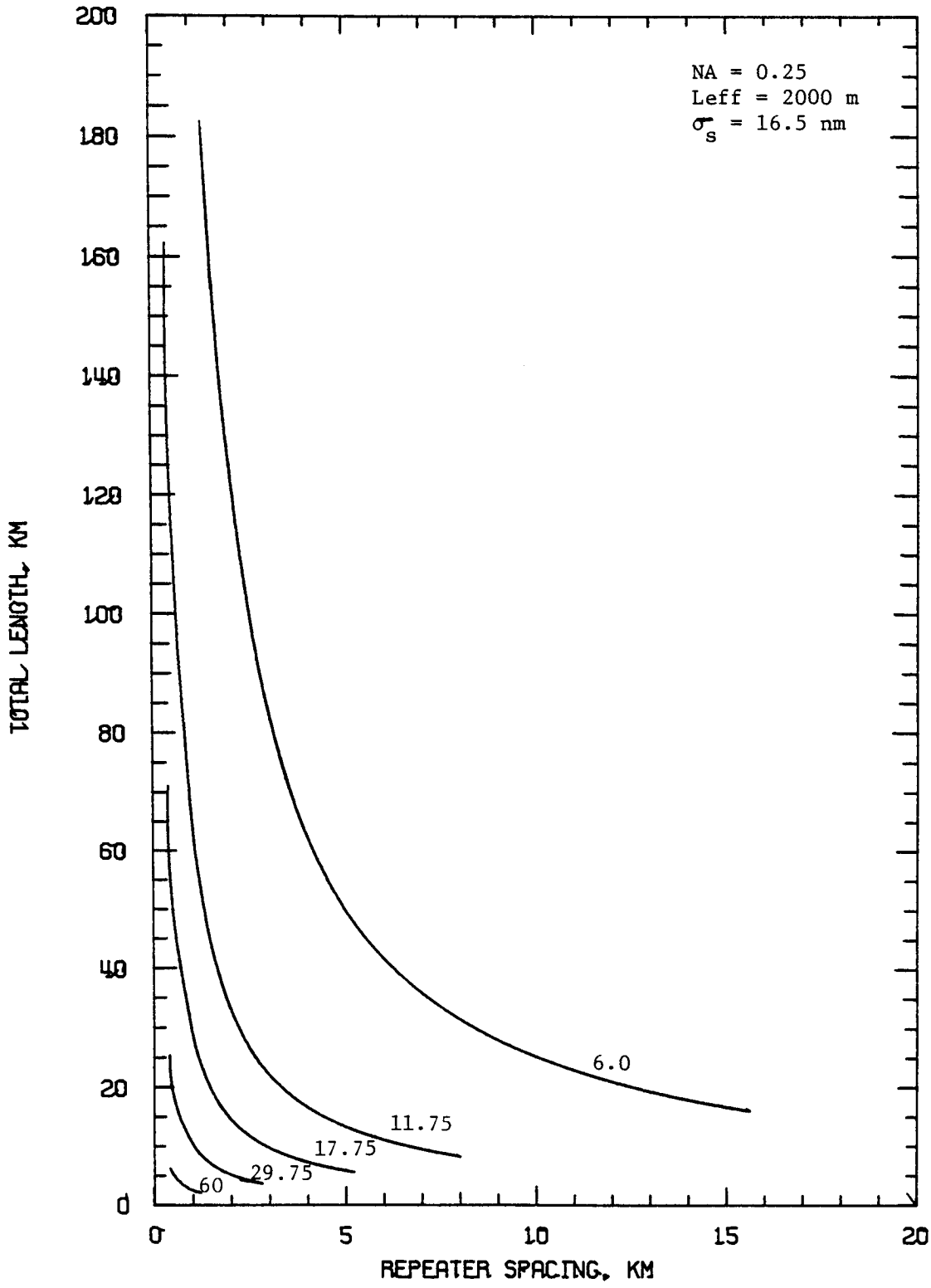

Figure 3.13 LED Systems Fiber Frequency Response: Ideal Graded Index Fiber.

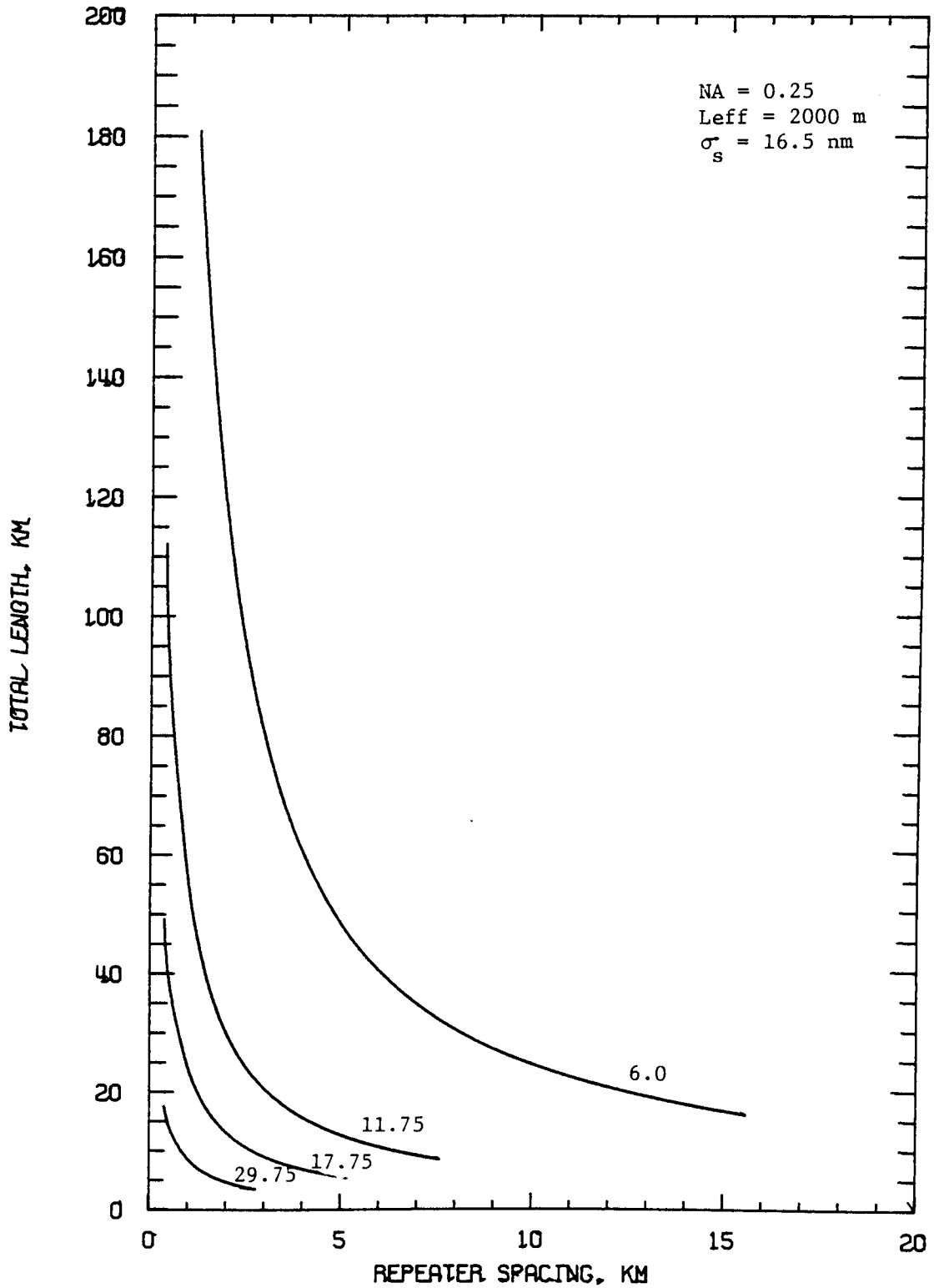

Figure 3.14 LED Systems Fiber Frequency Response : Practical Graded Index Fiber

For systems using laser sources and practical graded index fiber, line equalization may be required for multichannel systems, as shown in Figure 3.15.

The influence of the material dispersion can be seen by comparing the response of an ideal graded index fiber when illuminated by a laser source (Figure 3.16) to its response when the source is a LED (Figure 3.13). A material dispersion of 0.085 ns/km-nm is assumed.

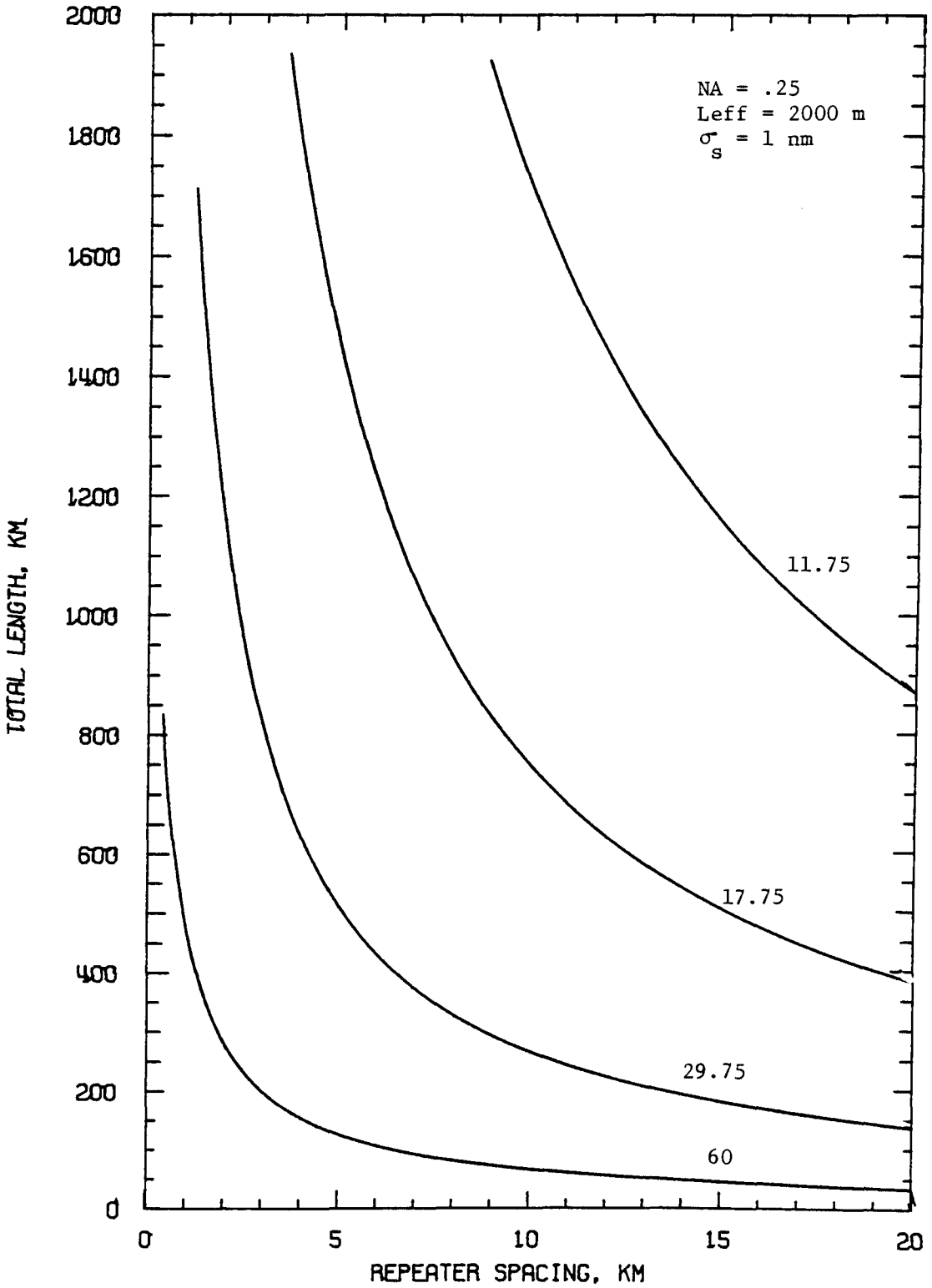

Figure 3.15 Laser Systems Fiber Frequency Response : Ideal Graded Index Fiber

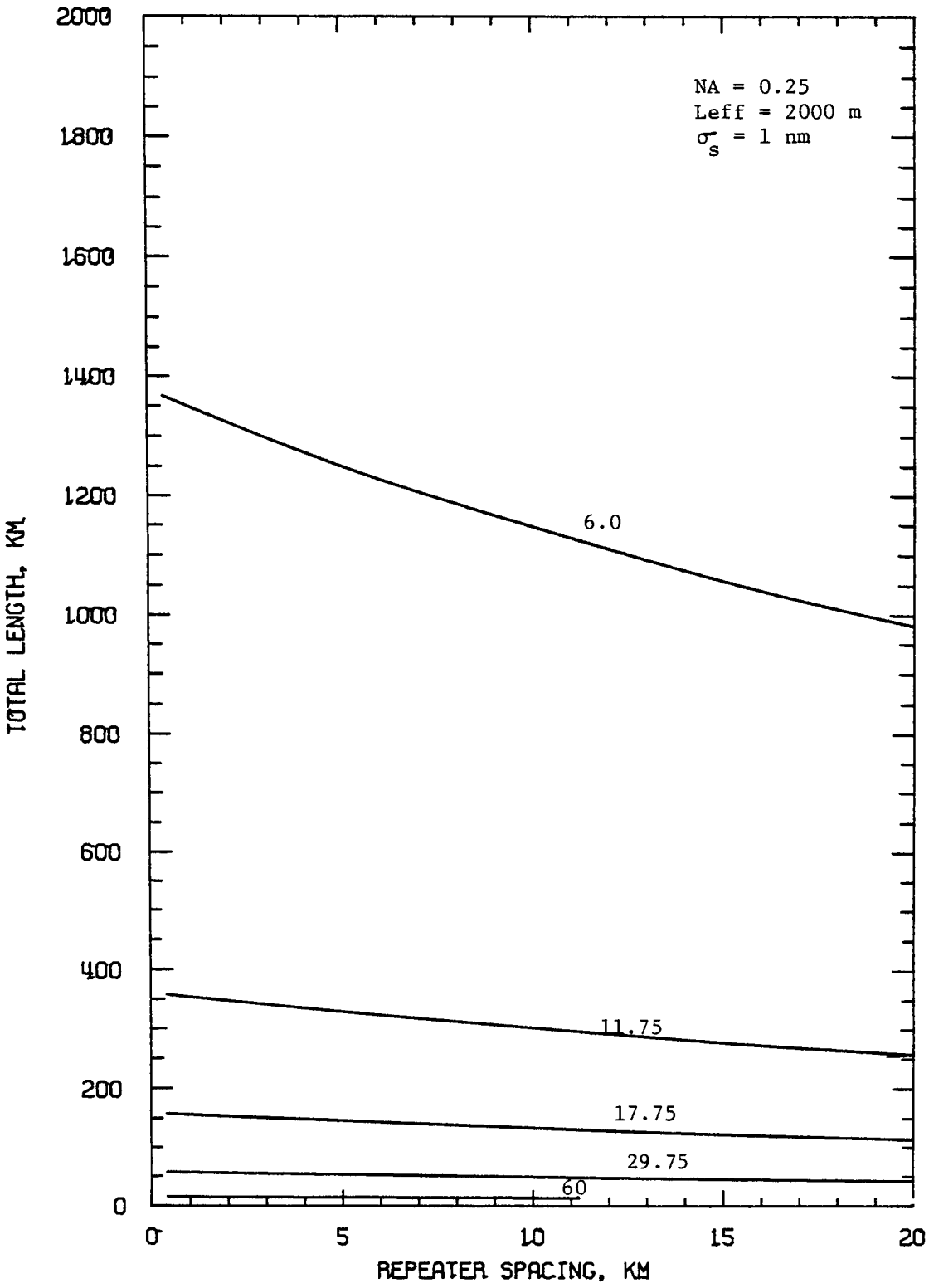

Figure 3.16 Laser Systems Fiber Frequency Response: Practical Graded Index Fiber

4. SYSTEM CAPABILITY

4.1 DESIGN GUIDELINES

Transmission problems are usually posed in terms of the number of video channels to be transmitted, the line required length, and the video quality standards to be met at the end of the line.

Before evaluating system performance, the transmission method and the components must be chosen. The characteristics that are required for the evaluation are summarized in Table 4.1. A source bias current and an initial optical modulation index that are compatible with long continuous operation are fixed. Then the nonlinear distortions for a given number of repeaters are evaluated (Section 2.4). If the linearity requirements are not met, the optical modulation index is reduced accordingly. After the minimum mean optical power required on the detector is evaluated following the analysis of Section 2.3. Knowing the mean optical power coupled into the fiber (Section 2.2) and the fiber attenuation, the maximum repeater spacing is evaluated (Section 2.1). The system bandwidth is then evaluated (Section 2.5). If the system bandwidth is not sufficient and the equalization cannot fully compensate, the repeater spacing is reduced accordingly. The preceding process can be repeated for different numbers of repeaters until the required line length is achieved.

Table 4.1

SYSTEM CHARACTERISTICS

1. Transmission Method
   - baseband - dc or ac
   - modulated carrier
   - multichannel system - standard FDM or HRC or mixed mode transmission
   - carrier frequencies
   - line equalization - if yes, maximum amount of compensation

2. Light Source
   - type LED or laser
   - external quantum efficiency
   - linearity
   - spectral width

3. Fiber
   - step or graded index
   - numerical aperture
   - effective coupling length
   - attenuation

4. Photodiode
   - PIN or APD type
   - quantum efficiency
   - leakage current
   - dark current (APD only)
   - excess noise factor k (APD only)

5. Amplifier
   - noise figure
   - photodiode equivalent load resistance

4.2 SYSTEMS MEETING BP-23

The BP-23 requirements which could limit the performance of a fiber optic transmission line are summarized in Table 4.2. The component characteristics that are assumed in the following calculations are listed in Table 4.3, except for the light sources whose characteristics are listed separately in Table 4.4.

For the LED's, second and third harmonics of -30 and -60 dB are typical of noncompensated devices. The figures of -70 dB for both second and third harmonics can be obtained if linearization techniques such as quasi-feedforward are used.

Limited data exists on the use of lasers for analog transmission. Measurements of the total harmonic distortion suggest that lasers have a similar behavior to LED's, though if the THD is -40 dB for a 10 mA peak-topeak signal, the THD increases by about 6 dB when the signal is doubled. Thus, the second-order distortion is dominant.[36] It may be assumed that the third-order distortion is about 20 dB lower than the second order, which gives second and third harmonics of -40 and -60 dB respectively at 10 mA peak-to-peak. Consequently, according to the source nonlinearity model of Section 2.4, the second and third harmonics corresponding to a peak-to-peak current of 20 mA are -34 and -48 dB respectively. Then, assuming that linearization techniques would give a similar result as for LED's, a laser with a second and third harmonic of -70 dB could become available.

Table 4.2

VIDEO TRANSMISSION PERFORMANCE REQUIREMENTS BP-23

Signal-to-Noise Ratio	40 dB
Crossmodulation	-48 dB
Single Frequency Interference	-57 dB*
Differential Gain	± 2 dB
Differential Phase	± 5°

*The exact curve is given in Figure 3.8.

Table 4.3

COMPONENT CHARACTERISTICS

FIBER	
	- Type: graded index (5% error in the index profile)
	- Numerical aperture: 0.25
	- Effective coupling length: 2 km
	- Attenuation: 3, 5, 8 dB/km
	- Material dispersion: 0.085 ns/km-nm
AMPLIFIER	
	- Noise figure: 3 dB
	- Equivalent load resistance: limited by the signal bandwidth and by an effective amplifier input capacitance of 0.12 picofarad
PHOTODIODE	
	- Optimum detector is chosen, PIN or APD
	- Quantum efficiency: 0.85
	- Leakage current: 1 nA
	- APD dark current: 0.1 nA
	- APD excess noise factor: k = 0.03

Table 4.4

SOURCE CHARACTERISTICS

LED	RADIANT INTENSITY ON AXIS mW/sr at 150 mA	SPECTRAL WIDTH nm	RELATIVE HARMONICS OF A 150 mA P-TO-P FUNDAMENTAL	
			$H_{2\alpha_{150}}$ dB	$H_{3\alpha_{150}}$ dB
1	3	40	-30	-60
2	3	40	-70	-70

LASER	DIFFERENTIAL QUANTUM EFFICIENCY mW/mA	SPECTRAL WIDTH nm	RELATIVE HARMONICS OF A 20 mA P-TO-P FUNDAMENTAL	
			$H_{2\alpha_{20}}$ dB	$H_{3\alpha_{20}}$ dB
1	0.34	2	-36	-48
2	0.34	2	-70	-70

However, it should be mentioned that the analog modulation of a laser for good quality video transmission poses significant problems such as bias stability, the elimination of relaxation oscillations, etc. It should also be verified whether or not long lifetime operation of the laser will require a reduced optical output power.

4.2.1 LED Systems

For LED systems, the source bias current and the initial optical modulation are set to 100 mA and 0.75 respectively. The system length in dB of optical loss is given in Figure 4.1 as a function of the repeater spacing optical loss for systems transmitting up to five video channels and when only the signal-to-noise ratio requirement is considered. For dc baseband transmission, the maximum number of repeaters is fixed to 12 in order to limit the number of clampers in tandem. For the other methods of transmission, the number of repeaters is limited to 50.

The system and repeater spacing losses found in Figure 4.1 can be converted in lengths knowing the fiber attenuation. In Figures 4.2 and 4.3 the system loss is evaluated for both LED sources when signal-to-noise ratio and linearity requirements are considered. For LED-1 (-30, -60), a carrier frequency allocation scheme which eliminates second-order distortion is taken. Otherwise, the transmission of two modulated carriers corresponding to channels T7 and T8 is practically impossible. A 10 log N law is assumed for the compounding of beats with the number of repeaters. Multichannel LED systems require line equalization. There is a limit, however, in the compensation that can be accomplished. For this reason, it is assumed that equalization can be provided without significant SNR penalty only when a repeater section considered individually has a bandwidth greater or equal to the signal bandwidth. In other words, equalization is provided to compensate for

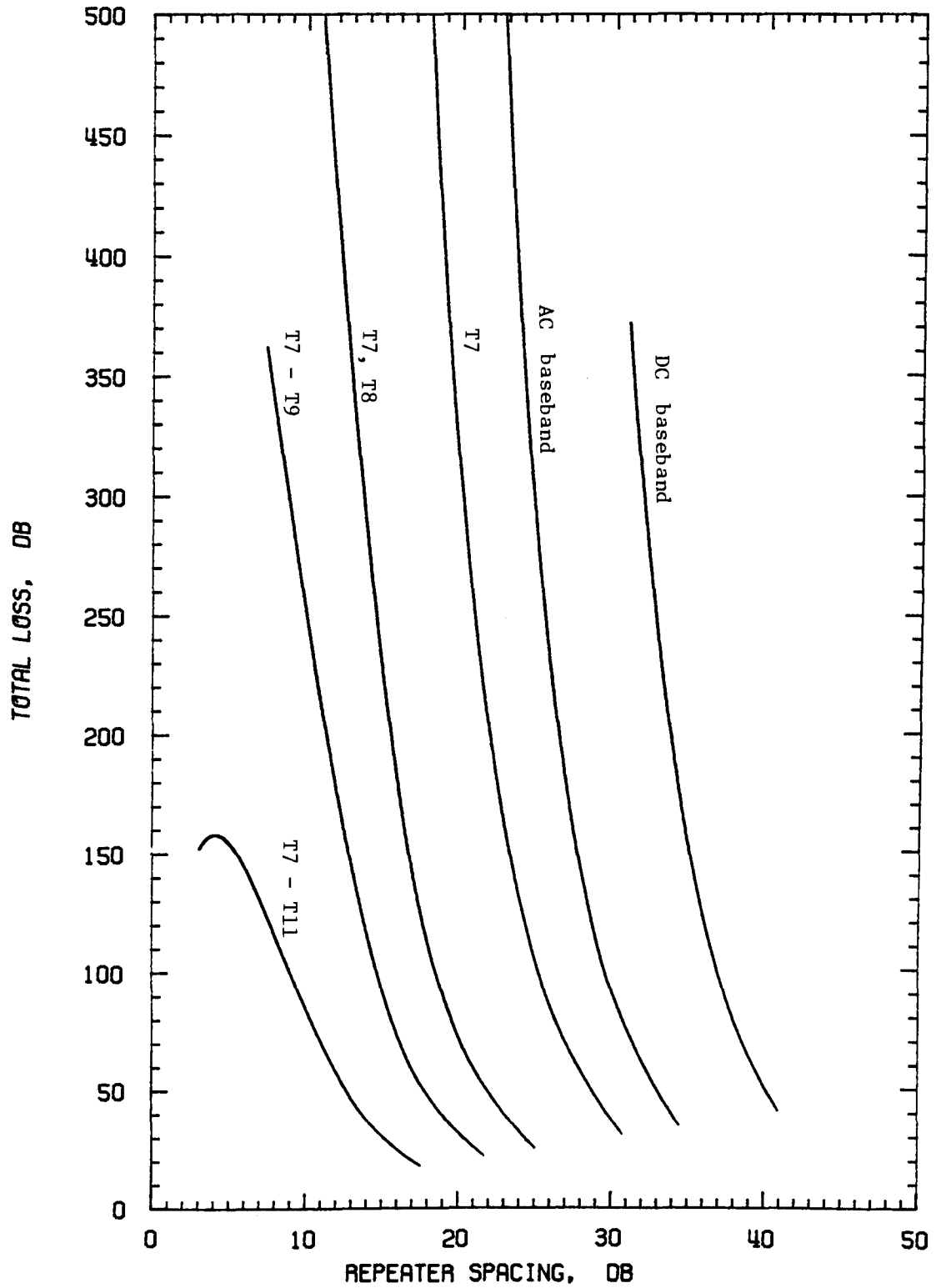

Figure 4.1 LED Systems - SNR Only

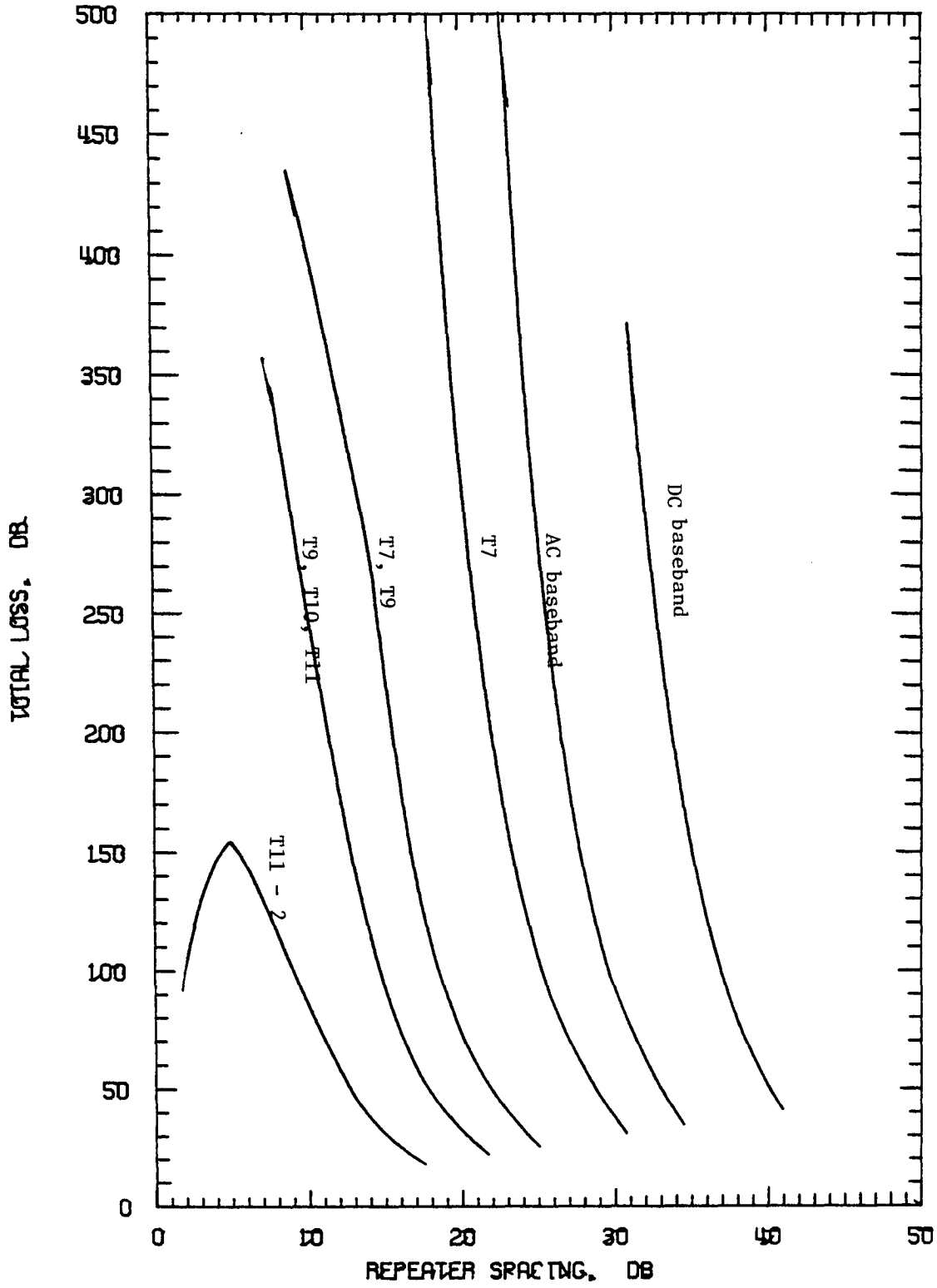

Figure 4.2 LED Systems - LED-1 (-30,-60)

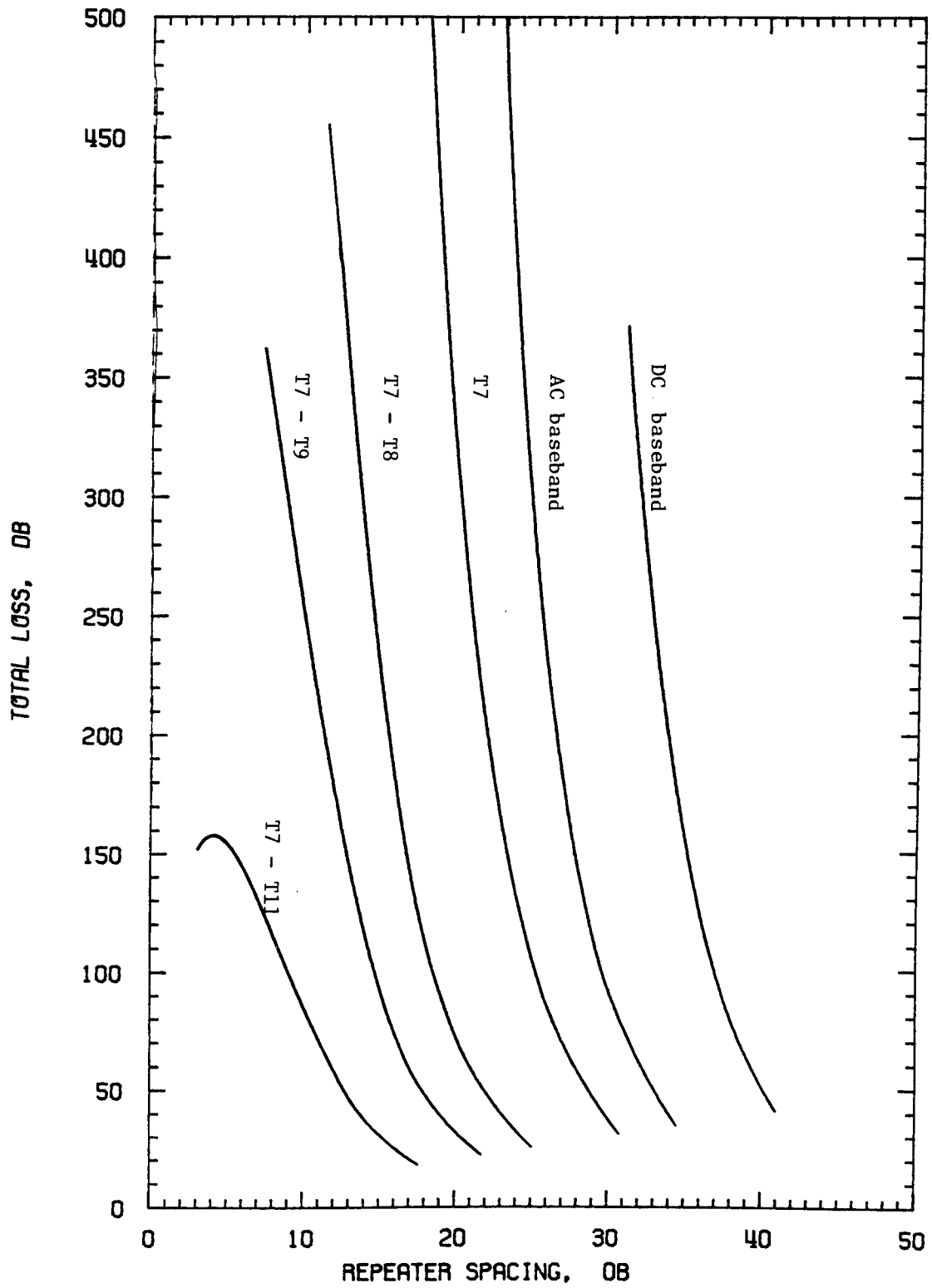

Figure 4.3 LED Systems - LED-2 (-70,-70)

the cascading effect on the system bandwidth. This is known as the practical equalization assumption.

The maximum system lengths when LED-2 (-70,-70) is used and when practical equalization is assumed are given in Figures 4.4 4.5 and 4.6 for fiber attenuations of 3, 5, and 8 dB/km respectively. From these figures, it is seen that LED systems are limited to low numbers (5) of video channels for reasons of power (SNR) and fiber bandwidth even if the linearity is sufficient.

4.2.2 Laser Systems

For laser systems, a source bias current of 13.3 mA above threshold with an optical modulation index of 0.75 are chosen. The total system optical loss for laser systems is given in Figures 4.7 4.8 and 4.9 as a function of the repeater spacing loss when SNR only, laser-1 (-34,-48) and laser-2 (-70,-70), respectively, are considered. In Figures 4.10, 4.11 and 4.12 the total system length is given for fiber attenuations of 3, 5 and 8 dB/km, respectively, when practical equalization is assumed. It can be seen that longer systems are feasible with laser sources. It should also be noted that the fiber frequency response does not limit the maximum system length for the numbers of channels considered.

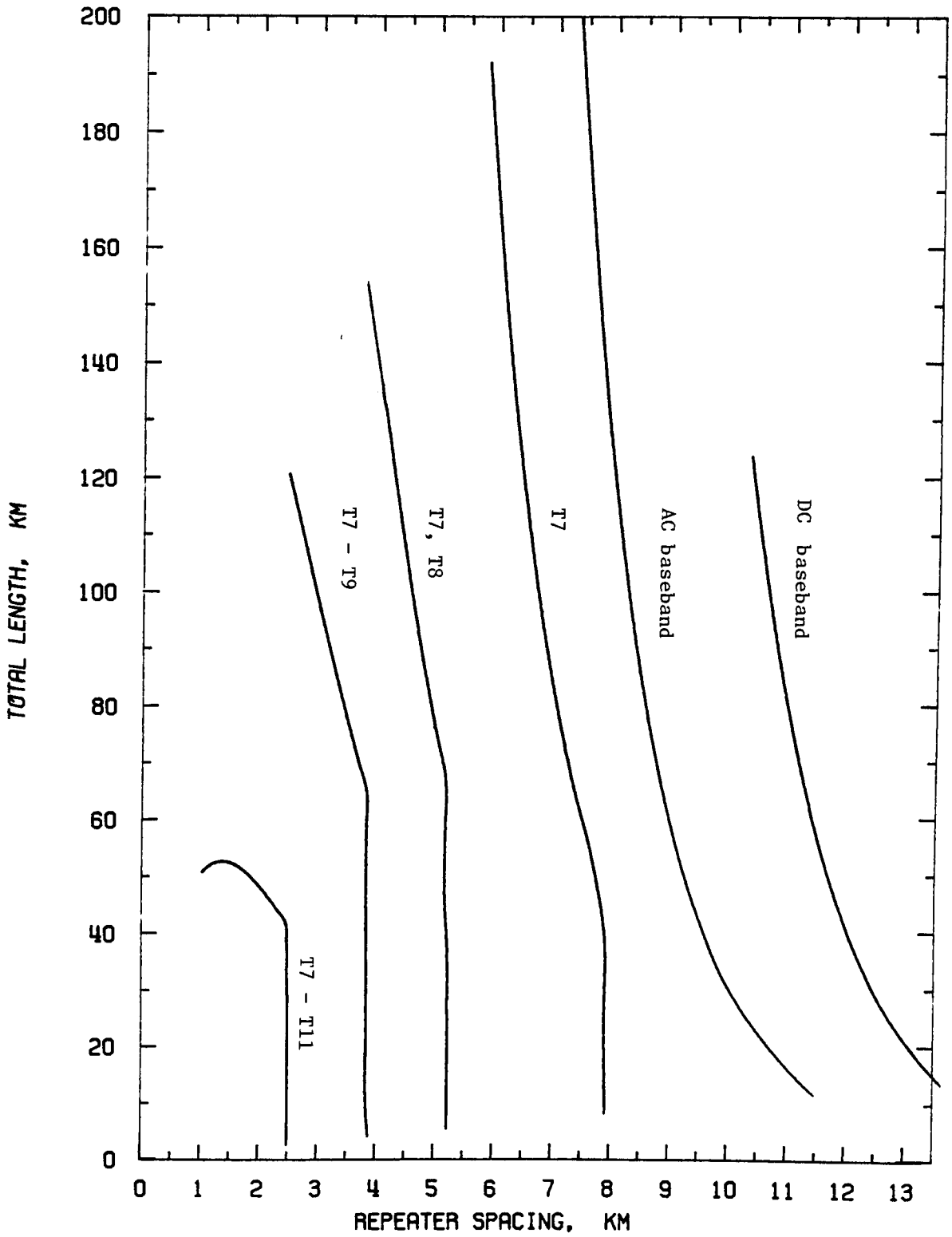

Figure 4.4 LED Systems Practical Equalization (α = 3 dB/km)

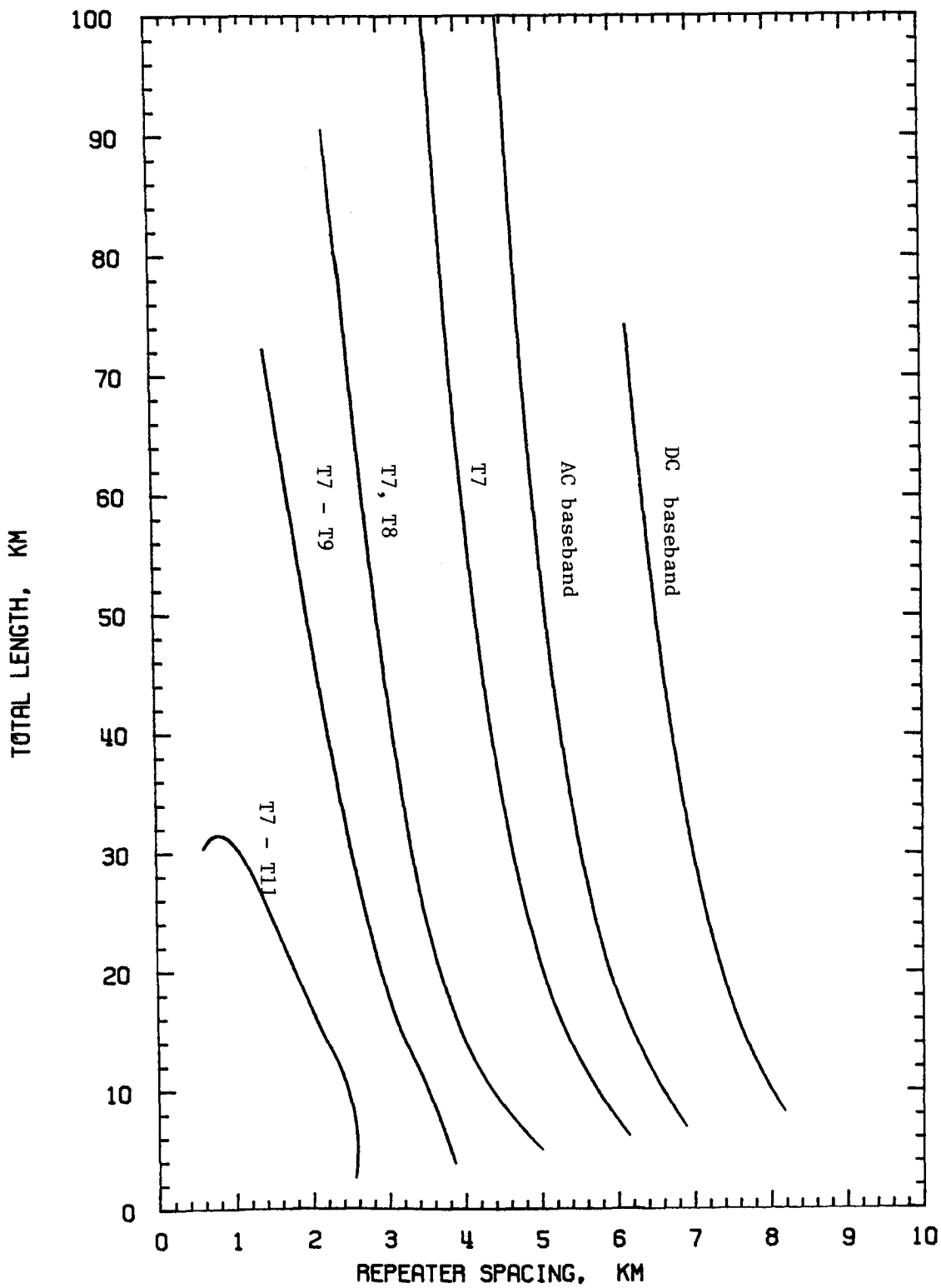

Figure 4.5 LED Systems Practical Equalization (α = 5 dB/km)

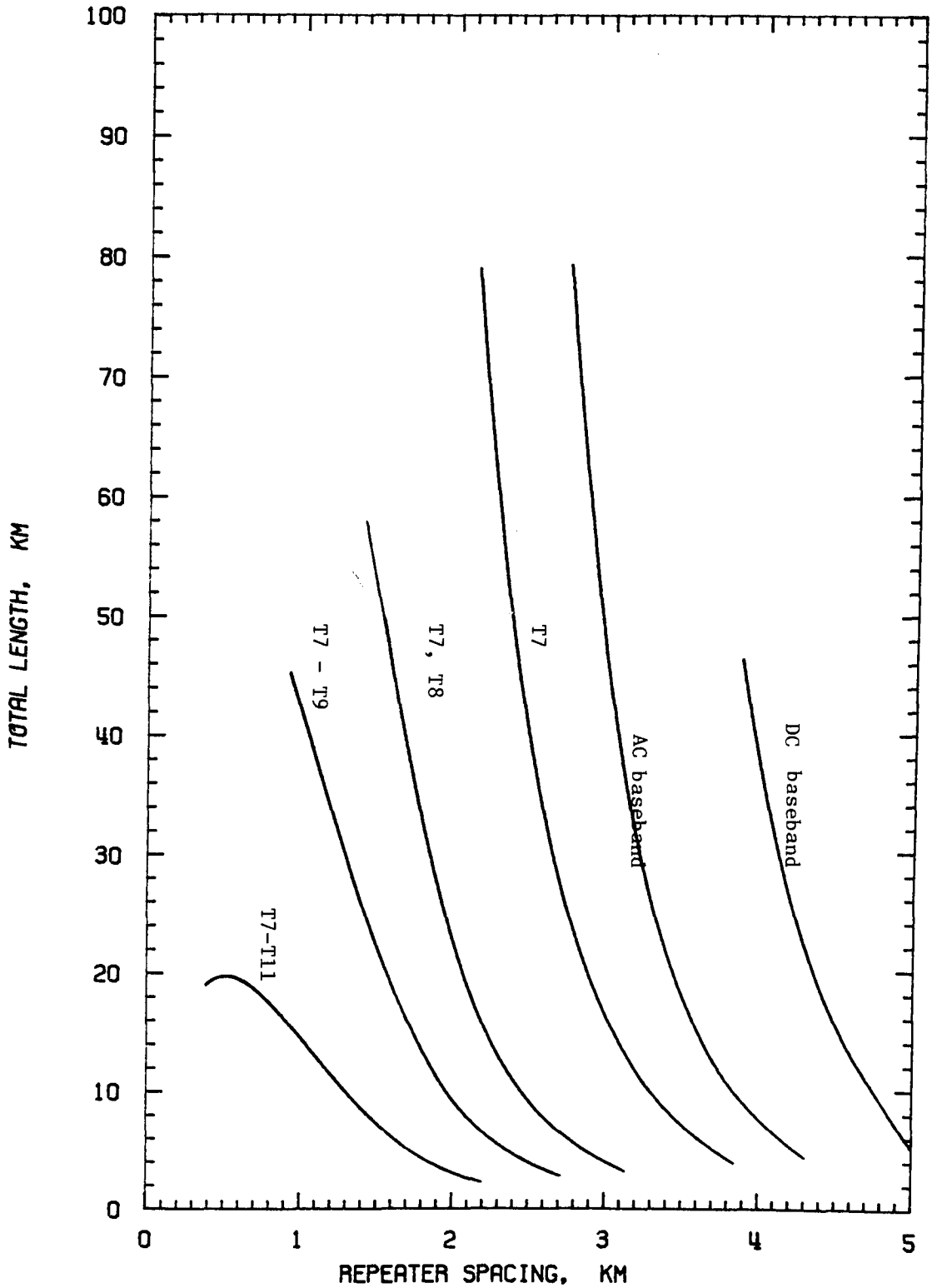

Figure 4.6 LED Systems Practical Equalization (α = 8 dB/km)

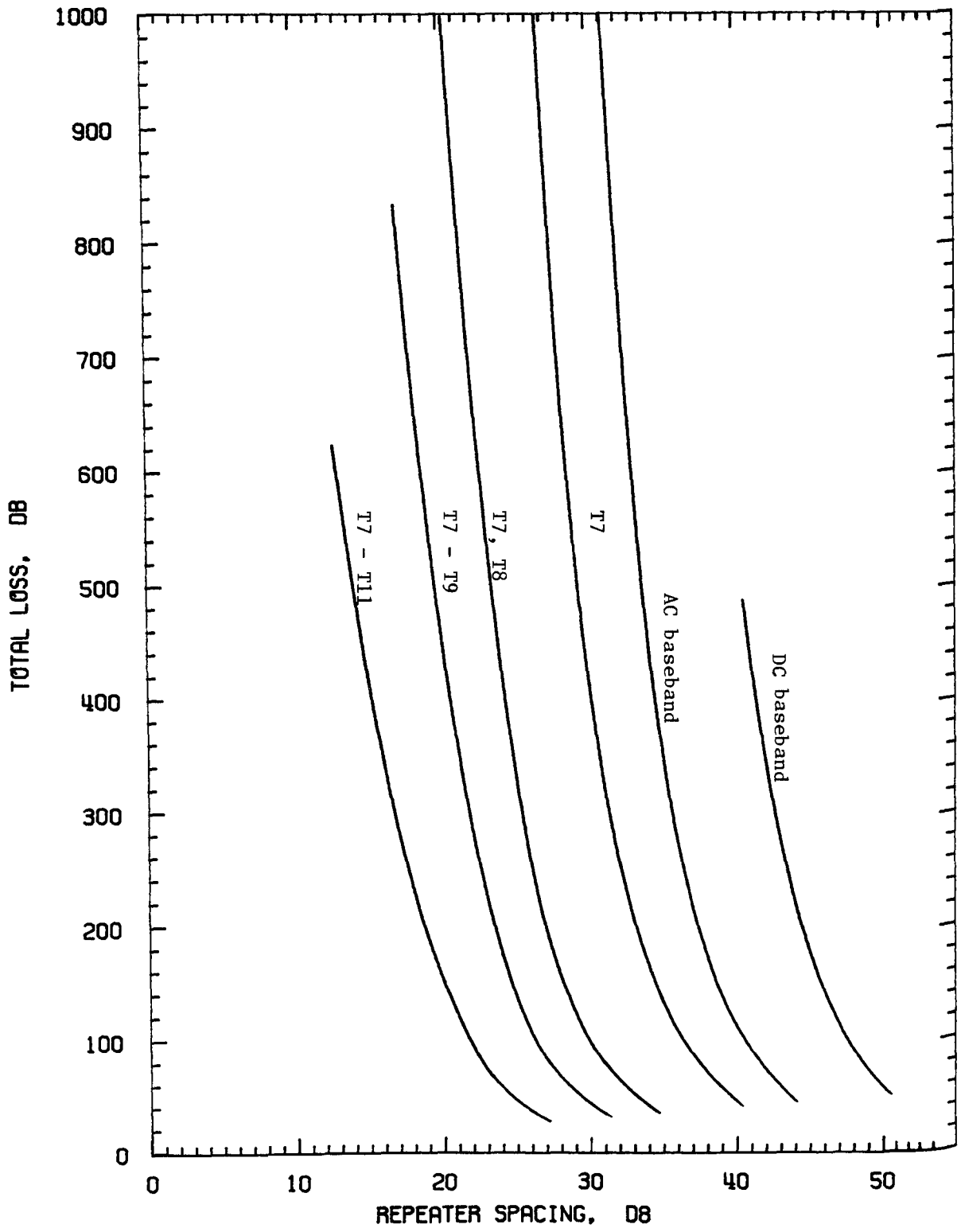

Figure 4.7 Laser Systems - SNR Only

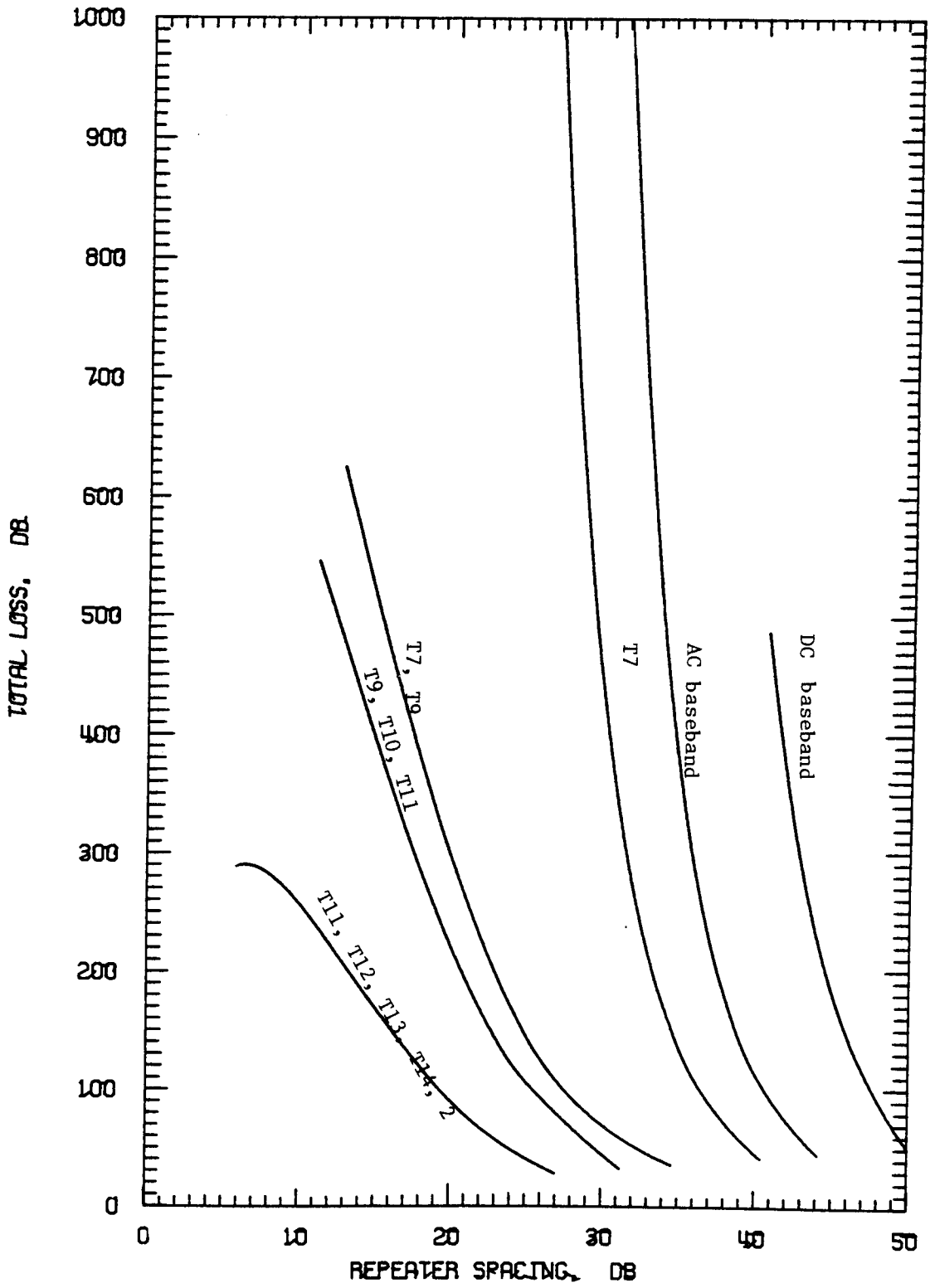

Figure 4.8 Laser Systems - Laser-1 (-36, -48)

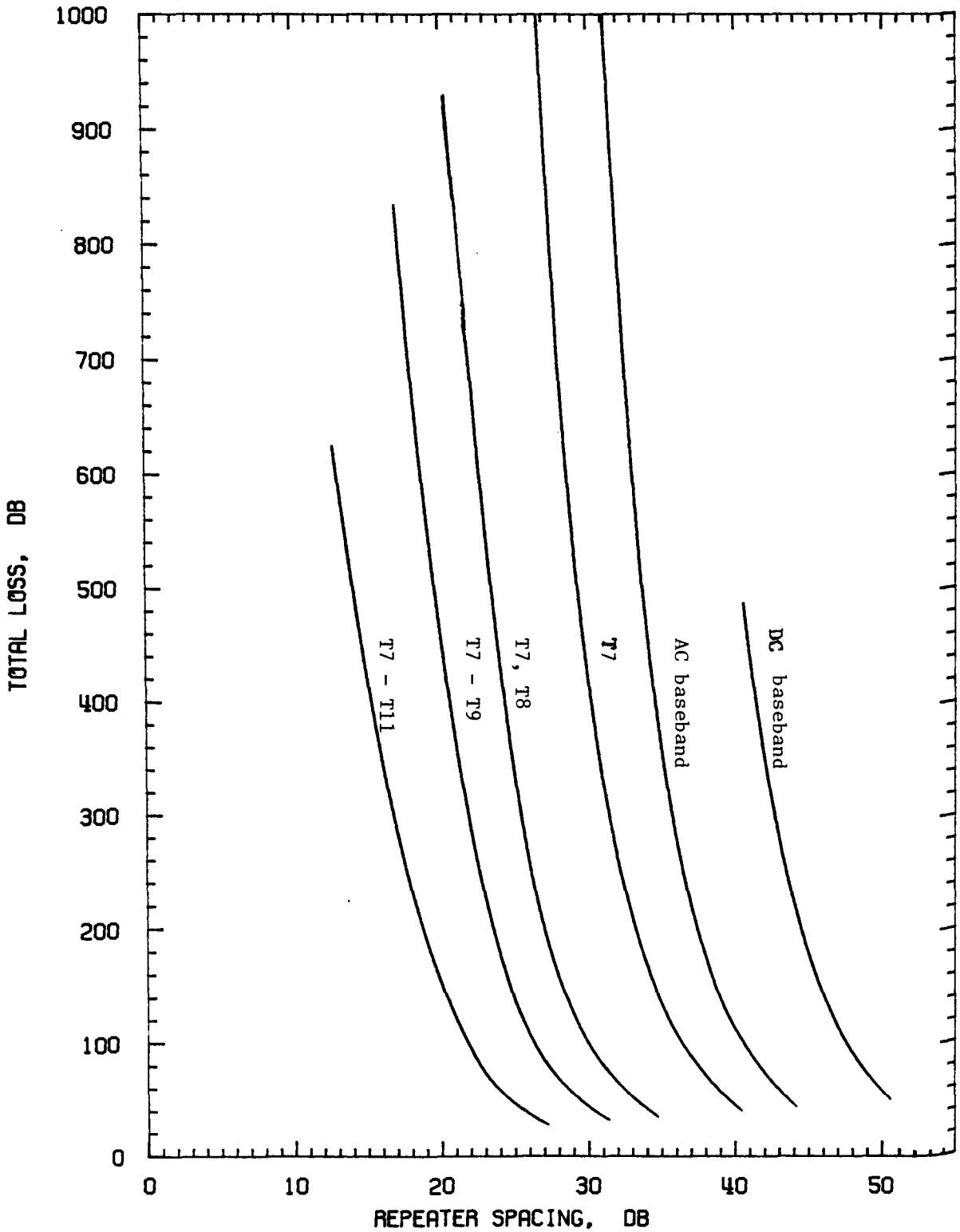

Figure 4.9 Laser Systems - Laser-2 (-70, -70)

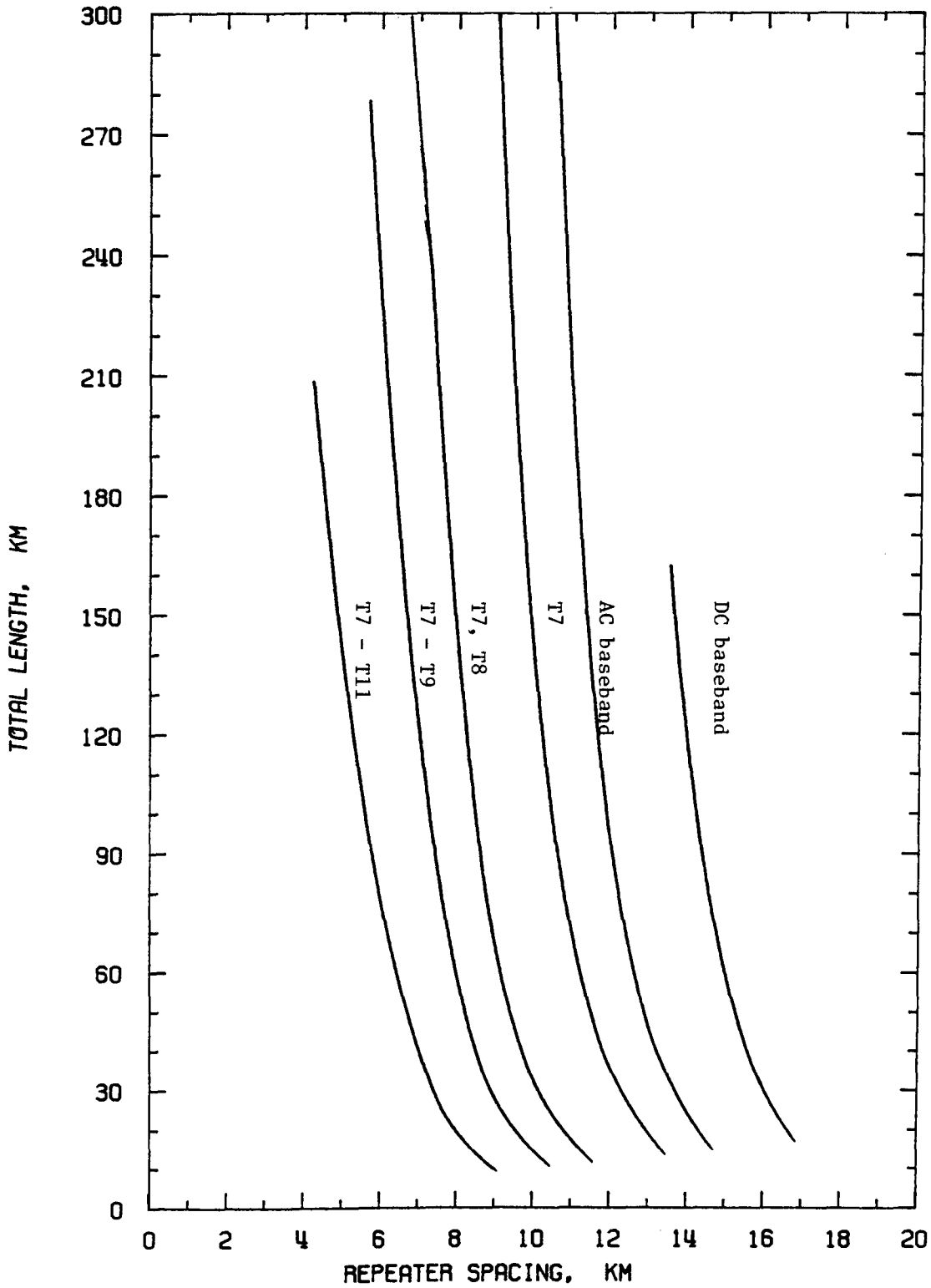

Figure 4.10 Laser Systems Practical Equalization (α = 3 dB/km)

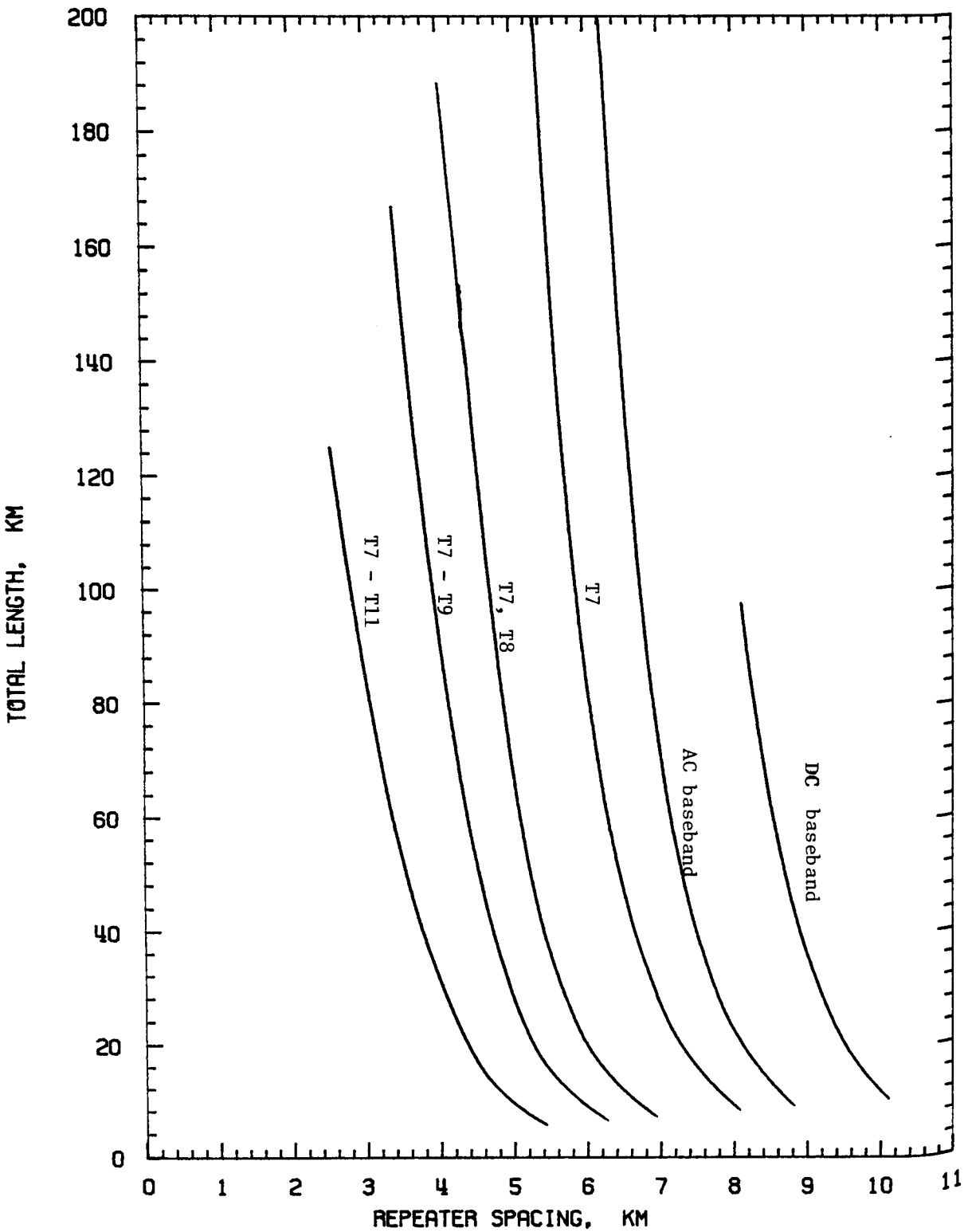

Figure 4.11 Laser Systems Practical Equalization (α = 5 dB/km)

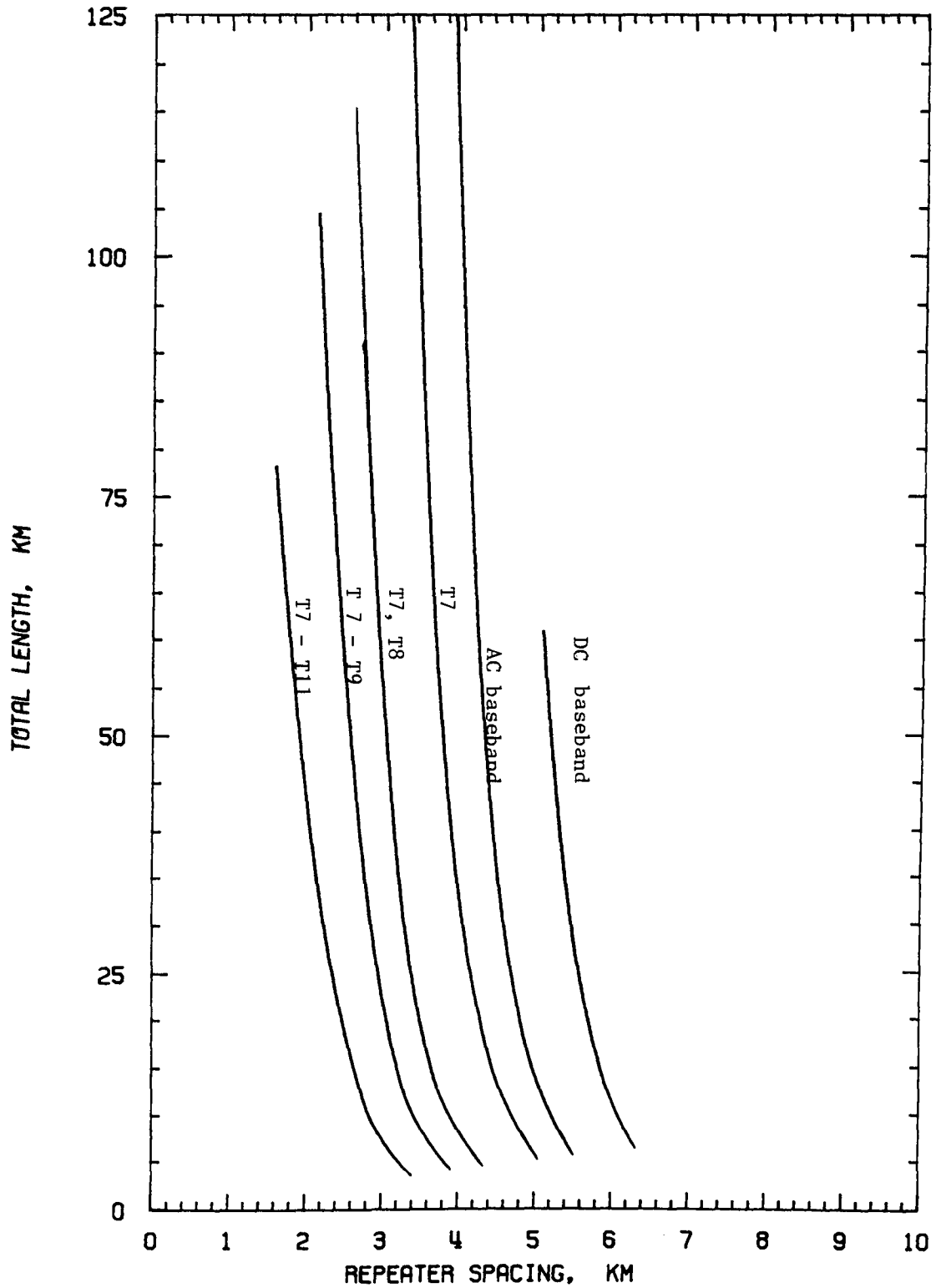

Figure 4.12 Laser Systems Practical Equalization (α = 8 dB/km)

4.2.3 Effect of the Law for the Compounding of Beats with the Number of Repeaters

As seen in Section 2.4, no reliable law for the compounding of beats with the number of repeaters exists. Intermodulation beats could compound following a 10 log N or a 20 log N law (or possibly following an intermediate law between the two). Also the law of compounding can differ depending on the type of beats involved, e.g., 10 log N for a second-order and 20 log N for third-order distortion.

The effect of the factor C on the system performance is evaluated for a system using laser-2 (-70,-70) and for the transmission of five video channels. In Figure 4.13 it is seen that the law of compounding has a significant effect on the system performance.

4.2.4 Effect of the Method of Transmission

Multichannel transmission can be achieved using different methods of transmission, such as HRC, mixed-mode transmission and standard FDM. In Figures 4.14 and 4.15 the methods of transmission are compared for systems transmitting five video channels and using LED-2 (-70,-70) and laser-2 (-70,70) sources respectively. The baseband channel in the mixed-mode transmission method is ac-transmitted. A 20 log N law for the compounding of beats is assumed in order to demonstrate the influence of nonlinear distortions. It is found that HRC systems represent a considerable improvement over the other methods of transmission. However, the linearity advantage could be reduced.

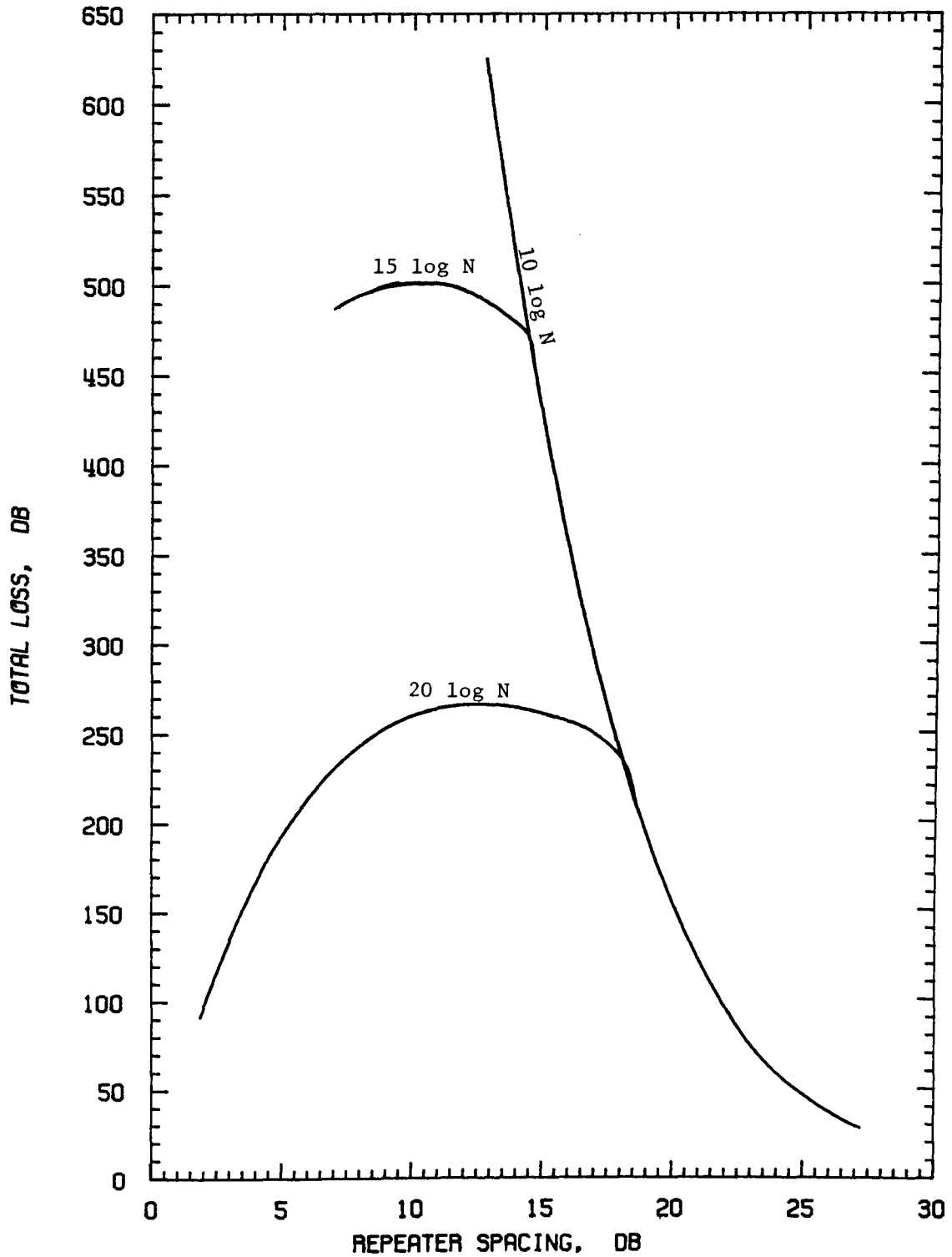

Figure 4.13 - Effect of the Beats Compounding Law(5 -Channel System)

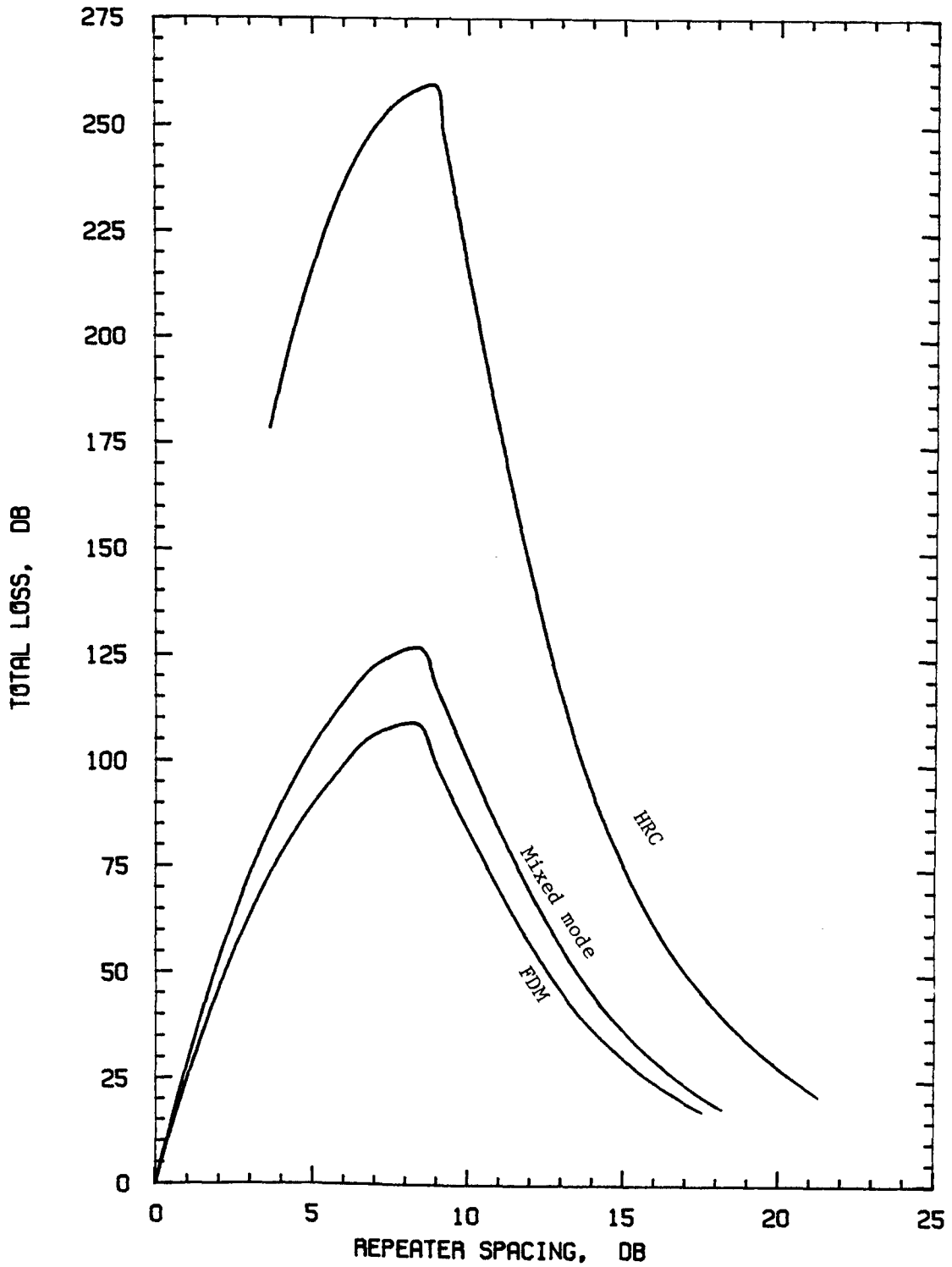

Figure 4.14 Effect of the Method of Transmission(5-Channel System)LED-2 (-70, -70)

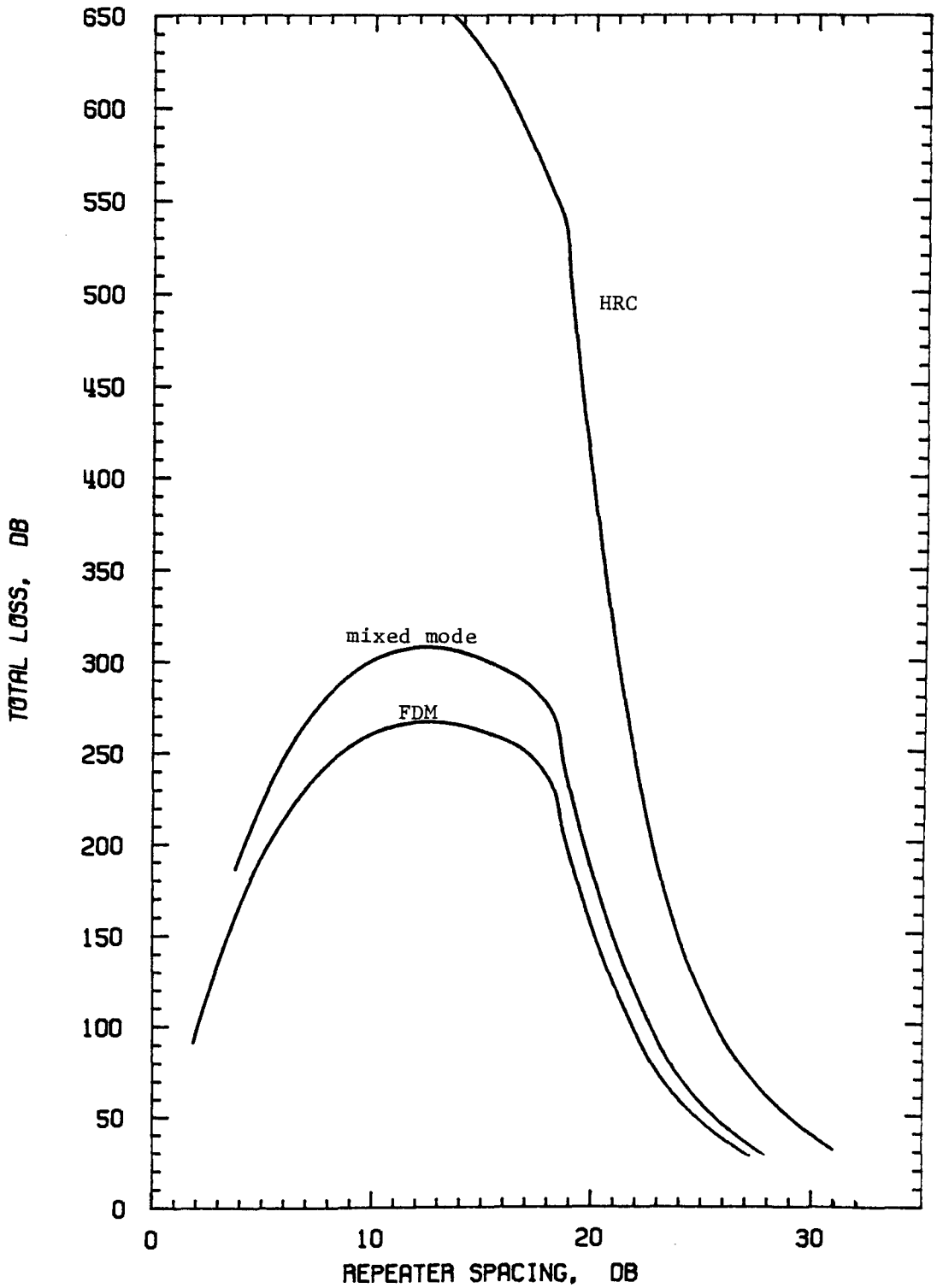

Figure 4.15 Effect of the Method of Transmission(5-Channel System)Laser-2 (-70,-70)

4.2.5 12-Channel Systems

LED's are not powerful enough to transmit 12 video channels that meet BP-23 requirements. However, high power lasers could become available, and their capability for 12-channel video systems should be assessed.

Three transmission methods are considered: HRC, FDM systems using the 12 lower adjacent channels starting at T7, and the 12 standard broadcast channels (channels 2 to 13). Figure 4.16 gives the total system loss as a function of the repeater spacing loss when the laser-2 transmitter and a 10 log N beats compounding law are assumed. In Figure 4.17 a 20 log N law is assumed. From these figures, it is concluded that 12-channel transmission over system losses of more than 400 dB is possible with a linearized high power laser. Again, the beats compounding law has a significant effect on the system performances.

4.3 TRANSPORTATION TRUNKS

In Activities 2 and 4, transportation trunks in the different proposed network configurations are required. Some must be transparent, and they are called high quality transportation trunks. Typical transmission performance requirements are summarized in Table 4.5. In some cases, a given amount of degradation is tolerated in the transportation trunk; these are referred to as medium quality transportation trunks. Possible transmission performance requirements are listed in Table 4.6.

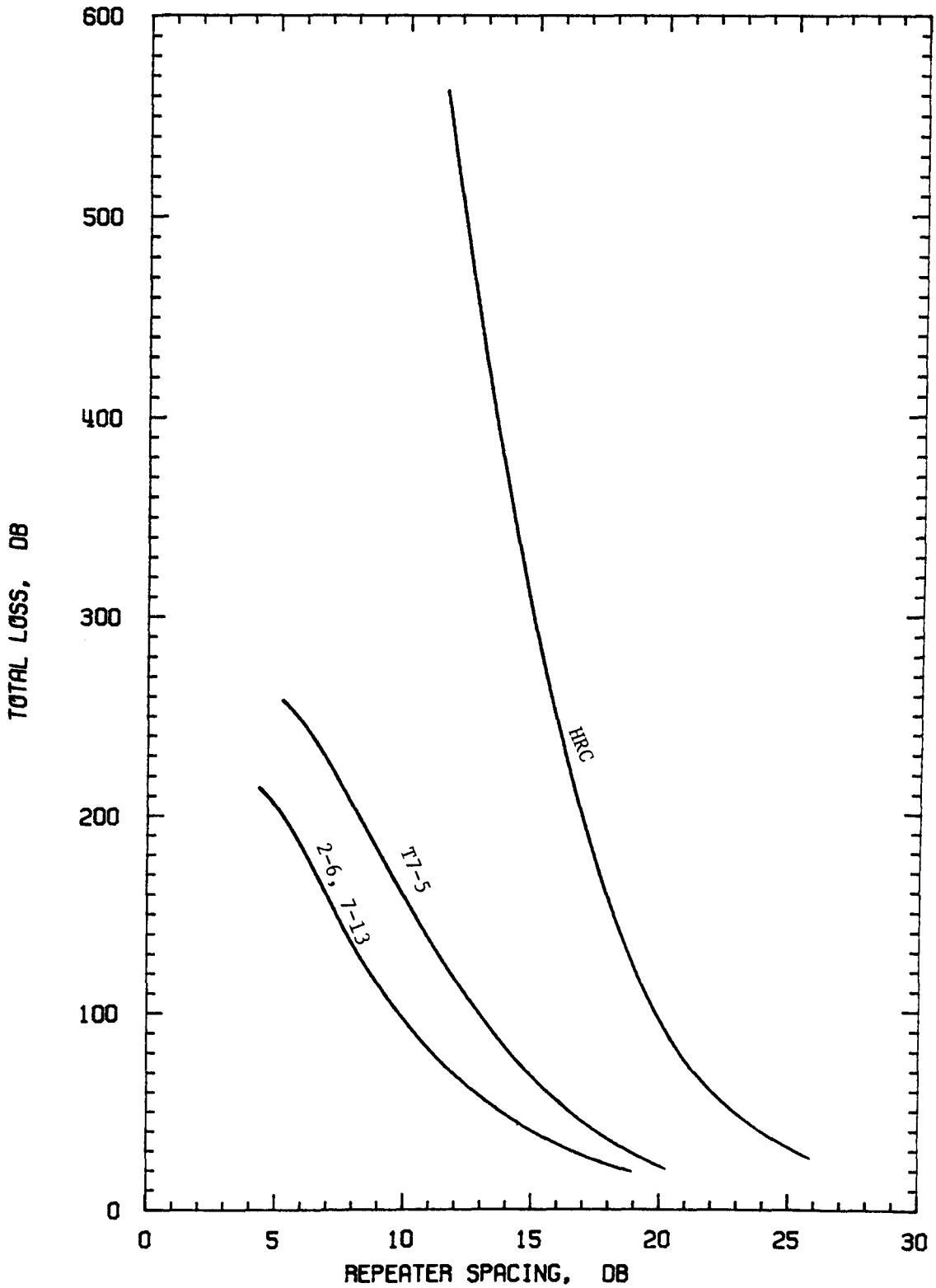

Figure 4.16 12-Channel Systems Laser-2 (-70, -70),10 log N Law

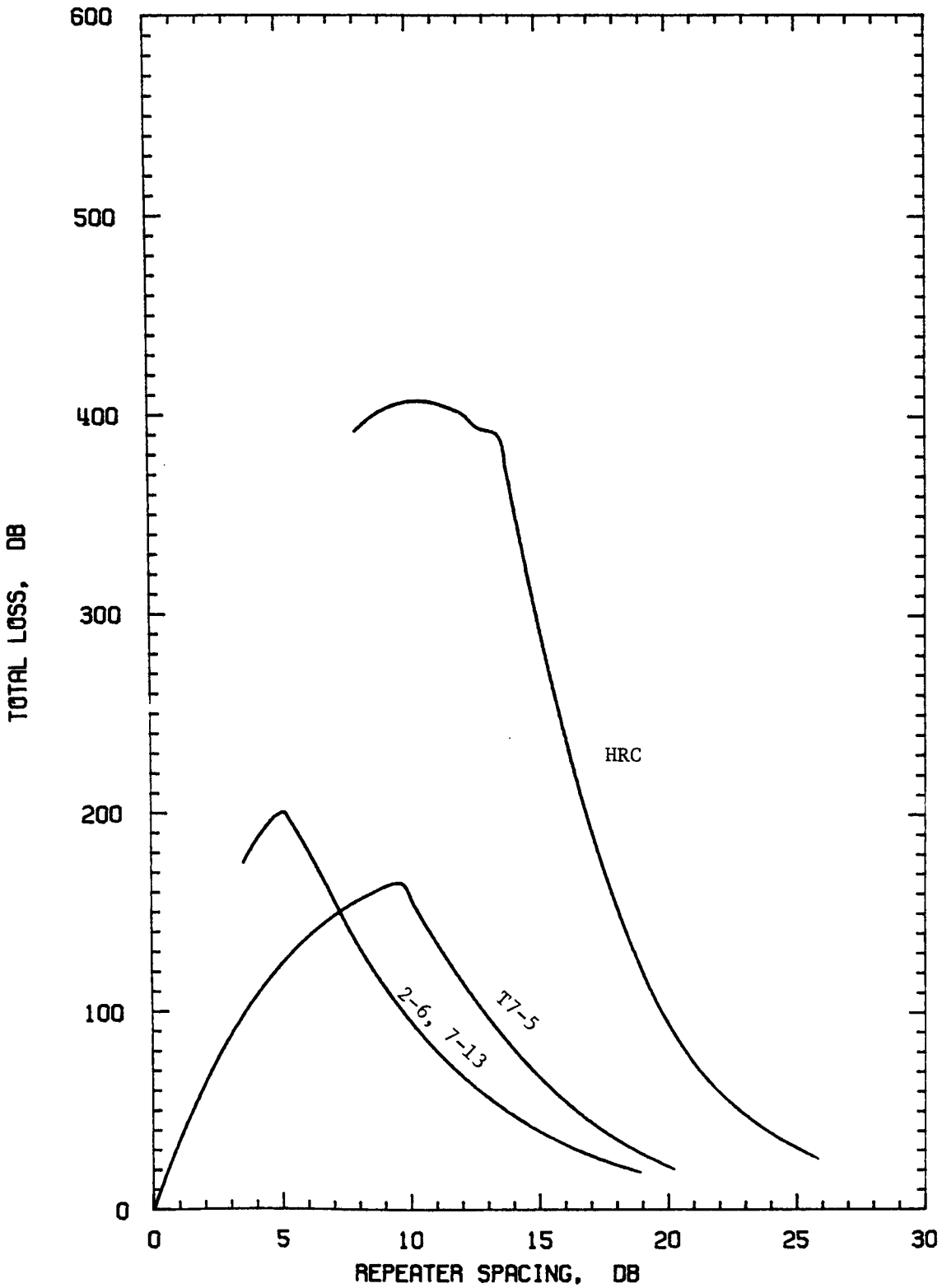

Figure 4.17 12-Channel Systems Laser-2 (-70,-70), 20 log N Law

Table 4.5

HIGH QUALITY TRANSPORTATION TRUNKS

Signal-to-noise ratio	56 dB
Crossmodulation	-61 dB
Single Frequency Interference	-6 dB*
Differential Gain	±0.4 dB
Differential Phase	±0.5°

*-9dB is added to the BP-23 curve.

Table 4.6

MEDIUM QUALITY TRANSPORTATION TRUNK
VIDEO TRANSMISSION PERFORMANCE REQUIREMENTS

Signal-to-noise ratio	46 dB
Crossmodulation	-51 dB
Single Frequency Interference	-60 dB*
Differential Gain	±1.0 dB
Differential Phase	±2.5°

*-3 dB is added to the BP-23 curve.

For these requirements, the total system losses are evaluated considering the four light sources.

Figures 4.18 through 4.21 correspond to medium quality transportation trunks and Figures 4.22 through 4.25 to high quality transportation trunks.

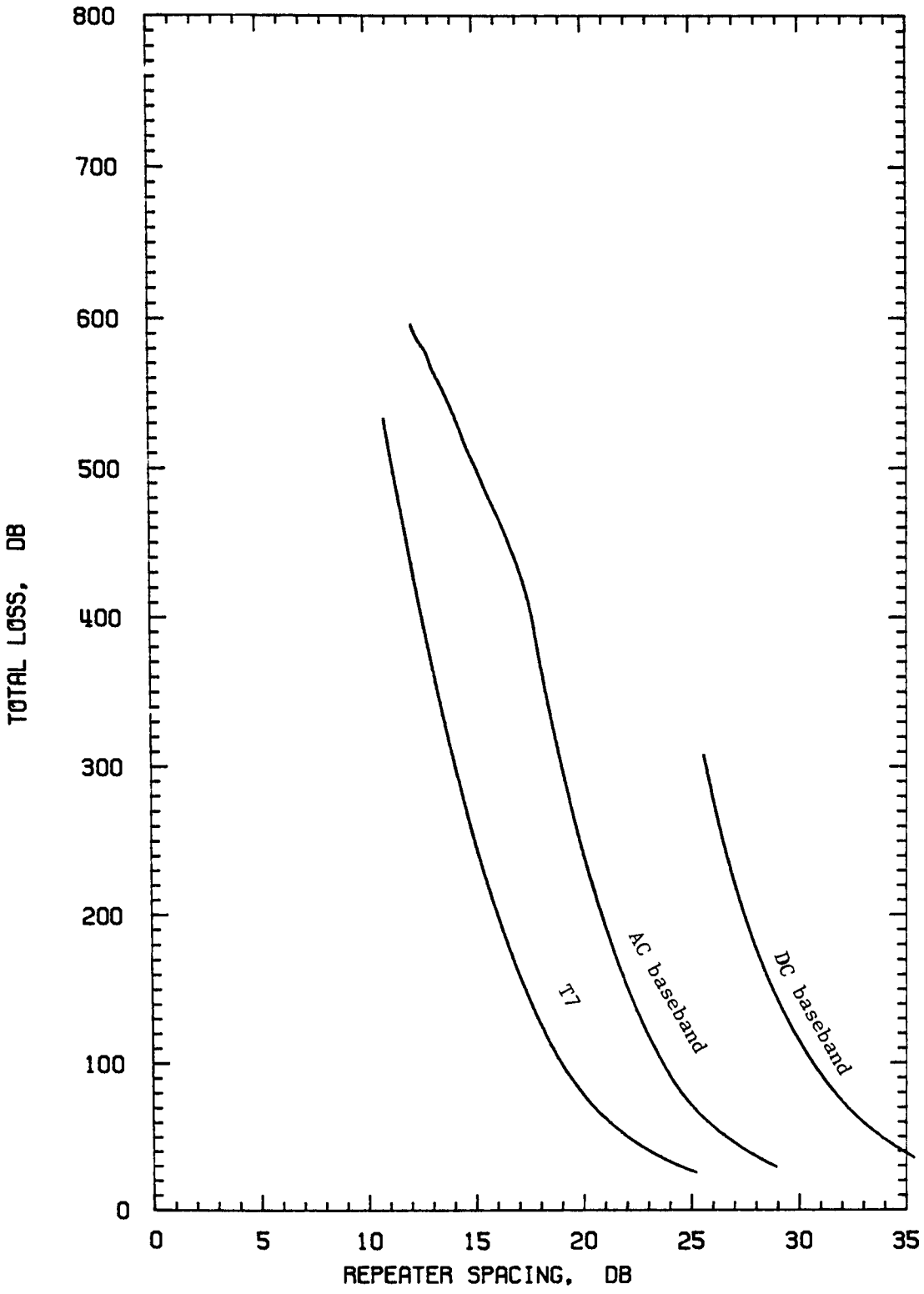

Figure 4.18-Medium Quality Transportation Trunk:
LED-1 (-30, -60)

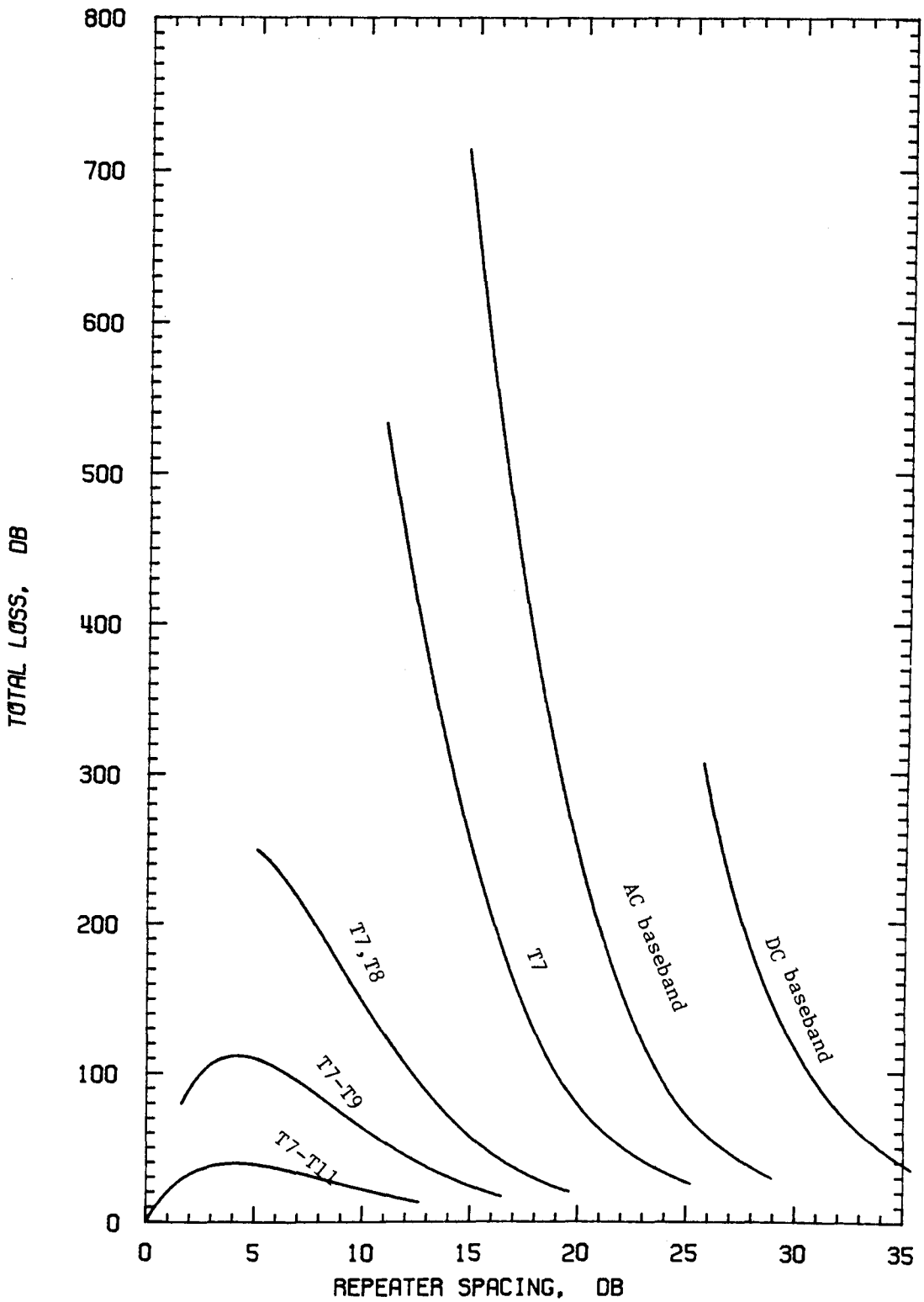

Figure 4.19 Medium Quality Transportation Trunk: LED-1 (-70, -70)

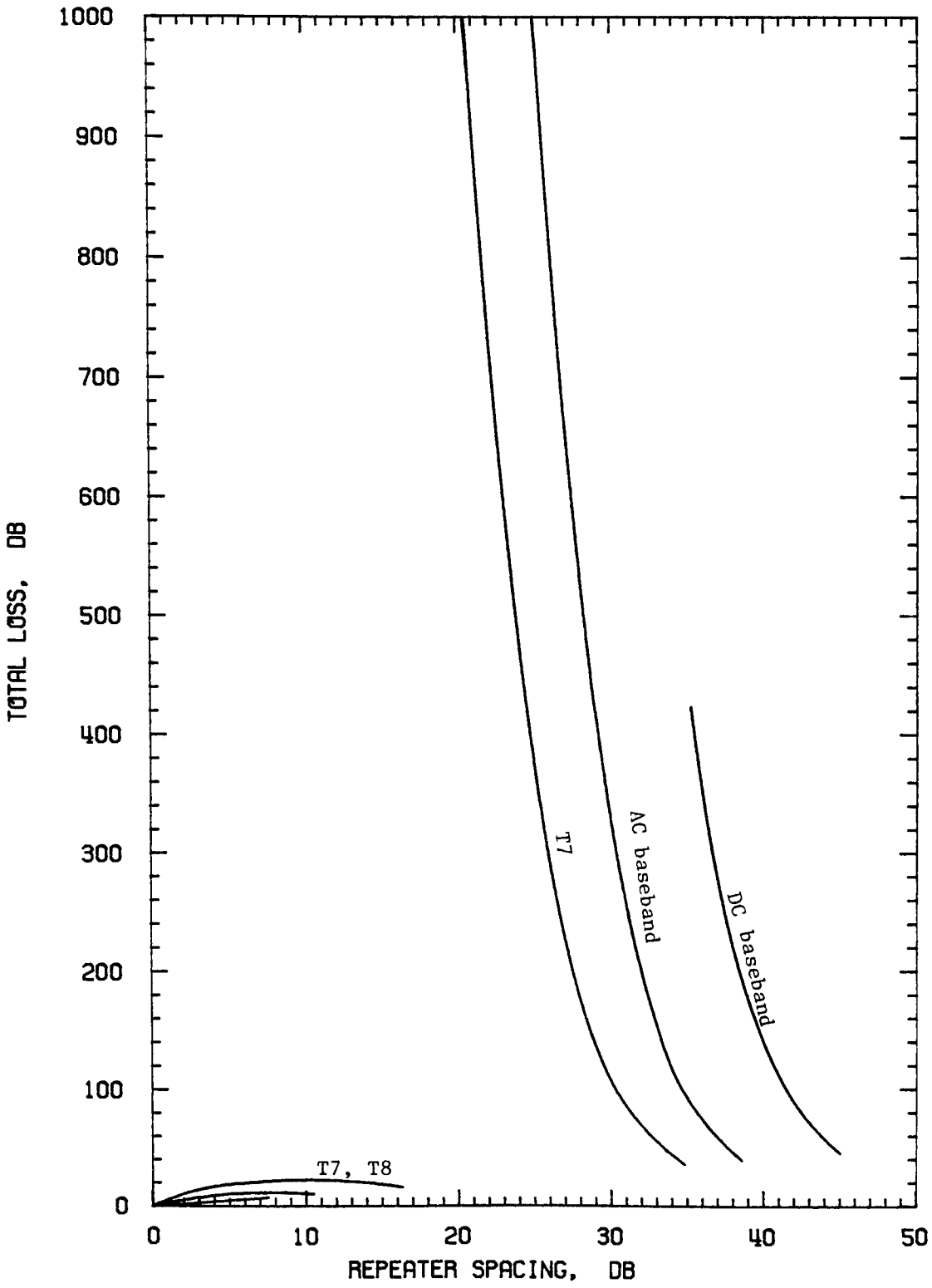

Figure 4.20 Medium Quality Transportation Trunk: Laser-1 (-36, -48)

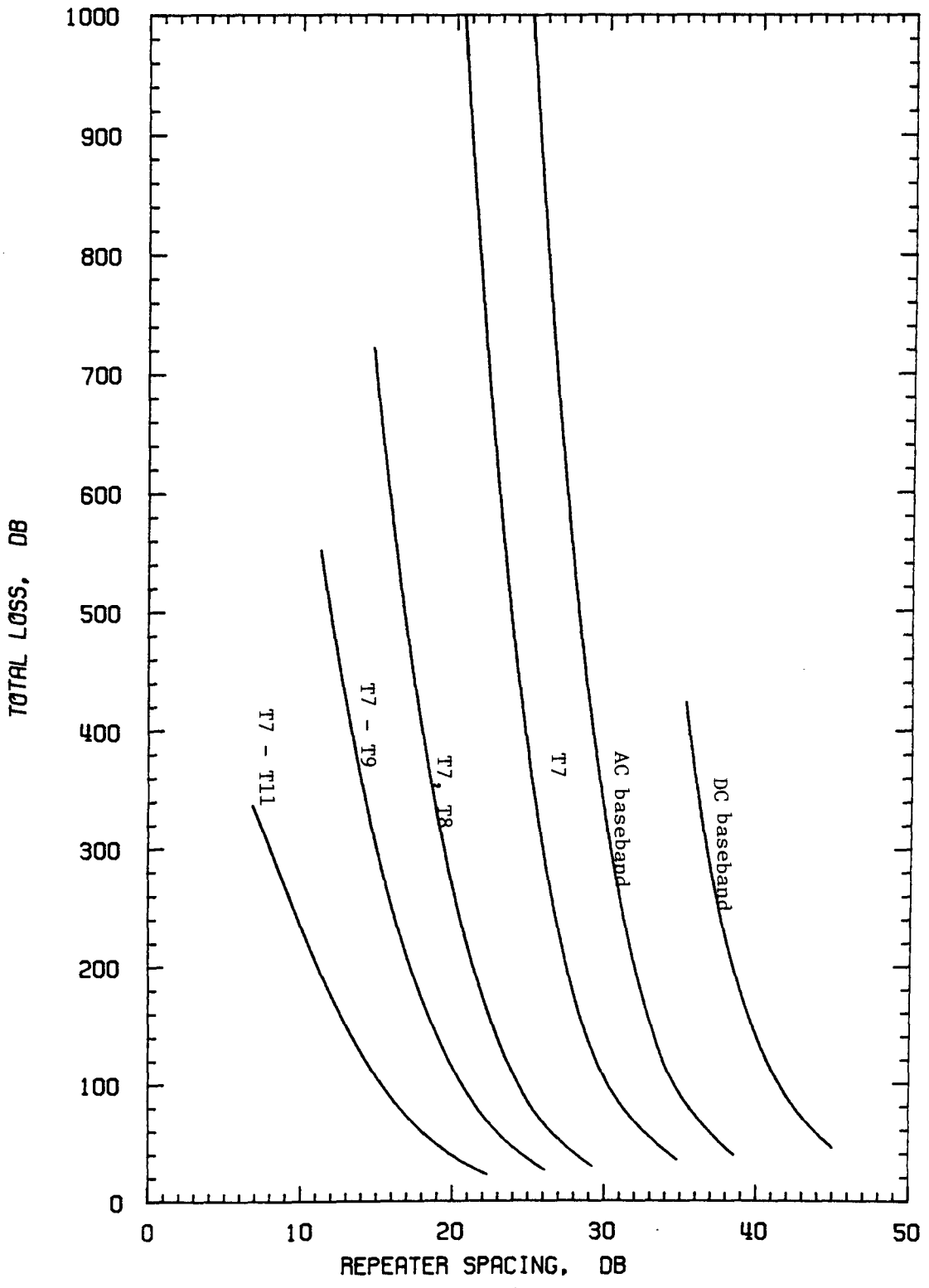

Figure 4.21 Medium Quality Transportation Trunks: Laser-2 (-70, -70)

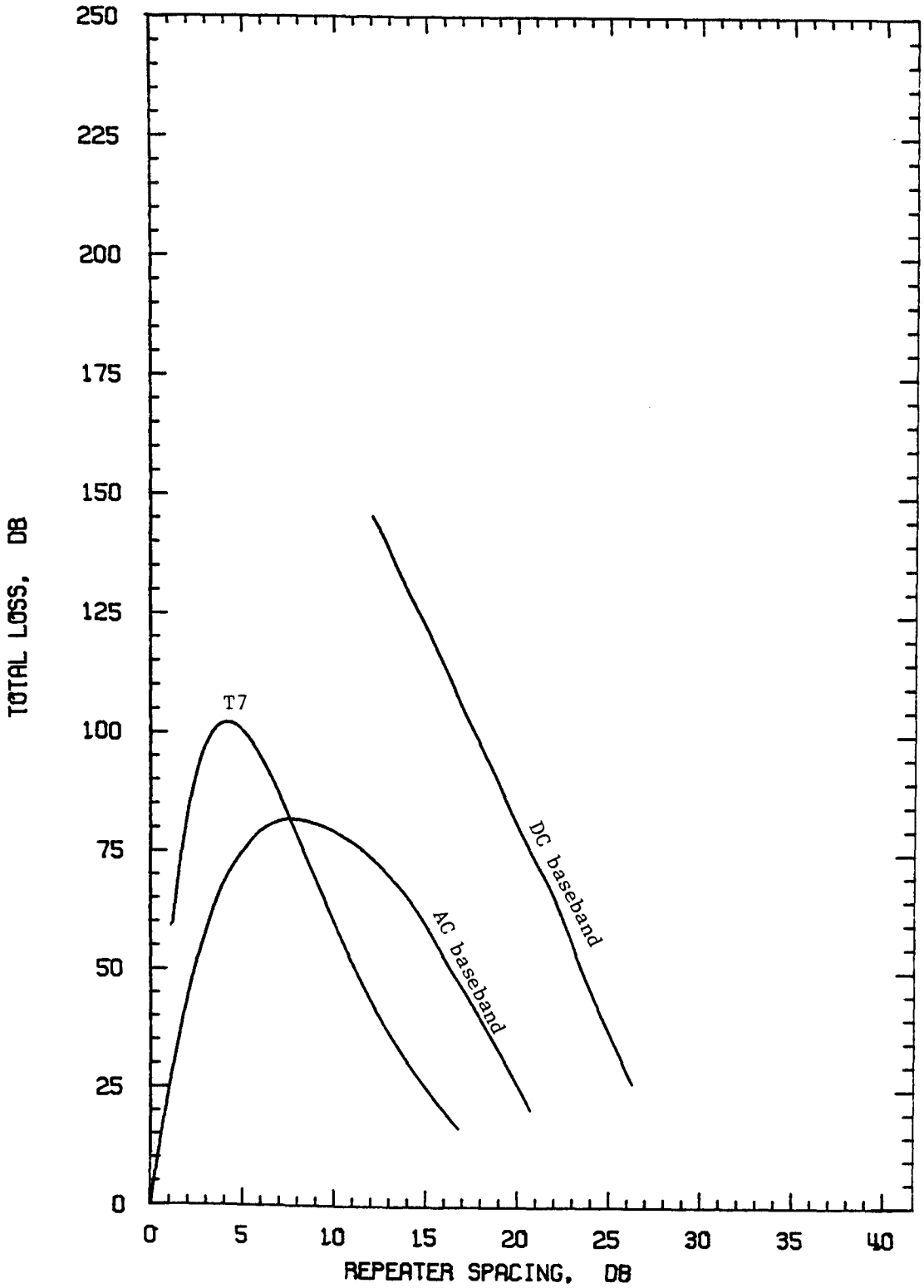

Figure 4.22 High Quality Transportation Trunks: LED-1 (-30, -60)

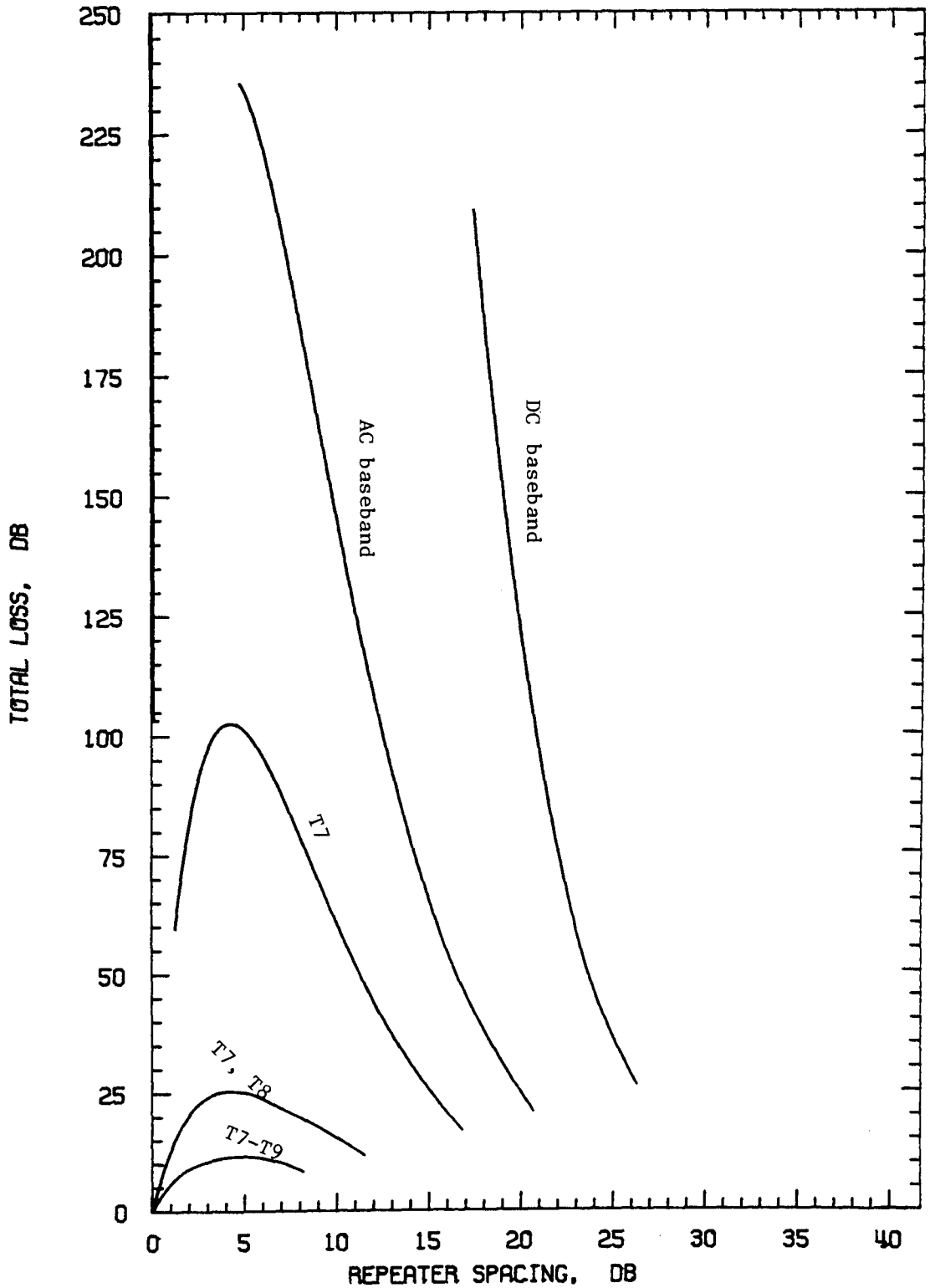

Figure 4.23 High Quality Transportation Trunks: LED-2 (-70, -70)

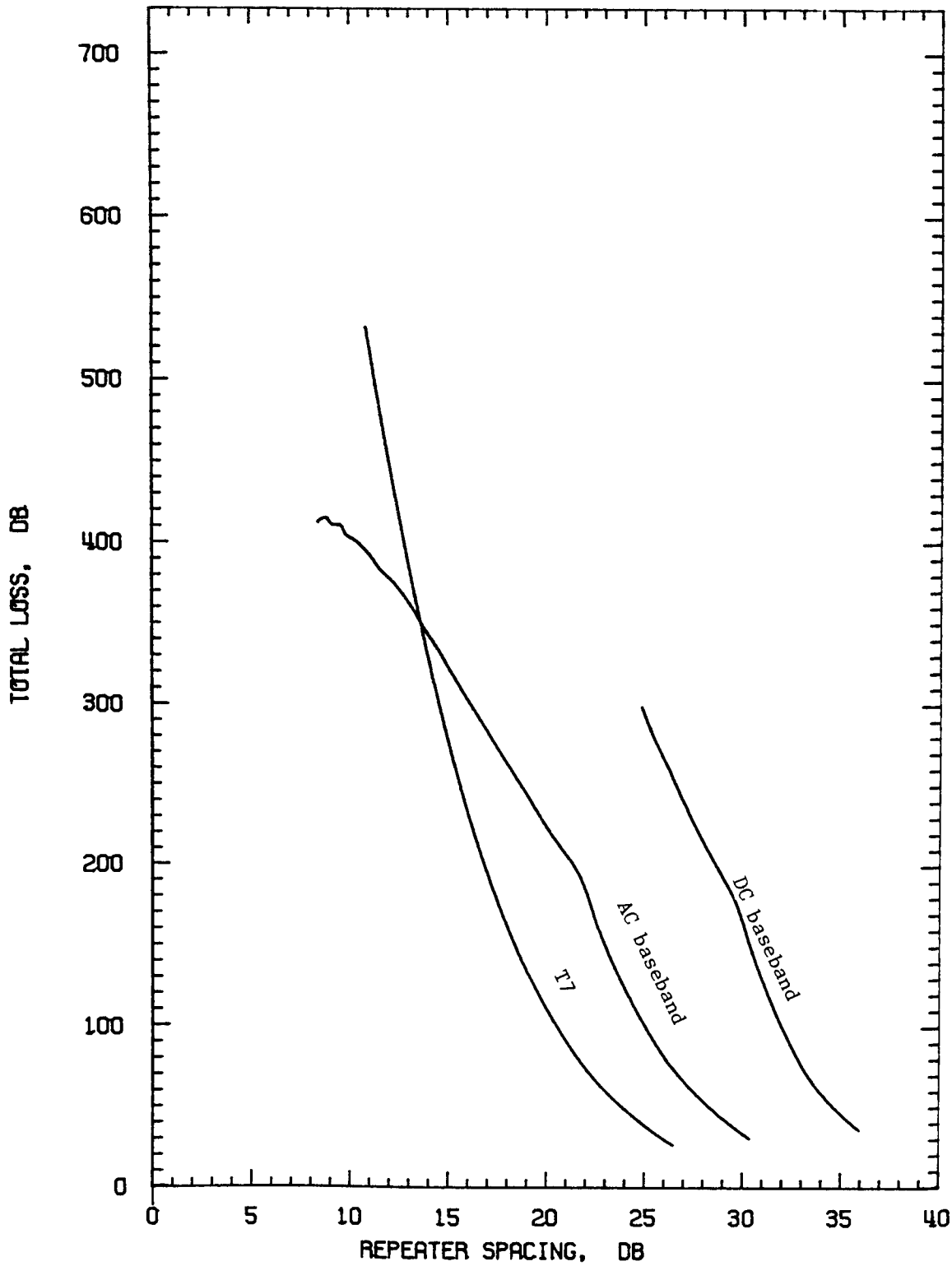

Figure 4.24 High Quality Transportation Trunks: Laser-1 (-36, -48)

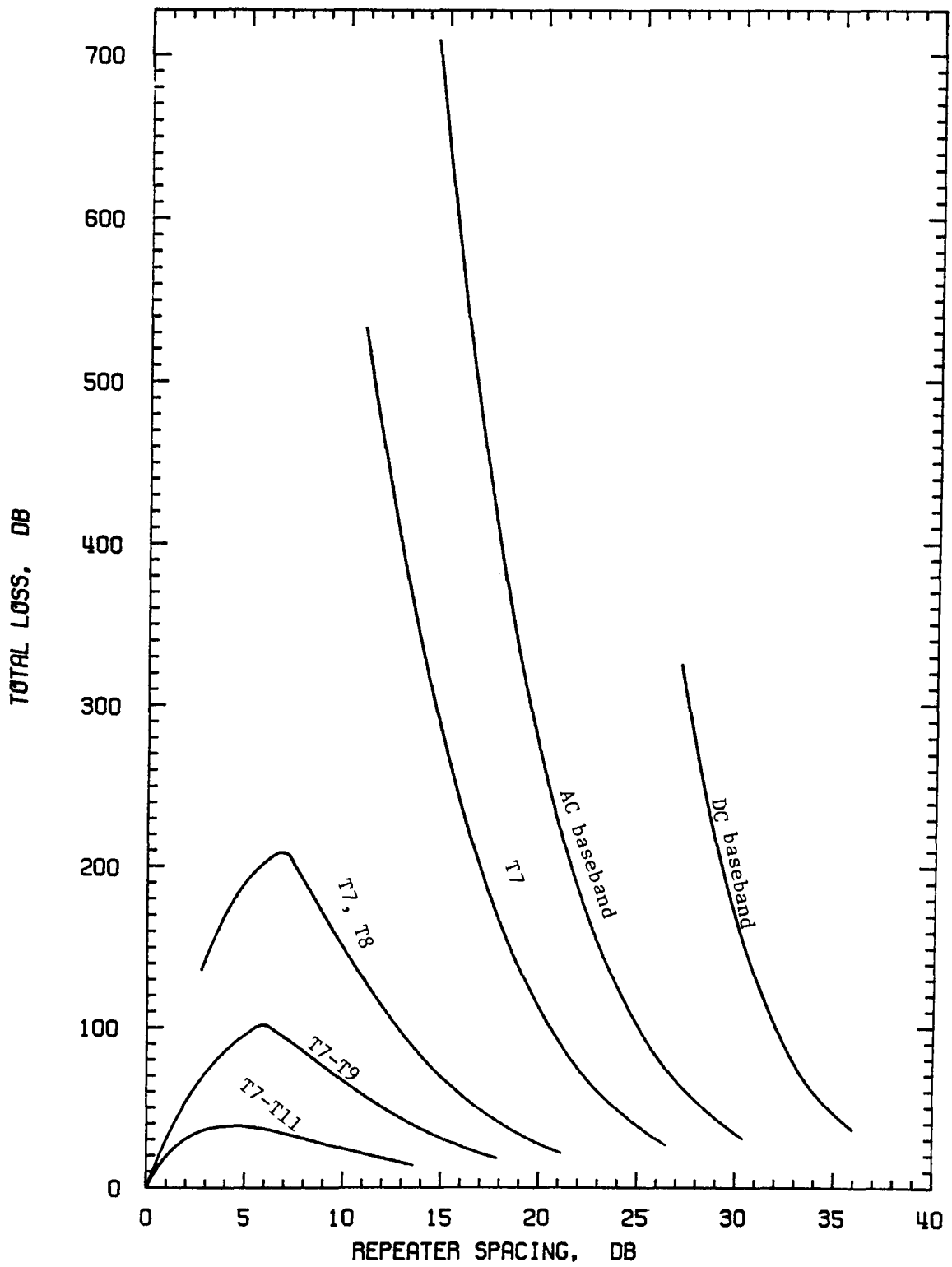

Figure 4.25 High Quality Transportation Trunks: Laser-2 (-70, -70)

For high quality transportation trunks, a single-channel transmission should be preferable for long systems. For lines having a high number of sources in tandem, the transmission on a modulated carrier is preferred because it is less sensitive to differential gain than baseband transmission.

5. DIGITAL VIDEO TRANSMISSION

Digital video transmission can be used for transportation trunk applications. Its use for the distribution of signals to the subscribers is unattractive at the moment because of the codec price level. Pulse Position Modulation was attractive when CW lasers did not exist and the available lasers were limited to low duty cycles. (See Appendix A). Now since CW lasers are available Pulse Code Modulation (PCM) is preferred.

Many coding schemes for video are proposed with different sampling frequencies and different code word lengths. The number of bits per code word sets the level of the quantization noise. For an 8-bit code word, the equivalent peak-to-peak signal over the rms noise ratio equals 54.8 dB.[37] For each bit reduction in the code word length the signal-to-noise ratio decreases by 6 dB. Therefore, an 8-bit code word should be used for high quality transportation trunks. A sampling frequency equal to three times the frequency of the color subcarrier is often used (10.74 MHz). NTSC video signals can also be sampled at sub-Nyquist frequencies due to the discrete nature of the video specturm which consists of harmonics of the line frequency.[38] The sampling frequency must be a harmonic of the quarter-line frequency in order that alias components caused by the sub-Nyquist sampling be removed by comb filtering. The proposed sampling frequencies are twice the color subcarrier frequency, plus or minus one-quarter of the line frequency.

Another way of reducing the transmission rate is to encode only the active area of the picture signal. The parts of the signal that are used for timing or for indicating a reference level do not need to be transmitted in digital video transmission. Therefore, a bit reduction of 20 percent can be achieved by transmitting only the active area of the picture signal.[39]

Differential pulse code modulation (DPCM) is another means of reducing the transmission rate. DPCM encodes the difference between the amplitide of a sample and a prediction based on previously encoded samples. However, it should be noted that all bit-rate reduction techniques are associated with an increase in the codec complexity. Therefore, a tradeoff between ease of transmission and codec complexity exists. Possible bit rates for high and medium quality transportation trunks are listed in Table 5.1.

The tolerable error rate in digital video transmission if the errors are not correlated is 10^{-7}.[40] This figure was obtained for the transmission of PAL video signals. However, the value for NTSC video signals should not differ significantly.

Table 5.1

BIT RATES FOR DIGITAL VIDEO TRANSMISSION

A. High Quality Transportation Trunks

CODING METHOD	BITS/ SAMPLE	SAMPLING FREQUENCY MHz	BIT RATE Mbps
PCM	8	10.74	85.6
PCM Sub-Nyquist	8	7.16	57.2
PCM Sub-Nyquist Active Area	8	7.16	45.8
DPCM	5	10.74	53.5
DPCM Active Area	5	10.74	42.8

B. Medium Quality Transportation Trunks

CODING METHOD	BITS/ SAMPLE	SAMPLING FREQUENCY MHz	BIT RATE Mbps
PCM	6	10.74	64.2
PCM Sub-Nyquist	6	7.16	42.9
PCM Sub-Nyquist Active Area	6	7.16	34.4
DPCM	5	7.16	35.8
DPCM Active Area	5	7.16	28.6

Transmission Performance

The transmission performances are evaluated assuming that the detector amplifier is a high-impedance front-end FET amplifier followed by an equalizer. For the higher bit rates considered, a FET amplifier may not be optimum, but for the purposes of this report, an approximation of the attainable performance is adequate.

The peak signal-to-noise ratio is expressed by[41]

$$SNR = \frac{\left(\frac{\eta e G}{h\nu}\right)^2 p^2}{\left[2\frac{kT}{h\nu} + eI_L + eG^2F_D I_D + \frac{e^2}{h\nu}\eta G^2 F_D P_{avg} + \frac{S_e}{R_{eq}^2}\left(1 + \left(\frac{\tau_1}{\tau_2}\right)^2\right)\right]\frac{1}{4\tau_2}} \quad (5.1)$$

where

p = peak optical power

s_e = double-sided power spectral density of the amplifier noise

$s_e = 2.8kT/gm$

g_m = FET transconductance

τ_1 = time constant of the high-impedance front end

$\tau_1 = R_{eq} C_{eq}$

τ_2 = time constant of the equalizer poles

The transfer function of the equalizer is

$$H_{eq} = \frac{1 + j\,w\,\tau_1}{(1 + j\,w\,\tau_2)^2} \quad (5.2)$$

τ_2 is adjusted for a -3 dB electrical bandwidth of the total system equal to the bit rate.

For a decision threshold corresponding to half of the peak power, the probability of error can be expressed by

$$P_e = \frac{1}{2} \operatorname{erfc}\left(\frac{1}{2}\sqrt{\frac{SNR}{2}}\right) \qquad (5.3)$$

For the transmission rates listed in Table 5.1, the corresponding repeater spacings are evaluated assuming square pulses with a 50 percent duty cycle and no line coding. The assumptions for the hardware characteristics are summarized in Table 5.2. The results are given in Table 5.3 in terms of the repeater spacing optical loss for different numbers of repeaters. The repeaters are assumed to be of the regenerative type. Therefore, the errors add from one repeater section to the other.

Table 5.2

HARDWARE CHARACTERISTICS

PARAMETER	VALUE	UNIT
Peak Power Coupled in the Fiber	2.04	mW
R_{eq}	1.0	MΩ
C_{eq}	0.12	pf
g_m	0.015	mhos
η	0.85	-
G	optimum (k=0.03)	-
I_L	1.0	nA
I_D	0.05	nA

Table 5.3

DIGITAL VIDEO TRANSMISSION
REPEATER SPACING OPTICAL LOSS (dB)

A. High Quality Transportation Trunks

TRANSMISSION RATE Mbps	NUMBER OF REPEATERS		
	1	10	100
85.6	53.9	53.3	52.8
57.2	55.6	55.0	54.4
45.8	56.4	55.9	55.3
53.5	55.8	55.2	54.7
42.8	56.7	56.10	55.6

B. Medium Quality Transportation Trunks

TRANSMISSION RATE Mbps	NUMBER OF REPEATERS		
	1	10	100
64.2	55.1	54.5	54.0
42.9	56.7	56.11	55.6
34.4	57.6	57.0	56.5
35.8	57.4	56.8	56.3
28.6	58.3	57.7	57.2

Since digital transmission is very sensitive to variation in SNR in this region of the error rate curve, a link margin factor should be included to take account of possible changes in the equipment performance while in operation. The magnitude of this safety factor depends on the tolerance associated with every component of the system.

Furthermore, the intersymbol caused by the fiber dispersion is not considered here. This could be a significant factor, especially for the higher transmission rates listed in Table 5.1. Based on noise considerations only, the repeater spacing is not very sensitive to variations of the transmission rate, six percent decrease when the rate is doubled (Table 5.3). Therefore the fiber dispersion could be the most significant factor in the choice of a transmission rate. Based on noise considerations, digital transmission is practically immune from the repeater cascading effect. This makes digital video transmission particularly suited for long-haul high-quality transportation trunks.

6. FM VIDEO TRANSMISSION

The frequency modulation of the intensity of a light source is an attractive modulation scheme when noise and source linearity are limiting factors. The signal-to-noise ratio of a baseband video channel that is FM-transmitted is (in terms of the BTL definition),

$$SNR_{BTL} = 24\ \beta^2\ \frac{I^2_C}{I^2_{NFM}} \qquad (6.1)$$

where β is the modulation index, I^2_C the carrier rms power, and I^2_{NFM} the rms noise power in an FM band centered at the carrier equal to twice the baseband bandwidth. Relating this SNR expression to the NCTA SNR definition and including a 2.5 dB that can be gained by using pre- and de-emphasis,[42]

$$SNR_{NCTA} = \frac{\left(\frac{\eta e G}{h\nu}\right)\ \frac{m_I^2 P_{DC}^2}{2}\ \beta^2}{2\left(N_T + N_Q + N_D + N_L + N_B\right) N} + 20.3\,dB \qquad (6.2)$$

Thus FM transmission represents a signal-to-noise ratio improvement over AM-VSB transmission for the same peak-to-peak driving current of,

$$\frac{SNR_{FM}}{SNR_{AM}} = 17.3 + 20 \log \beta \qquad (6.3)$$

The value of β is limited by the tolerable bandwidth expansion. The bandwidth that contains about 98 percent of the signal power can be approximated for a NTSC video channel by

$$B = 2\ (\beta + 1)\ 4.2\ \text{MHz} \qquad (6.4)$$

when the modulation index is low ($\beta << 1$). For the higher values of modulation index the significant bandwidth can be approximated by[43]

$$B = 2\ (\beta + 2)\ 4.2\ \text{MHz} \qquad (6.5)$$

Therefore, the system bandwidth should be greater than 1.5 B.

The total optical loss of a high quality transportation trunk is given in Table 6.1 as a function of the modulation index and the number of repeaters. The same hardware characteristics that are assumed in Section 4 are considered. Similarly, the total optical loss of a medium quality transportation trunk is given in Table 6.2.

Table 6.1

FM HIGH QUALITY TRANSPORTATION TRUNKS
(SNR = 56 dB) SYSTEM TOTAL OPTICAL LOSS (dB)

NUMBER OF REPEATERS	FM MODULATION INDEX					
	β=0.3		β=1.0		β=2.0	
	LED	LASER	LED	LASER	LED	LASER
1	22	32	32	41	37	46
3	54	83	81	110	98	127
5	81	129	125	174	153	201
10	138	234	223	319	277	373
20	226	419	391	583	499	692
40	344	730	672	1058	887	1273

Table 6.2

FM MEDIUM QUALITY TRANSPORTATION TRUNKS
(SNR=46 dB) SYSTEM TOTAL OPTICAL LOSS (dB)

NUMBER OF REPEATERS	FM MODULATION INDEX					
	β=0.3		β=1.0		β=2.0	
	LED	LASER	LED	LASER	LED	LASER
1	31	41	40	50	45	55
3	81	110	109	138	124	153
5	124	173	171	220	197	245
10	221	318	316	412	368	465
20	338	582	575	768	682	875
40	675	1062	1039	1425	1256	1642

The system length increases with the FM modulation index; varying β from 0.3 to 2.0 results in an improvement of 14 dB in the repeater spacing optical loss. The increase thermal noise due to the bandwidth extension with the modulation does not have a significant effect. However, the fiber frequency response should be considered, especially in LED systems where the performance could be limited by the line equalizer performance rather than by signal-to-noise ratio considerations.

For high quality transportation trunks, FM transmission with a modulation index of 0.3 does not represent any advantage compared to ac baseband transmission. The break-even point corresponds to a FM modulation index of about 1.0. However, transmission on a modulated carrier is preferred for long trunks (Section 4.3). In this case, FM

transmission represents a 5- to 6-dB improvement in the repeater spacing optical loss for an FM modulation index of 0.3.

For medium quality transportation trunks, FM transmission with a modualtion index of 0.3 already represents a marginal benefit over ac baseband transmission. The benefit is partly due to the fact that higher avalanche gains can be used for medium quality trunks than can be used for high quality trunks.

For a nonrepeatered line, the line optical loss for FM transmission is about 10 dB less than for digital transmission. However, FM transmission is subject to the compounding of noise with the number of repeaters. Therefore, digital transmission should be preferred for long repeatered transportation trunks, notwithstanding the tradeoff between digital codecs and FM head-end equipment.

REFERENCES

1. G. Comber, I.F. Macdiarmid
"Long-term Step Response of a Chain of AC-coupled Amplifiers"
Electronics Letters, 27 July 1972, Vol 8, No 15.

2. AT&T
"Telecommunications Transmission Engineering"
Vol. 3, 1975

3. J.P. Wittke, M. Ettenberg, H. Kressel
"High Radiance LED for Single-Fiber Optical Links"
RCA Review, Vol 37, June 1976

4. F.D. King, J. Straus, O.I. Szentesi, A.J. Springthorpe
"High-radiance Long-lived LED's for Analogue Signalling"
Proc. IEE, Vol 123, No 6, June 1976

5. M. Ettenberg, H. Kressel, I. Ladamy, H.F. Lockwood
"Injection Lasers and LED's for Optical Communications"
EASCON '76, Paper 117

6. E. Weidel
"Light Coupling Problems for GaAs Laser-Multimode Fibre Coupling"
Optical and Quantum Electronics 8 (1976)

7. T. Ozeki, B.S. Kawasaki
"Efficient Power Coupling Using Taper-Ended Multimode Optical Fibers"
Electronics Letters, 11 November 1976

8. W. M. Hubbard
"Utilization of Optical-Frequency Carriers for Low and Moderate Bandwidth"
BSTJ, Vol 52, No 5, May-June 1973

9. BNR
"A Systems Study of Fibre Optics for Braodband Communication: State-of-the-Art Review"
TR6259, April 1977

10. J. Conti, M.J.O. Strutt
"Optical Fluctuations of Light Emitting Diodes"
IEEE Journal of Quantum Electronics, QE-8, October 1972

11. W. Bolleter, J. Conti, G. Guekos, G. Tenchio
"Noise Correlation and Noise Reduction in GaAs Light-Emitting Diodes"
Solid-State Electronics, 1976, Vol 19, pp. 319-324

12. T. L. Paoli
"Noise Characteristics of Stripe-Geometry Double-Heterostructure Junction Lasers Operating Continuously - I. Intensity Noise at Room Temperature"

13. G. Tenchio
"Low-Frequency Intensity Fluctuations of C.W.D.H. GaAlAs-Diode Lasers"
Electronics Letters, 24 October 1976, Vol 12, No 21

14. T. M. Straus
"The Relationship Between the NCTA, EIA, and CCIR Definitions of Signal-to-Noise Ratio"
IEEE Transaction on Broadcasting, BC-20, No 3, September 1974

15. I. Switzer
"Phase Phiddling"
NCTA 74, Convention transcripts

16. R. J. McIntyre, J. Conradi
"The Distribution of Gains in Uniformly Multiplying Avalanche Photodiodes: Theory and Experimental"
IEEE Trans Electron Devices, ED-19, June 1972

17. Y. Takasaki, M. Maeda
"Receiver Designs for Fiber Optic Communications Optimization in Terms of Excess Noise Factors that depend on Avalanche Gain"
IEEE, Trans on Communications, December 1976

18. T. Ozeki, E. H. Hara
"Measurement of Nonlinear Distortion in Photodiodes"
Electronics Letters, 5 February 1976, Vol 12, No 3

19. J. Straus, private communication

20. J. Straus, O.I Szentesi
"Linearized Transmitters for Optical Communications"
IEEE Conference on Circuits and Systems, April 25-27
Phoenix, Arizona

21. Department of Communications
"Proof of Performance Procedure for Cable Television (CATV) Systems"
BP-24, Issue 1, August 1971

22. K. A. Simons
"The Decibel Relationship Between Amplifier Distortion Products"
IEEE Proceedings, Vol 58, No 7, July 1970

23. L. G. Cohen, D.S. Personick
"Length Dependence of Pulse Dispersion in a Long Multimode Optical Fiber"
Applied OPtics, June 1975, Vol 14, No 6

24. K. Y. Chang
"Nonlinear Distortion of Amplifiers and its Application to Analog Coaxial System Design"
BNR, TR2C40-3-73, October 1973

25. K. A. Simons, op. cit.

26. D. Chan, private communication

27 O. I. Szentesi, A. J. Szanto
"Fiber Optics Video Transmission"
SPIE/SPSE Tech Symposium, Reston, Virginia, March 22-23, 1976

28. G. D. Hillman, private communication

29. S. E. Miller, E. A. J. Marcatili, T. Li
"Research Toward Optical-Fiber Transmission Systems, Part 1: The Transmission Medium"
IEEE Proceedings, December 1973

30. D. Keck
"Fundamentals of Optical Fiber Communications"
Chapter 1, Academic Press, 1976

31. L. G. Cohen, H. W. Astle, I. P. Kaminov
"Frequency Domain Measurements of Dispersion in Multimode Optical Fibers"
Applied Physics Letters, Vol 30, No 1, January 1977

32. See Ref. 29

33. J. A. Arnaud
"Beam and Fiber Optics"
Academic Press, 1976

34. See Ref. 27

35. T. Witkowicz, private communication

36. See Ref. 20

37. A. A. Goldberg
"PCM Encoded NTSC Color Television Subjective Tests"
SMPTE Journal, Vol 82, No 8, August 1973

38. J. P. Rossi
"Sub-Nyquist Encoded PCM NTSC Color Television"
SMPTE Journal, Vol 85, No 1, January 1976

39. D. Connor
"Digital Television at Reduced Bit Rates"
Digital Video, published by SMPTE, March 1977

40. V. G. Devereux
"Application of PCM to Broadcast Quality Video Signals. Part 2: Subjective Study of Digit Errors and Timing Jitter"
The Radio and Electronic Engineer, Vol 44, No 9, September 1974

41. M. Redman, K.Y. Chang, private communication

42. CCIR Report AD/CMTT
Conclusions of the Interim Meeting of CMTT
Geneva, July 5-18, 1972

43. P.H. Panter
"Modulation, Noise, and Spectral Analysis"
Chapter 7, McGraw-Hill, 1965

APPENDIX A: PULSE POSITION MODULATION

BY N. TOMS

A.1

Pulse position modulation (PPM), encodes the instantaneous amplitude of a signal as the time delay between the transmission of an impulse and some reference time. It is classified as a form of block orthogonal coding (ref. A.1)

There are two main attractions in the use of PPM for optical communications. The first is that since PPM is a binary code, the light sources used to transmit it do not need to be linear. The second advantage is that PPM only requires the light source to operate at a low duty cycle.

The main disadvantage of PPM is that it requires a very large bandwidth. Ref. A-1 shows that a 100 bits/s may need a bandwidth of 10^{30} Hz for comparable error rate performed using PPM. With analogue systems there is a trade-off between the SNR of the detected signal and the bandwidth expansion used for PPM. By bandwidth expansion is meant the ratio of the bandwidth of the PPM signal to that of the baseband signal. The rest of this appendix will be concerned with the calculation of the SNR of a PPM system as a function of bandwidth expansion and power at the detector.

A.2 Computation of bandwidth expansion vs SNR for a 5 MHz signal.

The present report considers the transmission of a 5 MHz signal, approximating a TV signal, by PPM. The PPM version of this signal is used to modulate a light source, which may be a laser or LED. After attenuation this optical signal is detected by an avalanche photodetector. (A PIN photodiode may be modelled by an avalanche photodetector operating at a gain of unity). Although the bandwidth of the transmission medium between source and detector is not explicitlyincluded in the calculations it may be regarded as a factor limiting the bandwidth expansion.

The analysis on which the present calculations is based is due to Hubbard (ref. A.2), and the reader is referred there to study the assumptions underlying the analysis. Unfortunately, ref.A2 suffers from many misprints, and the crucial equation (15) should read:

$$SNR = \frac{\frac{\Pi^2}{2}(K-1)^2 \frac{ne}{h\nu} KP_o{}^2 G^2}{\langle i_n{}^2 \rangle + \frac{8\Pi^2}{3\sqrt{3}}(K-1)^3 \frac{ne}{h\nu} KP_o{}^2 G^2 e^{-XNR/2}} \qquad (A.1)$$

SNR = signal to noise ratio of the PPM

K = a measure of bandwidth expansion = T/2t, where

T = Nyquist sampling interval for the baseband signal, and

2t= full width of PPM pulse. It follows that the bandwith B, of a PPM signal = 45B', where B' is the bandwidth of the baseband signal

η = quantum efficiency of the photodetector.

e = charge of an electron.

h = Planck's constant.

ν = frequency of the light used.

P_o = average received optical power at the photodetector.

G = avalanche gain of photodetector (=1 for a PIN diode).

$\langle i_n^2 \rangle$ = mean square noise voltage (incorporating quantum noise, thermal noise in the resistors and dark currents.

XNR = $i_m^2/4\langle i_n^2 \rangle$, where i_m: peak signal level.

Finally, one minor change has been made from Hubbards' analysis--the quantum noise is calculated at the signal level corresponding to the decision threshold, and not at the peak level. This has a comparatively minor effect on the actual numbers obtained. Also, beat noise has been ignored in the present calculation.

Hubbard assumes the following characteristics for the system:

$\lambda = 0.85\ \mu m$

Dark current = 10^{-9} A

Leakage current = 10^{-8} A

$\eta = 0.5$

Input impedance = 1000 ohms

These values have been maintained, and a baseband signal bandwidth of 5MHz has been used as already mentioned. The 1000 ohm input impedance assumed above may be challenged, since in a practical system the input impedance is a function of bandwidth, decreasing with increasing bandwidth. With 1pf input capacitances available in present avalanche diodes, 1000 ohms gives a 3dB bandwidth of 1GHz. Thus, some improvement in SNR for low bandwidth expansions can be obtained by using larger values of input impedance. This refinement is not included in the present study.

To bring out the general trends of a PPM system as a function of P_o (power at detector) and K (bandwidth expansion), eq. A.1 may be written:

$$SNR \approx \frac{A\,K^3\,P_o^2}{B + CKP_o + DP_o^2\,K^4\,e^{-EKP_o^2}} \qquad (A.2)$$

where all the constants are derived from fundamental physical constants, or from the parameters stated above. For G = 1 and the above parameters:

$A = 0.5792$

$B = 3.2378 \times 10^{-16}$

$C = 2.1963 \times 10^{-12}$

$D = 1.7835$

$E = 1.8126 \times 10^{14}$

From equation A.2 it may be seen that, for a fixed avalanche gain and for large K, SNR varies as K^2. (The physical limitation here is the assumption that peak power from the light source can increase indefinitely as long as the average power is constant.) However, due to the exponential term in the denominator, it can happen that SNR varies as $\frac{1}{K}$ up to a certain value of K. The effect is obvious from the results plotted in fig. A.1 for a system using a PIN photodiode (avalanche gain = 1). Here the SNR (defined as r.m.s. signal power to r.m.s. noise) is plotted against bandwidth for various power levels incident on the detector. For values of Po = 10nW and 1nW, the SNR appears to decrease with increasing K due to the dominance of the exponential term in the denominator. Extended calculation shows that for Po = 10nW the SNR begins to increase for bandwidths over 1000MHz (K greater than 50), while for Po = 1nW the turning point is not reached till a bandwidth of 10,000 MHz (K = 500) has been passed.

In the case of avalanche gain, the general trend of SNR increasing with bandwidth still holds, but the dependence of the constants A, B, C, D, E above on G, which is itself a function of bandwidth and signal power, invalidates the simple argument above. Fig. A.2 plots the results for the optimum avalanche gain case. A point which arises is that the optimum gain for many points corresponding to Po = 100μW is less than unity, and hence unrealistic. The values of optimum avalanche gain are shown in Fig. A.3. (The optimum gain is caluculated as set out by Hubbard by differentiating the SNR expression as a function of gain, and setting differentiated expression to zero).

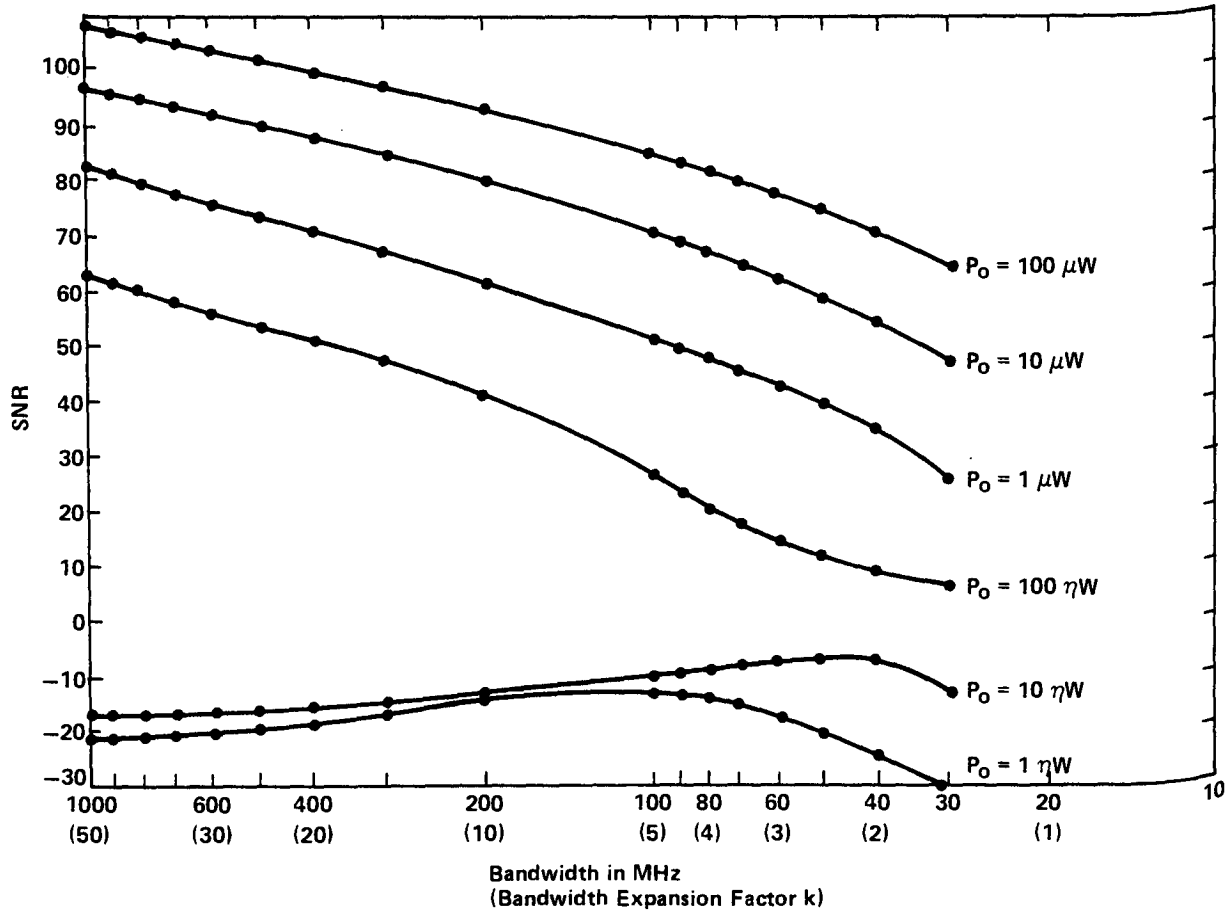

Figure A.1: SNR (r.m.s. Signal to r.m.s. Noise) V Bandwidth for PPM Systems (PIN Detector)

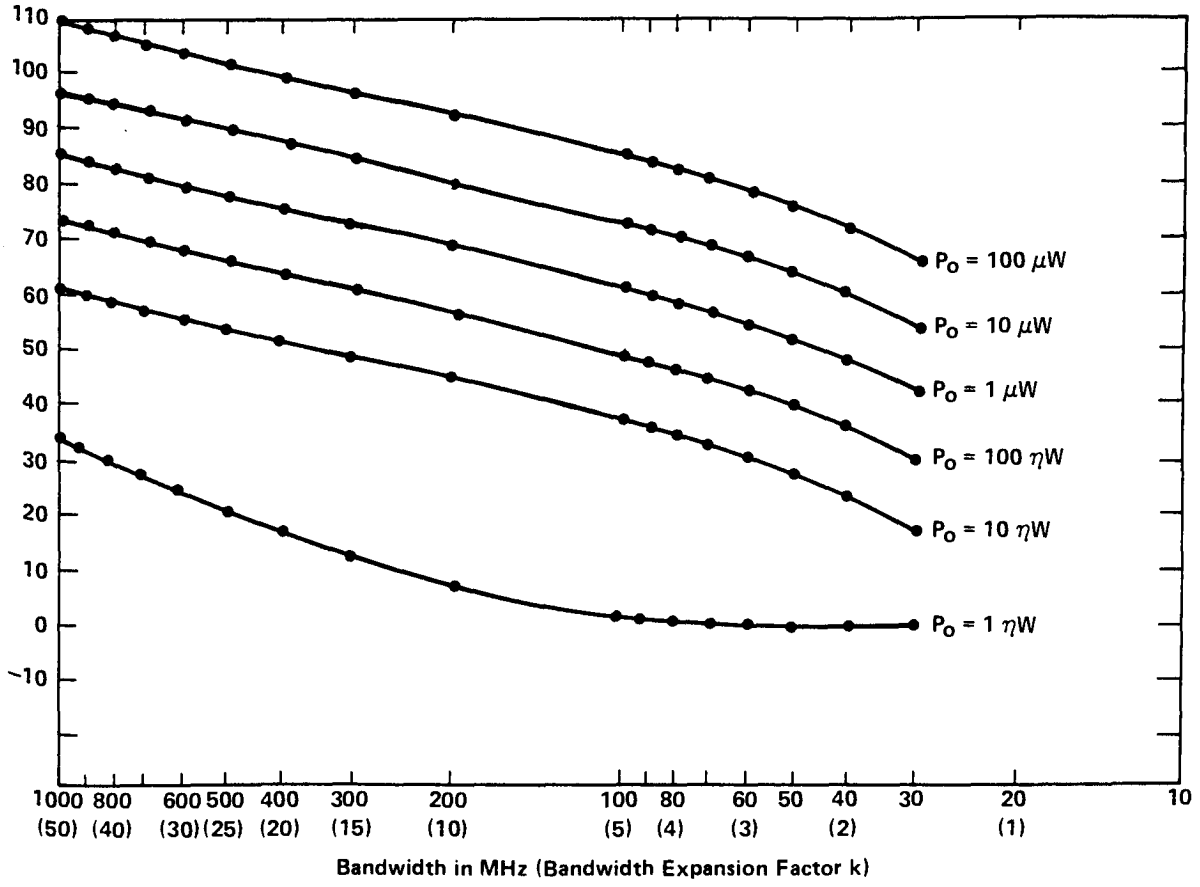

Figure A.2: SNR (r.m.s. Signal to r.m.s. Noise) V Bandwidth for PPM Systems Using Avalanche P.D.

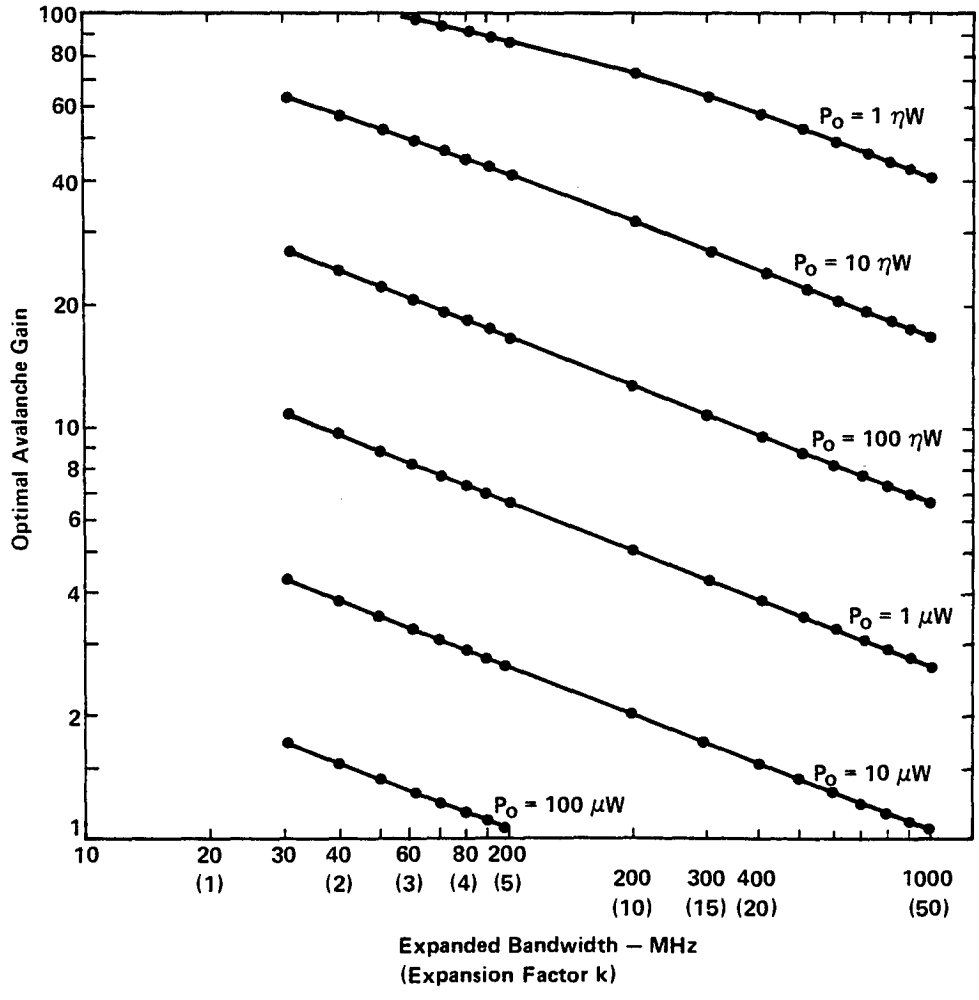

Figure A.3: Optimum Avalanche Gain v Bandwidth for PPM Systems

A.3 Timing extraction

The analysis above represents something of an ideal situation, since it assumes firstly that the signal has been encoded using a jitter-free clock, and secondly that the detector has managed to extract the jitter-free clock perfectly. In ref. A.3 Holden points out that over a large range of signal levels it is timing jitter which dominates all other degradation. Holden based his comments on experimental transmission of a 4kHz signal, and jitter will probably be worse at higher frequencies.

A.4 Peak light power

Throughout the calculations some average power P is assumed incident on the photodetector. When a bandwidth expansion of K is used, the light power during the peak of the pulse reaches a value of 2K times P_o. The physical limitations of a device trying to achieve such values must be kept in mind, especially of results for K greater than about 10 are to be used.

A.5 Interpretation of SNR

The calculations above were all for a sinusoidal, baseband signal whose amplitude swings between two levels +x and -x, causing the PPM pulse to move from one extreme of its time slot to the other. The mean signal power in this case is $x^2/2$. SNR for a television baseband signal which fluctuates between -x (white) and +x (synch tip) is expressed as the ratio of the voltage difference between these two levels to the r.m.s. noise voltage, hence as the rate of $4x^2$ to the mean noise power. Hence the SNR of a baseband vido signal is 9dB better than that calculated here. Further, as has been discussed in the body of the present report and in ref. A.4, this unweighted baseband SNR is equivalent to an NCTA figure 4dB higher. Thus system wanting a SNR equivalent to an NCTA figure of 40dB would use a value of 27dB on the curves of the present report, while a high quality transportation trunk objective of 56dB corresponds to 43dB on these curves.

Assuming a light source which launches a mean power of 1mW into a fibre, the following table summarizes the bandwidth expansion needed to achieve 40dB and 56 dB NCTA values for SNR:

Detector type	SNR (NCTA) (dB)	Attenuation due to fibre (dB)	Bandwidth required (MHz)
PIN	40	40	100
PIN	40	30	30
PIN	56	40	240
PIN	56	30	65
APD	40	40	< 30
APD	40	30	< 30
APD	56	40	60
APD	56	30	30

Although these figures look reasonably attractive, caution is needed in practical systems due to jitter. Further, a system which has 40dB loss in it may be over 8 km long using present day fibres. Such systems, using a PIN diode, need frequency responses of 800MHz-km from the fibre for a 40dB SNR, and nearly 2GHz-km for a 56dB SNR. Systems using APDs are superior, of course, needing only of the order of 200MHz-km and 480MHz-km in the two cases. However, multiplexing of several video channels by time division PPM demands a considerable bandwidth.

The real attraction of PPM lay in early systems with high fibre attenuations, where 40dB attenuation represented only 2km or less of fibre, and bandwidth was no major constraint. The combination of bandwidth requirements for multiplexed systems and the unquantified

effects of jitter accumulation in a cascaded PPM system make it unattractive in comparison with other modulation schemes.

A.7 References

A.1 "Principles of Communication Engineering". J.M. Wozencraft, I.M. Jacobs, J. Wiley & Sons, 1965. Ch.5.

A.2 "Utilization of optical-frequency carriers for low and moderate bandwidth channels". W.M. Hubbard. B.S.T.J. 52.5 (May/June 1973). PP 731-765.

A.3 "An optical-frequency pulse-position-modulator experiment". W.S. Holden. B.S.T.J 54.2 (February 1975) pp 285-296.

A.4 "The relationship between the NCTA, EIA, and CCIR definitions of signal to noise ratio". T.M. Straus. IEEE Trans. on Broadcasting BC-20 No.3 (Sept 74) pp 36-41.

APPENDIX B

WAVELENGTH DIVISION MULTIPLEXING

By N. Toms

INTRODUCTION

Wavelength division multiplexing (WDM) implies a three-stage process. Firstly, light sources of different spectral composition are individually modulated by independent signals. Secondly, the total light output from all these sources is transmitted over a common path. Thirdly, the total light energy at the end of the transmission path is analyzed on the basis of its spectral composition and each of the components resulting from this analysis is individually demodulated. The criteria by which a WDM system should be judged are the efficiency with which it launches the signal-modulated energy into the transmission pathway and the degree to which the signals resolved by the spectral analysis resembles the independent signals at the input.

Although some authors prefer to describe the above process as frequency, or optical frequency, division multiplexing, we feel that, semantically, wavelength division multiplexing conveys better the idea that sources of different spectral composition are used.

The rationale for studying WDM for use in fiber optics systems can be seen by considering the roles fiber optics is required to play within the telecommunications network. These fall into two principal categories, namely, high capacity trunks and medium capacity loops serving subscribers directly.

For high capacity trunking applications, the capacity of a single fiber is limited by three factors, namely modal dispersion, material dispersion and the modulation characteristics of the device. For analogue modulation, the third factor dominates due to nonlinearity in the response of LED's and lasers. For digital systems, instabilities in laser performance make reliable operation over 200 Mbit/s debatable. WDM would permit high transmission capacities while allowing devices to be operated within their linear range for analogue applications, or within their range of stability for digital applications.

However, it is in the second application category, that of medium capacity loops, that WDM offers its main advantages. Telecommunications systems are evolving towards an integrated network providing the subscriber with a range of video, data and telephone signals. Fiber is the obvious medium to transmit these signals to the subscriber. However, if the subscriber is to have a range of terminals, either he must have a separate fiber for each service, or his terminals must incorporate analogue or digital modems. The former increases transmission costs; the latter increases terminal costs. Furthermore, since different households will require different terminals, it becomes necessary to devise strict frequency or time allocations for each service. WDM differs from FDM and TDM by allowing the subscriber to transmit and receive all his signals at baseband, or at some other convenient frequency. His signals can be converted at a switching center into a suitable form for trunk transmission, if necessary, thereby allowing the expensive modulation and demodulation equipment to be shared by many users.

All of the above discussion is predicated on one assumption, namely that WDM systems with adequate performance can be constructed at a low cost. The rest of this paper looks at the performance objectives, and at the methods available to meet these objectives.

B.2 DISPERSIVE AND NONDISPERSIVE SYSTEMS

WDM systems could be implemented by two approaches: dispersive and nondispersive. In a nondispersive system the analysis (demultiplexing) is performed by spreading the total signal energy over an array of filters. Each filter only passes the light whose spectral composition equals that of one of the sources. These systems are inherently lossy, especially for large numbers of sources. In a system with N sources the energy from any one source which is incident on the appropriate filter is 10 log N dB down on the total available energy corresponding to that source. For this reason, nondispersive systems will be omitted from the present discussion. The problem of launching the light into the fiber may be solved either by running a dispersive system in reverse, or by using a power coupler such as that recently developed by D.O.C.

In a dispersive system the fiber output is imaged through a disperser into a plane containing an array of detectors. Because of the disperser the position of the image within the image plane is a function of the wavelength of the light in the fiber. This functional dependence will be assumed to be linear.

Figure B-1 illustrates this idea, and defines the coordinates to be used in the discussion below. The fiber end is located in the $\tilde{x}$-plane. The Cartesian coordinates chosen in this plane are x_d parallel

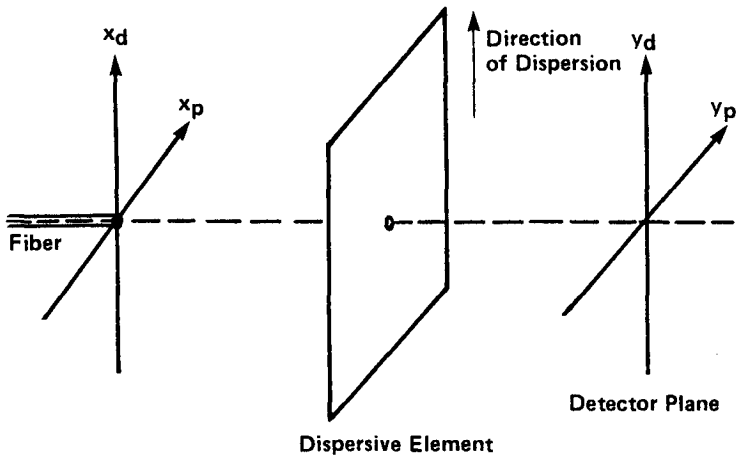

Figure B.1: Coordinate System for Analysis

to the direction of dispersion and x_p perpendicular to it. After emerging from the dispersive device, the image is formed in the $\tilde{y}$ plane. Again, the base vectors for this plane are taken parallel to and perpendicular to the direction of dispersion. These are y_d and y_p, respectively. (Note that the $\tilde{y}$ and $\tilde{x}$ planes are not necessarily parallel.)

B.3 ANALYSIS

The spatial and spectral distributions at the fiber output will be considered to be independent. Thus:

$$O(x,\lambda) \Rightarrow O'(x)\ S(\lambda) \qquad \text{(B-1)}$$

The dispersive system will image a monochromatic object:

$$O(\tilde{x},\lambda_i) = O'(\tilde{x}) \cdot \delta(\lambda-\lambda_i) \qquad \text{(B-2)}$$

by an image:

$$I'(\tilde{y}) = \frac{1}{k_1^2}\ O'\left(\frac{\tilde{y}}{k_1}\right) * \delta\left\{\left(y_d - k_2(\lambda_i-\lambda_o)\right), y_p\right\} \qquad \text{(B-3)}$$

where: k_1 represents the magnification of the system, and k_2 measures the dispersion in units of length in the y_d direction per unit of wavelength.

Thus, an infinitesimally small monochromatic image located at the origin in the $\tilde{x}$ plane:

$$O''(\tilde{x},\lambda_i) = \delta(\tilde{x})\ \delta(\lambda-\lambda_i) \qquad \text{(B-4)}$$

will be imaged by:

$$I''(\tilde{y}) = \delta(y_p)\cdot\frac{1}{k_2}\,\delta\left\{\frac{y_d}{k_2} - (\lambda_i-\lambda_o)\right\} \qquad \text{(B-5)}$$

(where the relation $\delta(ax) = \frac{1}{a}\delta(x)$ is used to put the dispersion factor outside the brackets in the same way as the magnification factor).

A point source at the origin in the $\tilde{x}$ plane whose optical power spectrum is $S(\lambda)$ will be imaged as:

$$I'''(\tilde{y}) = \delta(y_p) \cdot \frac{1}{k_2} S\left\{\frac{y_d}{k_2} + \lambda_0\right\} \qquad \text{(B-6)}$$

The Spatial and Spectral Distribution of the Fiber Output

The Spatial intensity variation at the output of a fiber may reasonably be modelled by a gaussian distribution. Thus:

$$O'(\tilde{x}) = C e^{-\frac{|\tilde{x}|^2}{2a^2}} = C e^{-\frac{x_d^2}{2a^2}} e^{-\frac{x_p^2}{2a^2}} \quad \text{for } |\tilde{x}| = \sqrt{x_p^2 + x_d^2} \leq r_f$$

$$= 0 \qquad \text{elsewhere} \qquad \text{(B-7)}$$

where r_f is the fiber core radius, and the fiber is assumed to the centred on the origin in the $\tilde{x}$ plane.

The power spectrum of the fiber output arises from the combination of the light from a number (N) of different sources. If each of these is modelled as having a gaussian distribution in wavelength, then the power spectrum is given by:

$$S(\lambda) = \sum_{i=1}^{N} A_i e^{-\frac{(\lambda-\lambda_i)^2}{2\sigma_i^2}} \qquad \text{(B-8)}$$

$$= \sum_{i=1}^{N} S_i(\lambda) \qquad \text{(B-9)}$$

where

$$S_i(\lambda) = A_i e^{-\frac{(\lambda-\lambda_i)^2}{2\sigma_i^2}} \qquad \text{(B-10)}$$

is the power spectrum due to the i^{th} source alone.

Detected Signal Power

In order to detect the N signals emitted by the fiber, there will be an array of N detectors located in the $\tilde{y}$ plane. The detector intended for the i^{th} signal, whose optical power spectrum is given by equation B-10 , will be centred at:

$$y_d = k_2(\lambda_i - \lambda_0) = y_{di}$$
$$y_p = 0 \qquad \text{(B-11)}$$

In front of each detector will be a slit, or mask of transmittance $T(\tilde{y})$, such that:

$$T(\tilde{y}) = 1, \left(y_{di} - \frac{\alpha}{2}\right) \leq y_d \leq \left(y_{di} + \frac{\alpha}{2}\right); -\infty < y_p < \infty \qquad \text{(B-12)}$$
$$= 0 \qquad \text{elsewhere}$$

The image in the $\tilde{y}$-plane due to the output of a fiber whose spatial intensity distribution $O^1(\tilde{x})$ is given by B-7 , and whose optical power spectrum $S(\lambda)$ is given by equation B-8 , is the convolution of the function $I'''(\tilde{y})$ of equation B-6 with the function $\frac{1}{k_1^2} O'\left(\frac{\tilde{y}}{k_1}\right)$.

Considering, for the moment, only the signal due to the i^{th} source, the signal power at any point $\tilde{y}$ of the detector plane is given by:

$$D_i(\tilde{y}) = \delta(y_p) \cdot \frac{1}{k_2} S_i\left\{\frac{y_d}{k_2} + \lambda_0\right\} * \frac{1}{k_1^2} O'\left\{\frac{\tilde{y}}{k_1}\right\} \qquad \text{(B-13)}$$

where * signifies convolution

using eq. B-7 for $O'\left\{\frac{\check{y}}{k_1}\right\}$:

$$O'\left\{\frac{\check{y}}{k_1}\right\} = C\, O_p'\left\{\frac{y_p}{k_1}\right\} \cdot O_d'\left\{\frac{y_d}{k_1}\right\}.$$

where: $O_p'\left\{\frac{y_p}{k_1}\right\} = \sqrt{C}\, e^{-\frac{y_p^2}{2k_1^2a^2}}$ when: $-k_1\tau \le y_p \le k_1\tau$

$= 0$ elsewhere

$$O_d'\left\{\frac{y_d}{k_1}\right\} = \sqrt{C}\, e^{-\frac{y_d^2}{2k_1^2a^2}} \quad \text{when: } -\sqrt{k_1^2\tau_f^2 - y_p^2} \le y_d \le \sqrt{k_1^2\tau_f^2 - y_p^2}$$

$= 0$ elsewhere

(B-14)

$$\therefore D_i(\check{y}) = \frac{1}{k_2 k_1^2}\, O_p'\left(\frac{y_p}{k_1}\right) \int_{z=-\infty}^{\infty} O_d'\left(\frac{z}{k_1}\right) S_i\left\{\frac{y_d - z}{k_2} + \lambda_0\right\} dz \qquad \text{(B-15)}$$

substituting for $O_d'\left\{\frac{z}{k_1}\right\}$ from B-14 and for S_i from B-10, gives:

$$D_i(\check{y}) = \frac{1}{k_2 k_1^2}\, C\, O_p'\left(\frac{y_p}{k_1}\right) A_i \int_{z=-\sqrt{k_1^2\tau_f^2 - y_p^2}}^{\sqrt{k_1^2\tau_f^2 - y_p^2}} e^{-\frac{z^2}{2k_1^2a^2}}\, e^{-\frac{\left\{\frac{y_d - z}{k_2} - \lambda_i + \lambda_0\right\}^2}{2\sigma_i^2}} dz \qquad \text{(B-16)}$$

To evaluate the integral in B-16 , put:

$$u = \sqrt{k_1^2\tau_f^2 - y_p^2}$$

$$\alpha^2 = 2k_1^2a^2$$

$$\beta = y_d - k_2\lambda_i + k_2\lambda_0 = y_d - y_{di}$$

$$\gamma^2 = 2 k_2^2 \sigma_i^2$$

The integral in 16 becomes:

$$I_i(\tilde{y}) = \int_{z=-u}^{u} e^{-\frac{z^2}{\alpha^2}} e^{-\frac{(z-\beta)^2}{\gamma^2}} dz$$

This may be evaluated by some algebraic manipulation to give:

$$I_i(\tilde{y}) = \frac{\alpha\gamma}{2}\sqrt{\frac{\pi}{\alpha^2+\gamma^2}}\, e^{-\frac{\beta^2}{\alpha^2+\gamma^2}}\left[\operatorname{erf}\left\{\frac{u}{\alpha\gamma}\sqrt{\alpha^2+\gamma^2}-\frac{\alpha\beta}{\gamma\sqrt{\alpha^2+\gamma^2}}\right\}+\operatorname{erf}\left\{\frac{u}{\alpha\gamma}\sqrt{\alpha^2+\gamma^2}+\frac{\alpha\beta}{\gamma\sqrt{\alpha^2+\gamma^2}}\right\}\right] \quad \text{(B-17)}$$

The function $erf(x)$ is defined as usual by:

$$erf(x) = \frac{2}{\sqrt{\pi}} \int_0^x e^{-t^2} dt$$

Erf(x) is a tabulated function, and is available in Fortran programs as a standard function. For values of x greater than 3, it may be approximated by noting that:

$$erf(x) = 1 - 2Q(\sqrt{2}x) \qquad \text{(for all values of x)}$$

and $$Q(x) \approx \frac{1}{\sqrt{2\pi}x}\left(1-\frac{1}{x^2}\right) e^{-\frac{x^2}{2}} \quad \text{for} \quad x \geq 3$$

The total power on the i^{th} detector due to the i^{th} source is:

$$Y_i = \int_{y_d = y_{di} - \frac{\alpha}{2}}^{y_{di} + \frac{\alpha}{2}} \int_{y_p = -k_1 r_f}^{k_1 r_f} D_i(\tilde{y})\, dy_p\, dy_d \qquad \text{(B-18)}$$

where, from B-16:

$$D_i(\tilde{y}) = \frac{1}{k_2 k_1^2} O_p'\left(\frac{y_p}{k_1}\right) A_i \cdot I_i(\tilde{y})$$

and $I_i(\tilde{y})$ is given by B-17.

Having derived the desired signal power incident on a given detector, the next problem is to calculate the undesired signal, or cross-talk, incident on the detector. This comes from two sources: stray scattering due to imperfections in the dispersive element or reflection at surfaces, and the tail of the energy distribution centred at adjacent detectors. The calculations which follows deal with the second effect.

It will be assumed that the only significant crosstalk contributions come from the light destined for the two detectors immediately adjacent to the detector under consideration. Further, it will be assumed that all light sources have the same spectral width $\sigma=\sigma_i$, and the same level $A=A_i$. The latter assumption can easily be changed later - it merely aids the orderly presentation. One further assumption is made, namely that the wavelengths λ_{i+1} and λ_{i-1} are equidistant from λ_i .

The power falling in the slit already described in front of the detector intended for $S_i(\lambda)$ due to the spectra $S_{i+1}(\lambda)$ and $S_{i-1}(\lambda)$ is given by:

$$Z_i = 2 \cdot \int_{y_d = y_{di} + \Delta y_d - \frac{\alpha}{2}}^{y_{di} + \Delta y_d + \frac{\alpha}{2}} \int_{y_p = -k_i \tau_f}^{k_i \tau_f} D_i(\tilde{y})\, d y_p\, d y_d \qquad \text{(B-19)}$$

where $\Delta y_d = k_i (\lambda_{i+1} - \lambda_i)$ represents the separation between the centres of adjacent photodetectors.

Only one more step is needed to complete the analysis, namely a normalisation for the constants A,C. These will be normalised so that the total power due to one source $S_i(\lambda)$ (all i) emerging from the fiber is unity. Thus:

$$AC \int_{\theta=0}^{2\pi} \int_{r=0}^{r_f} \int_{\lambda=-\infty}^{\infty} e^{-\frac{r^2}{2a^2}} \, r \, e^{-\frac{(\lambda-\lambda_i)^2}{2\sigma^2}} \, d\lambda \, dr \, d\theta = I \qquad \text{(B-20)}$$

from this it follows that:

$$AC = \left[(2\pi)^{\frac{3}{2}} \sigma a^2 \left\{ 1 - e^{-\frac{r_f^2}{2a^2}} \right\} \right]^{-1} \qquad \text{(B-21)}$$

The above completes the analysis of the dispersive system. It is clear that the system has two parameters which may be varied independently, namely the magnification k_1 and the dispersion k_2. In the simple system of fig. B-2 a transmission grating is placed between the two lenses. It is stressed that this is a most inefficient system, and a real system will almost certainly use a blazed reflection grating for efficiency, but the same analysis applies in both cases. The magnification k_1 is determined by the ratio of the focal lengths of the two lenses:

$$k_1 = f_2/f_1$$

The dispersion is determined by the spacing of the grating, d_g and f_2:

$$k_2 = f_2/d_g \ ,$$

Thus the ratio

$$k_1 : k_2 = d_g : f_1$$

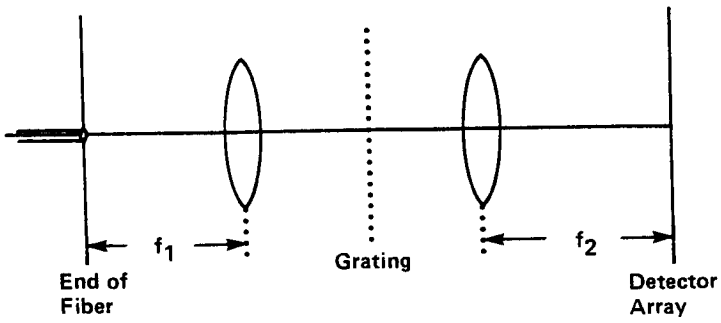

Figure B.2: A Simple Diffraction Grating Arrangement

A computer program was written to evaluate equations B-19 B-20 above, using the normalisation of equation B-21.

Because of time and space limitations, only a few results are presented here. The basic parameters common to all are:

$k_2 = 20{,}000$

$r_f = 50\,\mu m$

$a = 25\,\mu m$

$\lambda_0 = 800nm$

$\lambda_i = 850nm$

$\sigma = 2.\sqrt{2}\,nm$

The first curve, fig. B-3, shows the signal level, Y_i, as a function of d, the slit width. The results were computed from the above parameters, but are generalised in fig. B-3 by expressing d as a multiple of $k_2\sigma$. At the same time, to preserve generality, the magnification k_1 must be expressed as a function of σ . Four values of k_1 have been used as parameters, namely $k_1 = \sigma/\sqrt{2}$, σ, 2σ and 4σ (where σ is expressed in nanometres). These curves allow one to design the system to give a desired signal level at the detector.

Fig. B-4 shows the distance by which adjacent detectors must be separated to get a desired isolation against crosstalk, for a fixed value of $k_1 = \sigma/\sqrt{2}$. Note that the isolation for systems purposes is 20 log of the axis.

As a numerical example, if one had a source of:

$\sigma = 2\sqrt{2}$ nm.

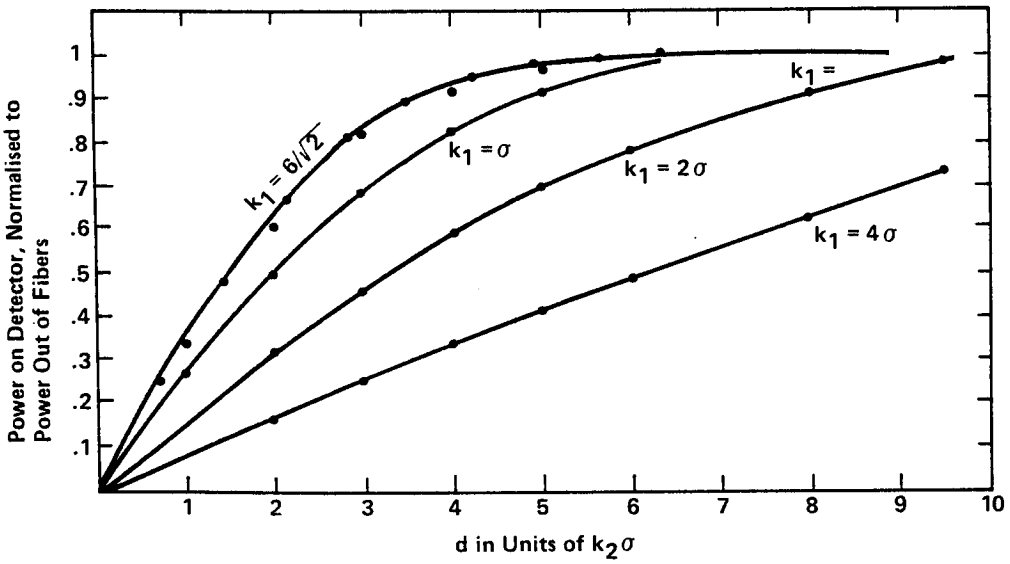

Figure B.3

SIGNAL LEVEL

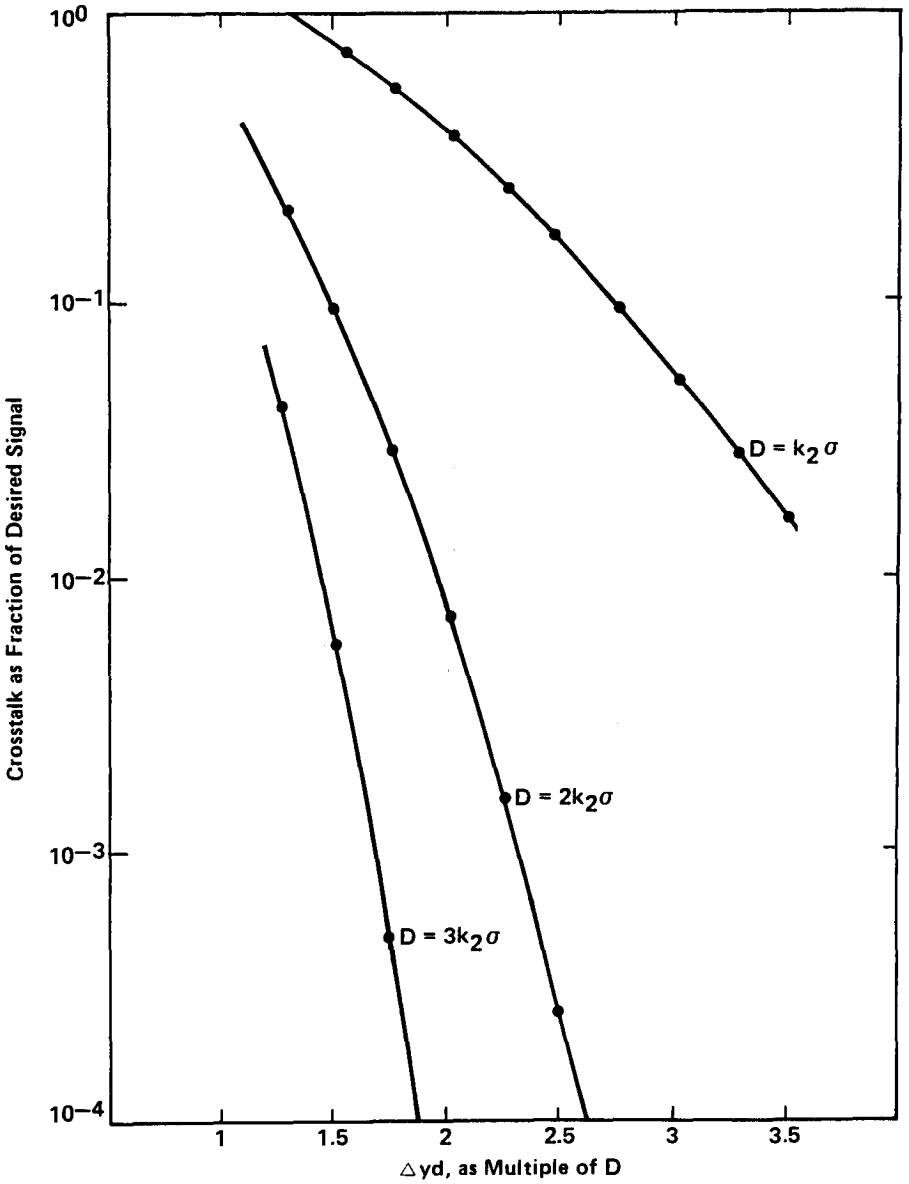

Figure B.4

SEPARATION DISTANCE BETWEEN DETECTORS

and needed to detect 65% of the light at a given wavelength, fig. B-3 shows that $d=2k_2\sigma$ is needed. If a crosstalk isolation of 60dB is needed, Fig. B-4 shows that $\Delta\gamma_d$ =2.26D is needed, or a center wavelength spearation of about 12nm. Thus, nine different sources within a 100nm band could be used.

This analysis is intended as a preliminary look at WDM. Factors such as light scattering from imperfections in gratings or other sources are ignored, but may be serious in a real system. Spectral components in a light source other than that described by the gaussian shape of $S_i(\lambda)$ may also need attention.